

Activity 10: Ambient air quality monitoring



Activity 10.1: E-bam deployment and air quality assessment (baseline) for eZamokuhle



Document by:



Final Report

3rd November 2023

Document Title

Client		Eskom
Title		E-bam deployment and air quality (AQ) assessment (baseline) for eZamokuhle
Our Reference		ESKPMV-2023- ACT-10.1-00
Issued to Client		3rd November 2023
Classification		Company Confidential

Document Change Record

Revision Number	Date	Description of Revision
00A	21 st July 2023	Creation of Document
00B	20 th August 2023	Peer Review of Document
00	6 th September 2023	Draft Document issued to Eskom
01	3 rd November 2023	Final Document issued to Eskom

Document Approval

	Name	Date
Prepared by	Avishkar Ramandh & Anesu Shamu	21 st July 2023
Reviewed by	Fred Goede	20 th August 2023
Approved by	Fred Goede	3 rd November 2023

TABLE OF CONTENTS

EXECUTIVE SUMMARY 8

1. BACKGROUND 11

 1.1 Air Quality Offsets Guideline 11

 1.2 ESKOM’S Approach to Air Quality Offsets 11

 1.3 ESKOM’s Planning, Monitoring and Verification (PMV) Project 13

 1.4 Scope of Work..... 14

2. METHODOLOGY 15

 2.1 Sampling Methodology 15

 2.2 Sampling locations 15

3. RESULTS AND DISCUSSION..... 19

 3.1 Meteorological Results 19

 3.2 Pollutant Trend & Analysis 28

 4.3 Emission Source Contribution 66

5. CONCLUSIONS 80

 5.1 Particulate Matter (PM₁₀)..... 80

 5.2 Particulate Matter (PM_{2.5})..... 80

6. ACKNOWLEDGEMENTS 82

7. REFERENCES 83

DISCLAIMER..... 89

COPYRIGHT..... 90

TABLE OF FIGURES

Figure 1: Concept Schedule for the implementation of Eskom's air quality offsets (Matimolane, 2020)	12
Figure 2: Eskom's Phased approach to the rollout of air quality offset interventions (Matimolane, 2020)	12
Figure 3: E-Bam Instrument	15
Figure 4: E-Bam instrument commissioned at House 5	16
Figure 5: Close-up of the sampling sites in eZamokuhle community	17
Figure 6: Map indicating the sampling sites in relation to the Majuba Power Station.	17
Figure 7: Layout of eZamokuhle in the Highveld.	18
Figure 8: Wind roses for the Eskom eZamokuhle and Eskom Majuba AQMS for the sampling period	21
Figure 9: Diurnal wind speeds recorded at the eZamokuhle and Majuba AQMS (m/s).	23
Figure 10: Monthly mean wind speeds recorded at the eZamokuhle and Majuba AQMS (m/s).	24
Figure 11: Daily average temperature at the eZamokuhle and Majuba AQMS (°C).	26
Figure 12: Daily total precipitation (rainfall) at the eZamokuhle and Majuba AQMS (mm).	27
Figure 13: Hourly ambient PM ₁₀ concentrations (ug/m ³) measured at the sampling locations during the sampling survey.	30
Figure 14: Mean hourly ambient PM ₁₀ concentrations (ug/m ³) measured at the sampling locations during the sampling survey.	31
Figure 15: Mean hourly diurnal PM ₁₀ concentrations (ug/m ³) measured at the sampling sites during the sampling survey	32
Figure 16: Daily ambient PM ₁₀ concentrations (ug/m ³) measured at the sampling sites during the sampling survey	33
Figure 17: Daily ambient PM ₁₀ concentrations (ug/m ³) measured at the sampling sites during the sampling survey	34
Figure 18: Average weekday ambient PM ₁₀ concentrations (ug/m ³) measured at sampling sites during the sampling survey	35
Figure 19: Monthly mean ambient PM ₁₀ concentrations (ug/m ³) measured at sampling sites during the sampling survey.	36

Figure 20: Weekly diurnal PM ₁₀ concentrations (ug/m ³) measured at the sampling sites during the sampling survey	37
Figure 21: Hourly ambient PM _{2.5} concentrations (ug/m ³) measured at the sampling sites during the sampling survey	40
Figure 22: Mean hourly ambient PM _{2.5} concentrations (ug/m ³) measured at the sampling sites during the sampling survey.	41
Figure 23: Hourly diurnal PM _{2.5} concentrations (ug/m ³) measured at the sampling sites during the sampling survey.	42
Figure 24: Daily ambient PM _{2.5} concentrations (ug/m ³) measured at the sampling sites during the sampling survey	43
Figure 25: Daily ambient PM _{2.5} concentrations (ug/m ³) measured at the sampling sites during the sampling survey	44
Figure 26: Weekday ambient PM _{2.5} concentrations (ug/m ³) measured at the sampling sites during the sampling survey	45
Figure 27: Mean monthly ambient PM _{2.5} concentrations (ug/m ³) measured at sampling sites during the sampling survey.	46
Figure 28: Weekly diurnal PM _{2.5} concentrations (ug/m ³) measured at sampling sites during the sampling survey.	47
Figure 29: Hourly ambient SO ₂ concentrations (ppb) measured at the Eskom eZamokuhle and Eskom Majuba AQMS during the sampling survey (Hourly SO ₂ NAAQS = 134ppb)	50
Figure 30: Hourly mean ambient SO ₂ concentrations (ppb) measured at the Eskom eZamokuhle and Eskom Majuba AQMS during the sampling survey (Hourly SO ₂ NAAQS = 134ppb)	51
Figure 31: Mean hourly diurnal ambient SO ₂ concentrations (ppb) measured at sampling sites during the sampling survey	52
Figure 32: Daily ambient SO ₂ concentrations (ppb) measured at the Eskom eZamokuhle and Eskom Majuba AQMS during the sampling survey (Hourly SO ₂ NAAQS = 48ppb)	53
Figure 33: Daily ambient SO ₂ concentrations (ppb) measured at the Eskom eZamokuhle and Eskom Majuba AQMS during the sampling survey (Hourly SO ₂ NAAQS = 48ppb).	54
Figure 34: Mean weekday and mean monthly ambient SO ₂ concentrations (ppb) measured at sampling sites during the sampling survey	55

Figure 35: Weekly diurnal SO ₂ concentrations (ppb) measured at sampling sites during the sampling survey	56
Figure 36: Hourly ambient NO ₂ concentrations (ppb) measured at Eskom eZamokuhle AQMS during the sampling survey (Hourly NO ₂ NAAQS = 106ppb).	59
Figure 37: Hourly mean ambient NO ₂ concentrations (ppb) measured at Eskom eZamokuhle AQMS during the sampling survey (Hourly NO ₂ NAAQS = 106ppb).	60
Figure 38: Mean hourly diurnal NO ₂ concentrations (□g/m ³) measured at sampling sites during the sampling survey	61
Figure 39: Daily ambient NO ₂ concentrations (ppb) measured at Eskom eZamokuhle AQMS during the sampling survey	62
Figure 40: Daily ambient NO ₂ concentrations (ppb) measured at Eskom eZamokuhle AQMS during the sampling survey	63
Figure 41: Mean weekday and mean monthly ambient NO ₂ concentrations (ppb) measured at sampling sites during the sampling survey	64
Figure 42: Weekly diurnal NO ₂ concentrations (□g/m ³) measured at sampling sites during the sampling survey	65
Figure 43: Pollution roses indicating which wind directions contribute most to overall mean concentrations for PM ₁₀	67
Figure 44: Pollution roses indicating which wind directions contribute most to overall mean concentrations for PM _{2.5}	68
Figure 45: Pollution roses indicating which wind directions contribute most to overall mean concentrations for SO ₂	69
Figure 46: Pollution roses indicating which wind directions contribute most to overall mean concentrations for NO ₂	70
Figure 47: Polar plot of hourly mean PM ₁₀ concentration at the Eskom AQMS for the sampling period	71
Figure 48: Polar plot of hourly mean PM _{2.5} concentration at the Eskom AQMS for the sampling period	72
Figure 49: Polar plot of hourly mean SO ₂ concentration at the Eskom AQMS for the sampling period	74
Figure 50: Polar plot of hourly mean NO ₂ concentration at the Eskom AQMS for the sampling period	75
Figure 51: Polar plot of hourly mean PM ₁₀ concentration at the Eskom AQMS for the sampling period	77

Figure 52: Polar plot of hourly mean PM_{2.5} concentration at the Eskom AQMS for the sampling period 77

Figure 53: Polar plot of hourly mean SO₂ concentration at the Eskom AQMS for the sampling period 78

Figure 54: Polar plot of hourly mean NO₂ concentration at the Eskom AQMS for the sampling period 79

EXECUTIVE SUMMARY

This study performed an analysis of the baseline trends, correlations and general relations which were based on collected ambient air quality measurement data obtained from the: Eskom eZamokuhle Station (the in-situ station), the Eskom Majuba Station (the industrial station), as well as three sampling locations in the eZamokuhle residential region. It is noted that these measurements at eZamokuhle were conducted prior to the rollout of the Eskom AQO Project interventions in the eZamokuhle community and thus serves as the status quo air quality baseline herein. The Openair model was utilised to statistically analyse the semi-empirical mathematical relationships between air pollutant concentrations and meteorological parameters for these three stations.

Three E-BAM Environmental Beta Attenuation Mass Monitors were commissioned at three residential sampling sites in the eZamokuhle region. The E-BAMs were placed outdoors in the yard of each of the residential sampling sites. The E-BAM instrument is a portable, real-time beta gauge comparable to U.S.-EPA methods for PM_{2.5} and PM₁₀ particulate measurements. The E-BAM automates particulate measurement by continuously sampling and reporting concentration data. The sampling assessment was conducted from mid-August to mid-October 2022 at the three residential sampling sites.

The hourly diurnal PM cycle at House 4 is indicative of residential fuel burning. Maximum hourly ambient PM₁₀ concentrations of 400 ug/m³ were recorded at House 4 during the survey. Maximum daily ambient concentrations of 120 ug/m³ were recorded, with exceedances of the daily NAAQS for PM₁₀. These exceedances were prominent during the colder months during the sampling period. No exceedances of the daily NAAQS for PM₁₀ were recorded for the second half of September, as well as the October at House 4. A daily mean ambient PM₁₀ concentration of 57.1 ug/m³ were recorded for House 4 during the sampling period.

The hourly diurnal cycle at House 1 and House 5 are indicative of residential fuel burning. Maximum hourly ambient PM₁₀ concentrations of 500ug/m³ were recorded at House 1 and House 5 during the survey. Maximum daily ambient concentrations of 80ug/m³ were recorded at both Houses, with exceedances of the daily NAAQS for PM_{2.5}. These exceedances were more prominent during the colder months during the sampling period, but exceedances were also reported during October for both Houses. A daily mean ambient PM_{2.5} concentration of 40.0 ug/m³ and 43.7 ug/m³ were recorded for House 1 and House 5 respectively during the sampling period.

An analysis of the Eskom eZamokuhle and Eskom Majuba air quality monitoring stations (AQMS) data for PM₁₀, PM_{2.5}, SO₂ and NO₂ are also given for the same period as the particulate sampling survey in eZamokuhle for reference purposes. The Eskom eZamokuhle and Majuba ambient monitoring stations as well as the three residential E-BAM sampling sites in the eZamokuhle recorded multiple exceedances of the daily NAAQS for both PM₁₀ and PM_{2.5}. Due to the bi-modal particulate matter peaks and localised contribution evident in the study analysis, these elevated concentrations show a typical profile for residential fuel burning. These elevated concentrations were more pronounced in the winter months with the increased space heating requirements of the eZamokuhle households in winter.

There were no exceedances of the SO₂ or NO₂ NAAQS recorded at the Eskom eZamokuhle and Eskom Majuba AQMS. The SO₂ concentrations were generally associated with a typically industrial signature whereas the analysis indicated that the variability of NO₂ concentration was associated with vehicle emissions.

In summary the results of this study has demonstrated that residential fuel burning has a significant impact in terms of ambient PM₁₀ loading for Ezamokuhle. This coupled with the colder temperatures & poor air pollution dispersion potential of Ezamokuhle in winter, results in elevated localised ambient PM₁₀ concentrations. Hence there is an opportunity

herein to reduce human exposure to harmful levels of air pollution by reducing emissions from residential burning. Thus supporting the roll-out of Eskom’s PMV air quality offset intervention project in Ezamokuhle.

The analysis provided indicated serves as a baseline for the impact of the Eskom air quality offset programme with the monitoring being repeated once the intervention is eZamokuhle is completed.

1. BACKGROUND

1.1 AIR QUALITY OFFSETS GUIDELINE

An environmental offset is an action(s), designed to compensate for a negative environmental impact of resource use, a discharge, emission or other activity. The Department of Environment, Forestry & Fisheries (DEFF) defines air emissions offsets as an intervention, or interventions, specifically implemented to counterbalance the adverse and residual environmental impact of atmospheric emissions in order to deliver a net ambient air quality benefit within, but not limited to, the affected airshed where ambient air quality standards are being or have the potential to be exceeded and whereby opportunities and need for offsetting exist (Notice 333 of 2016).

1.2 ESKOM'S APPROACH TO AIR QUALITY OFFSETS

DEFF's Air Quality Offset Guideline has shaped and informed Eskom's Air Quality Offsets Implementation Plan. This Plan has been based on a scientific process of feasibility studies, testing and demonstration, and on consultation with key stakeholders. Figure 1 illustrates the concept schedule for the phased implementation of Eskom's air quality offsets.

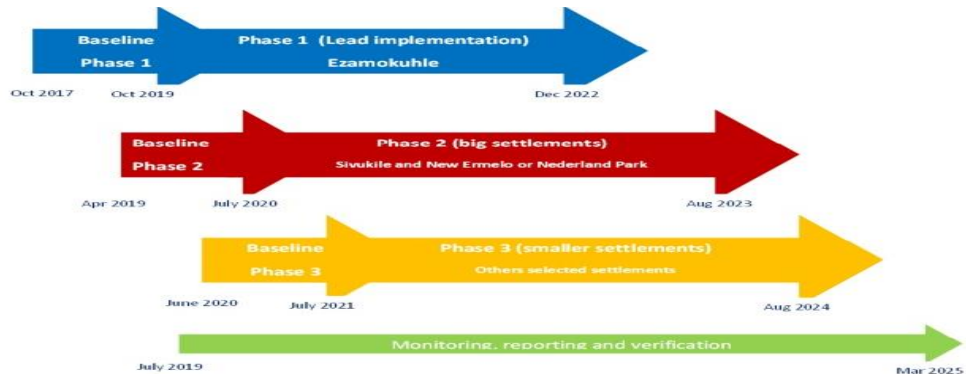


Figure 1: Concept Schedule for the implementation of Eskom’s air quality offsets (Matimolane, 2020)

Eskom has adopted the phased approach (Figure 2) herein to increase the probability of success and to ensure that learnings from early phases are incorporated into the large-scale roll-out. (Matimolane, 2020).

Figure 2: Eskom’s Phased approach to the rollout of air quality offset interventions (Matimolane, 2020)

Phase 1	Phase 2	Phase 3
<ul style="list-style-type: none"> •Lead Phase •The intervention is tested on an entire community in order to determine the best way forward for scaling up the initiative. 	<ul style="list-style-type: none"> •Full implementation on the remaining households in the larger settlements •Learnings from the Lead Phase incorporated herein. •Intervention will be rolled out simultaneously at several large communities across the three district municipalities and selected areas in the Vaal. 	<ul style="list-style-type: none"> • Full implementation on the remaining households in the smaller settlements • Learnings from the Lead Phase incorporated herein. • The intervention will be rolled out simultaneously at several small semi-rural communities the three district municipalities and selected areas in the Vaal.

Eskom's air quality offsets programme is designed to reduce human exposure to harmful levels of air pollution by reducing emissions from local sources, like domestic coal burning and waste burning. Thus, air quality offsets can improve ambient air quality in low-income communities in the vicinity of Eskom's power stations. Eskom has developed air quality offset (AQO) implementation plans for Majuba Power Station (eZamokuhle township); Hendrina Power Station (KwaZamokuhle township) and Lethabo Power station (Sharpeville).

1.3 ESKOM'S PLANNING, MONITORING AND VERIFICATION (PMV) PROJECT

For Eskom's PMV Project, interventions to reduce household emissions from domestic coal/wood burning will be rolled out in KwaZamokuhle and eZamokuhle in the Mpumalanga Highveld. For formal dwellings the intervention will be a thermal insulation retrofit and an electricity starter pack and installation. The intervention for informal dwellings still needs to be selected and tested. Interventions also need to be identified and implemented to improve air quality in Sharpeville, Gauteng. Since domestic coal burning is less prevalent in Sharpeville, it is expected that a community-scale intervention, like reducing waste burning, will be more suitable there.

Air Resource Management (ARM) (Pty) Ltd has been appointed by Eskom to support the PMV services in support of the *Phase 1: Lead implementation* at: KwaZamokuhle; eZamokuhle and Sharpeville. Its ARM (Pty) Ltd understanding that the overall objective *Lead Implementation Phase* is to benefit the specific local communities, minimize implementation risk, increase practical and scientific knowledge, and develop and refine monitoring, reporting and verifications processes. To achieve this, Eskom has included sixteen targeted work package Activities (Table 1) for these respective communities. This report focuses on *Activity 10.1 The E-bam deployment and AQ assessment (baseline) for eZamokuhle*.

Table 1: Eskom PMV Activity Schedule (Eskom PMV NEC Contract,27082020)

Activities	Kwazamokuhle	Ezamokuhle	Sharpeville
Activity 1: Preliminary air quality assessment		✓	
Activity 2: Gather Area intelligence		✓	
Activity 3: Rapid in situ assessment		✓	
Activity 4: Obtain ethical clearance		✓	
Activity 5: Census	✓	✓	✓
Activity 6: Community source survey		✓	
Activity 7: Fuel source survey		✓	
Activity 8: Household surveys		✓	
Activity 9: Annual (household/community) surveys and monitoring of project effectiveness	✓	✓	✓
Activity 10: Ambient air quality monitoring	✓	✓	✓
Activity 11: Conduct indoor air quality monitoring	✓	✓	
Activity 12: Atmospheric Dispersion Model	✓	✓	✓
Activity 13: Design of Intervention		✓	✓
Activity 14: Development of Database Reporting	✓	✓	✓
Activity 15: Strategic Assistance and offsets methodology	✓	✓	✓
Activity 16: Research and Development	✓	✓	✓

1.4 SCOPE OF WORK

In accordance with the scope of work, for Activity 10: *Conduct Ambient Air Quality Monitoring*, ARM is to conduct ambient air quality monitoring utilising the Environmental beta Attenuation Monitors to monitor baseline PM concentrations in eZamokuhle before the implementation and rollout of the intended Eskom household interventions.

2. METHODOLOGY

2.1 SAMPLING METHODOLOGY

Three E-BAM Environmental Beta Attenuation Mass Monitors were commissioned at three residential sampling sites in the eZamokuhle region. The E-BAM instrument is a portable, real-time beta gauge comparable to U.S.-EPA methods for PM_{2.5} and PM₁₀ particulate measurements. The E-BAM automates particulate measurement by continuously sampling and reporting concentration data. Data records are updated every minute. Figure 3 is a graphical representation of the E-BAM instrument.



Figure 3: E-Bam Instrument

2.2 SAMPLING LOCATIONS

Table 2 is a summary of the E-BAM site locations as well as the sampling duration. Figure 4 is a picture of the E-BAM instrument commissioned at House 5 whereas Figure 5 is a close-up of these sampling locations in the eZamokuhle residential region. Figure 6 is

locality map of the E-BAM samplers in relation to the Eskom eZamokuhle and Eskom Majuma AQMS, whilst Figure 7 is indicative of the eZamokuhle residential region in the Highveld.

Table 2: Summary of E-BAM sampling locations

Site	Pollutant Measured	Latitude (°S)	Longitude (°E)	Sampling Duration
House 1	PM _{2.5}	27.000325°	29.853501°	6 August 2023 to 21 October 2023
House 4	PM ₁₀	27.001456°	29.856803°	14 August 2023 to 21 October 2023
House 5	PM _{2.5}	27.000133°	29.855321°	8 August 2023 to 19 October 2023



Figure 4: E-Bam instrument commissioned at House 5



Figure 5: Close-up of the sampling sites in eZamokuhle community



Figure 6: Map indicating the sampling sites in relation to the Majuba Power Station.

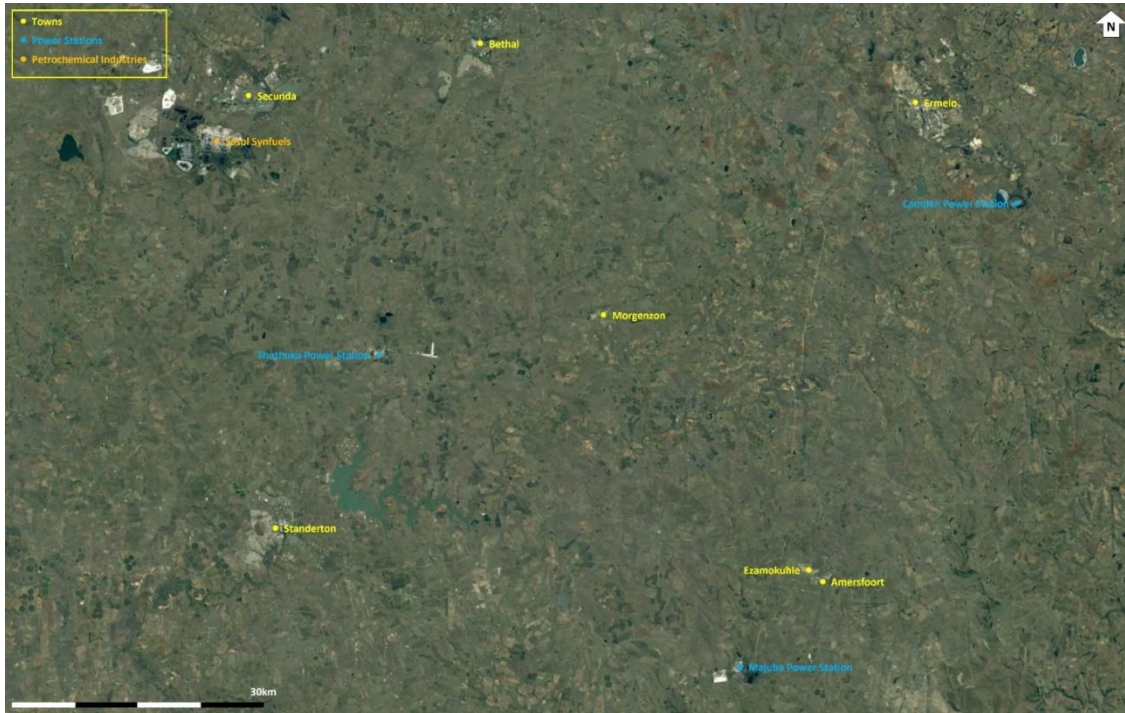


Figure 7: Layout of eZamokuhle in the Highveld.

3. RESULTS AND DISCUSSION

3.1 METEOROLOGICAL RESULTS

Air quality is strongly influenced by meteorology. Meteorological mechanisms govern the dispersion and eventual removal of pollutants from the atmosphere (Seaman, 2000). The analysis of hourly average meteorological data is necessary to facilitate a comprehensive understanding of the dispersion potential of the site. The horizontal dispersion of pollution is largely a function of the wind field. The wind speed determines both the distance of downward transport and the rate of dilution of pollutants. The wind rose is a very useful way for showing how wind speed and wind direction conditions vary by year. Meteorological data for the sampling period were obtained from the Eskom eZamokuhle and Eskom Majuba AQMS.

3.1.1 WIND SPEED AND WIND DIRECTION

Wind drives the atmospheric transport and strongly affects vertical air mixing and thus the ventilation of the urban air (Grundstrom et al., 2015). The understanding of how wind speed affects ground-level air pollution concentrations is relatively well established.

Stagnant atmospheric conditions with calm, clear weather often led to stable atmospheric stratification which can transform into strong nocturnal temperature inversions due to rapid surface cooling. The resulting restriction in vertical air mixing near the surface consequently leads to poor air quality (Delaney and Dowding, 1998; Janhall et. al., 2006; Olofson et al., 2009). Low wind speeds deteriorate air quality with respect to pollutants emitted near the ground due to restricted air ventilation (Jones et al., 2010). In contrast higher wind speeds are associated with increased dispersion and mixing of atmospheric pollutants which may result in low ambient pollution concentrations. Figure 4 illustrates

the predominant wind directions for the sampling period for the Eskom eZamokuhle and Eskom Majuba AQMS.

For the Eskom eZamokuhle AQMS station the average wind speed for the sampling period (Figure 8) was recorded at 3.04m/s with calm condition 0%. Calm condition means that wind speed is recorded at zero meter/second (Carlaw, 2015). The predominant wind direction was westerly ($\approx 17\%$ frequency of occurrence) followed by north westerly and easterly winds ($\approx 13\%$ frequency of occurrence) with maximum wind speed of 8 – 11m/s.

For the Eskom Majuba AQMS station the average wind speed for the sampling period (Figure 8) was recorded at 4.31m/s with calm condition 0.3%. Calm condition means that wind speed is recorded at zero meter/second (Carlaw, 2015). The predominant wind direction was south westerly ($\approx 16\%$ frequency of occurrence) followed by westerly and north easterly winds ($\approx 13\%$ frequency of occurrence) with maximum wind speed of 8 – 11m/s.

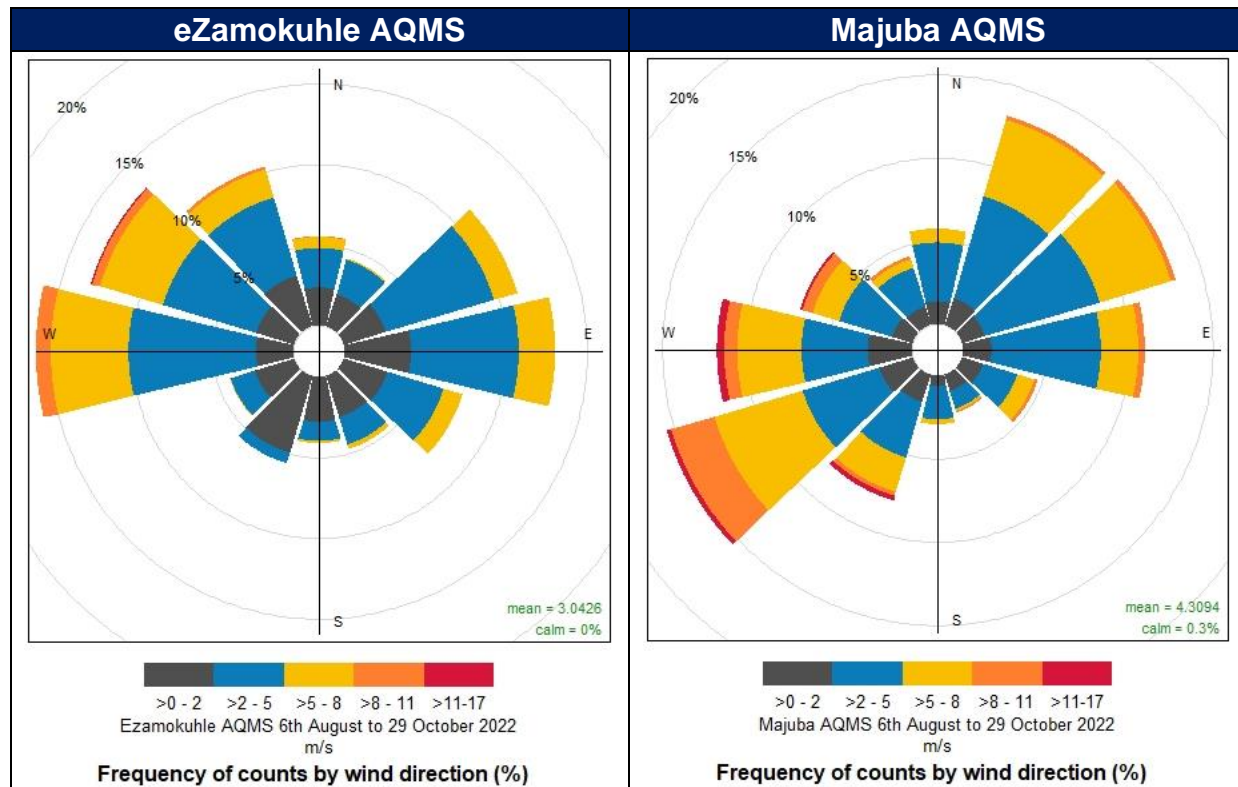


Figure 8: Wind roses for the Eskom eZamokuhle and Eskom Majuba AQMS for the sampling period

Figure 9 provides the diurnal wind speed, whilst Figure 10 is indicative of the monthly mean ambient wind speeds recorded at the Eskom eZamokuhle and Eskom Majuba AQMS respectively.

It is evident from Figure 9 that the wind speed for both stations increase at 08:00 with a decrease at around 17:00. Maximum wind speeds are recorded for both stations at 15:00. Figure 10 illustrates slightly higher monthly mean wind speeds for the Majuba AQMS in comparison to the eZamokuhle AQMS.

As a norm, wind speeds in excess of 5.4m/s potentially have sufficient energy to pick-up and transport loose and/or disturbed particulate matter, which gives rise to visible nuisance dust and clouds of dust at ground level. The extent, to which this occurs / can

occur, depends on several parameters, such as the properties and characteristics of the particulate matter, moisture content, etc.

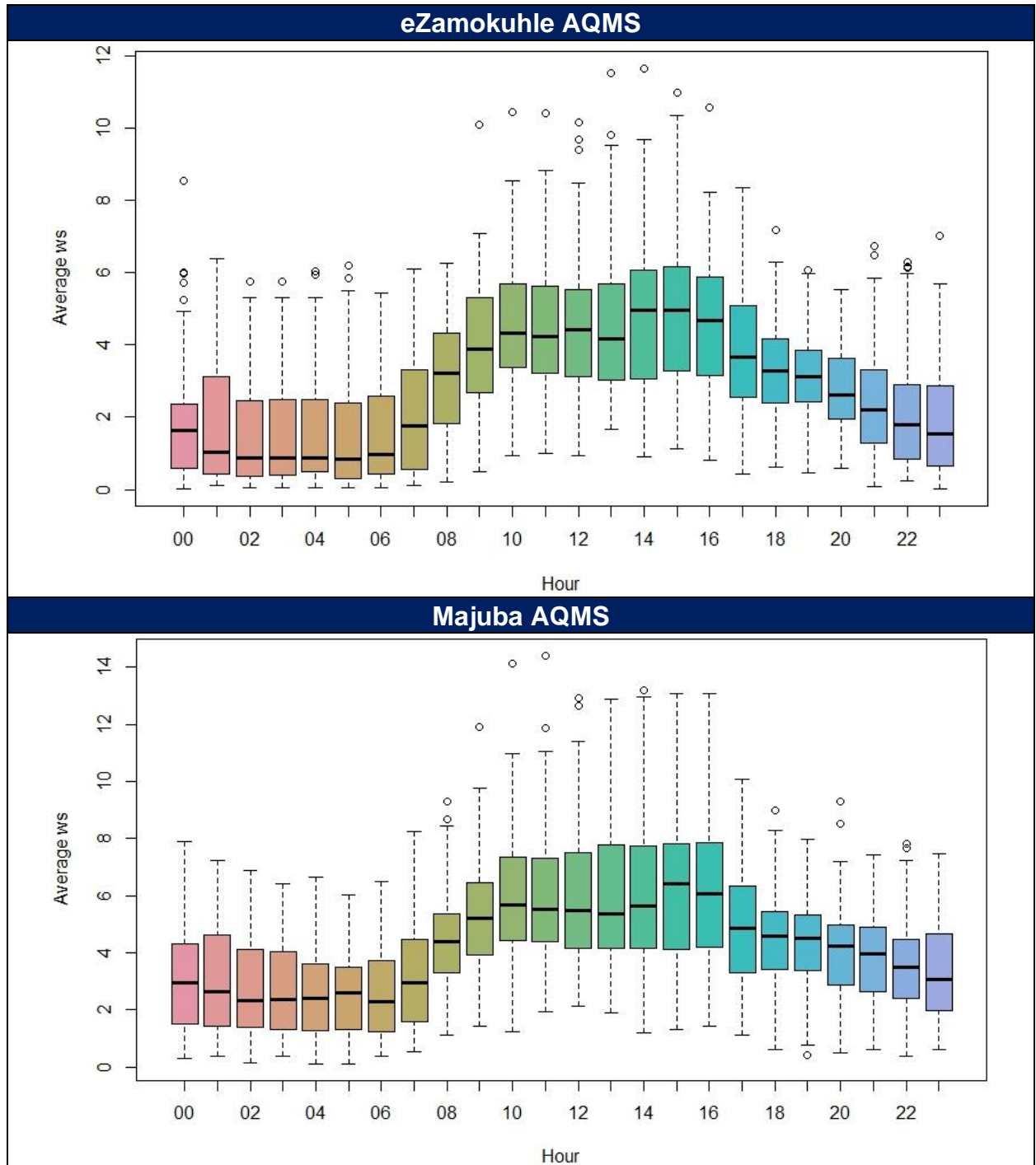


Figure 9: Diurnal wind speeds recorded at the eZamokuhle and Majuba AQMS (m/s).

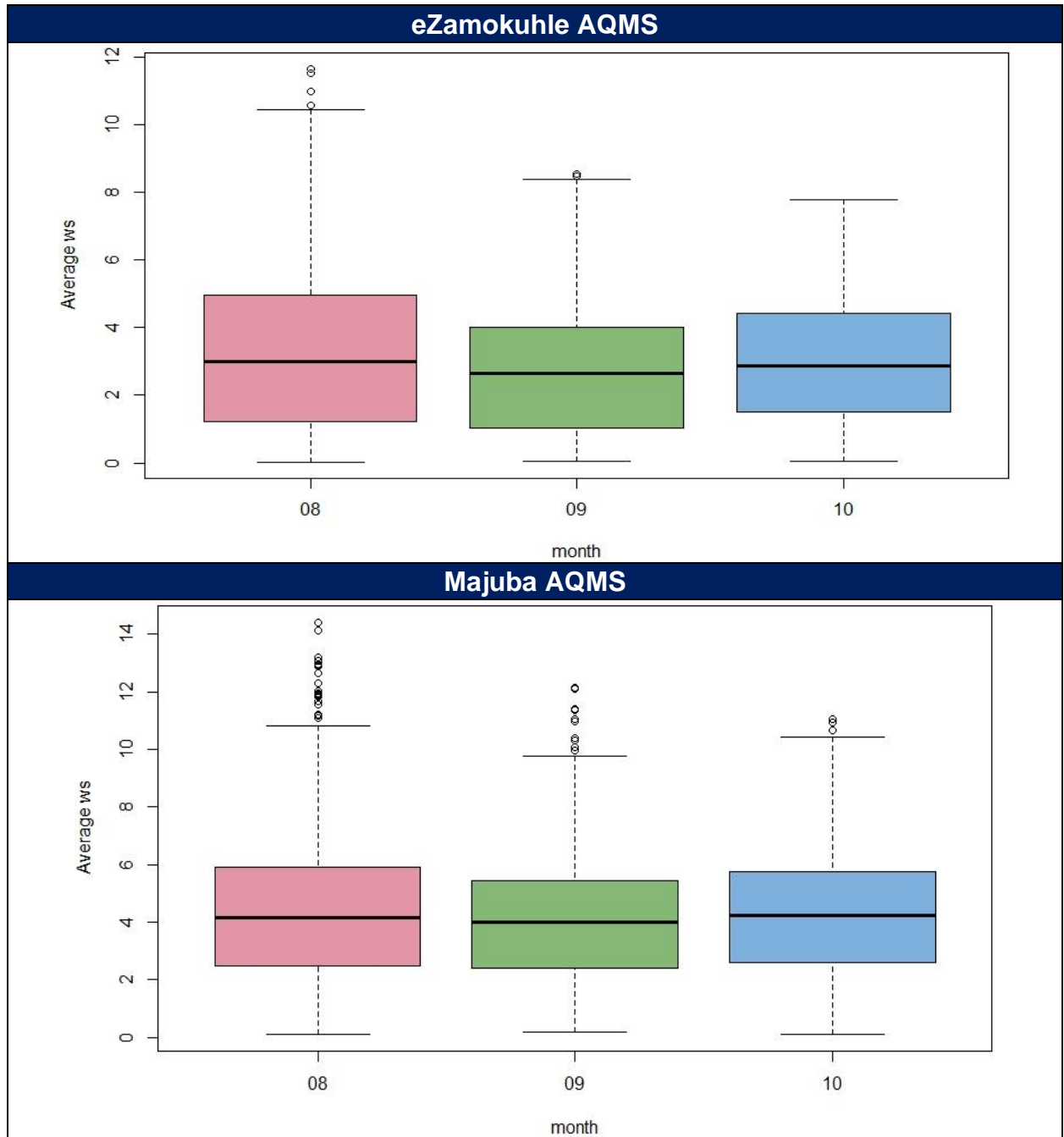


Figure 10: Monthly mean wind speeds recorded at the eZamokuhle and Majuba AQMS (m/s).

3.1.2 TEMPERATURE

Air temperature is important, both for determining the effect of plume buoyancy (the larger the temperature difference between the plume and the ambient air, the higher the plume can rise), and determines the development of the mixing and inversion layers. Figure 11 provides daily mean ambient temperatures for the Eskom eZamokuhle and Eskom Majuba AQMS respectively. From Figure 11, it is evident how the average ambient air temperatures are between 5 and 15°C for August, and slowly increasing to 15 and 22°C for the month of October. An increase in wind speed and ambient temperature improves the dispersion of air pollutants in the air.

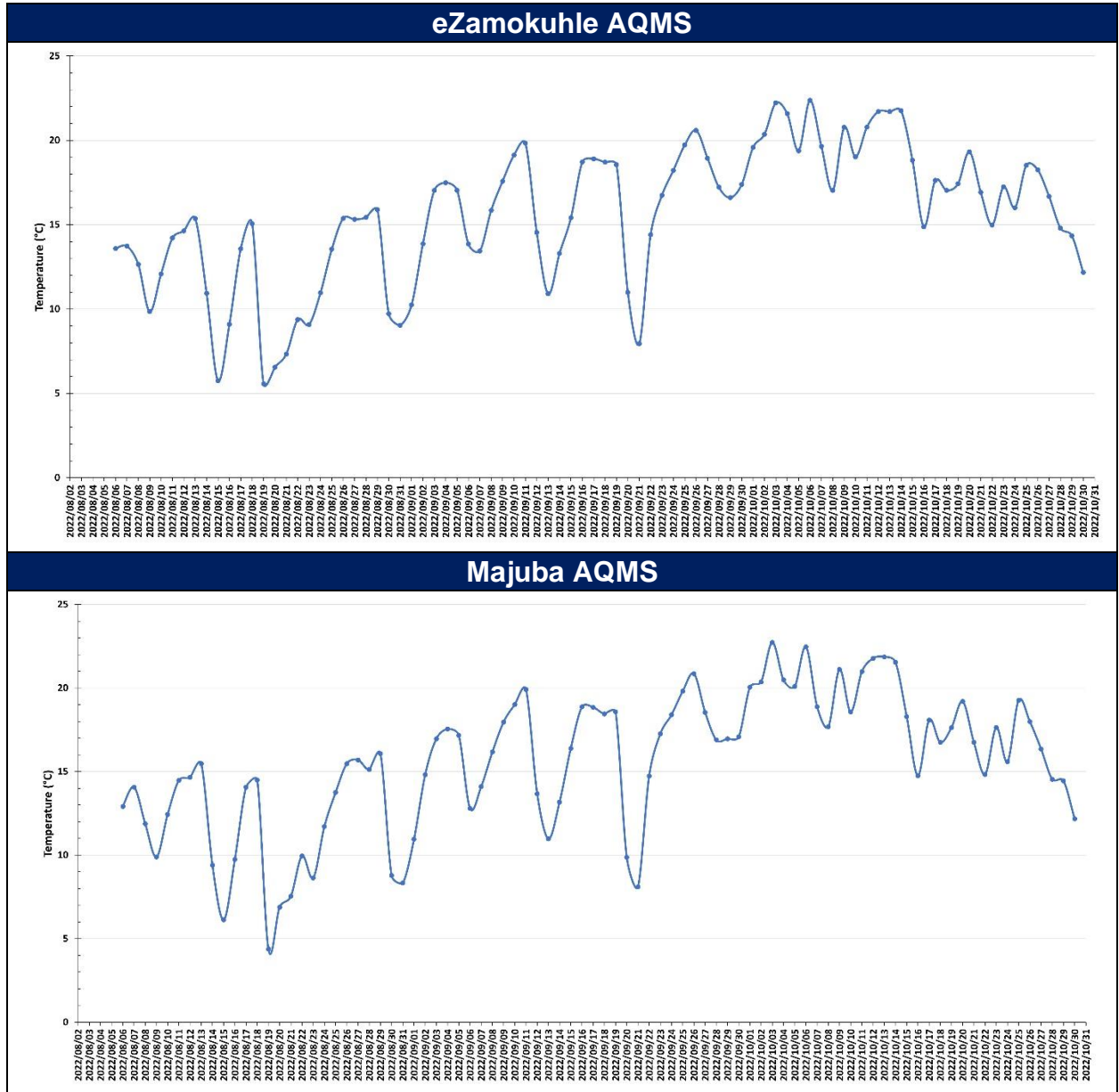


Figure 11: Daily average temperature at the eZamokuhle and Majuba AQMS (°C).

3.1.3 TEMPERATURE RAINFALL ?

Figure 12 provides daily total rainfall/precipitation recorded for the Eskom eZamokuhle and Eskom Majuba AQMS respectively. From Figure 12, it is evident both stations recorded a maximum rainfall of 17mm on 20 August 2022. Frequent rainfall events were recorded for both stations from 18 to 28 October 2022.

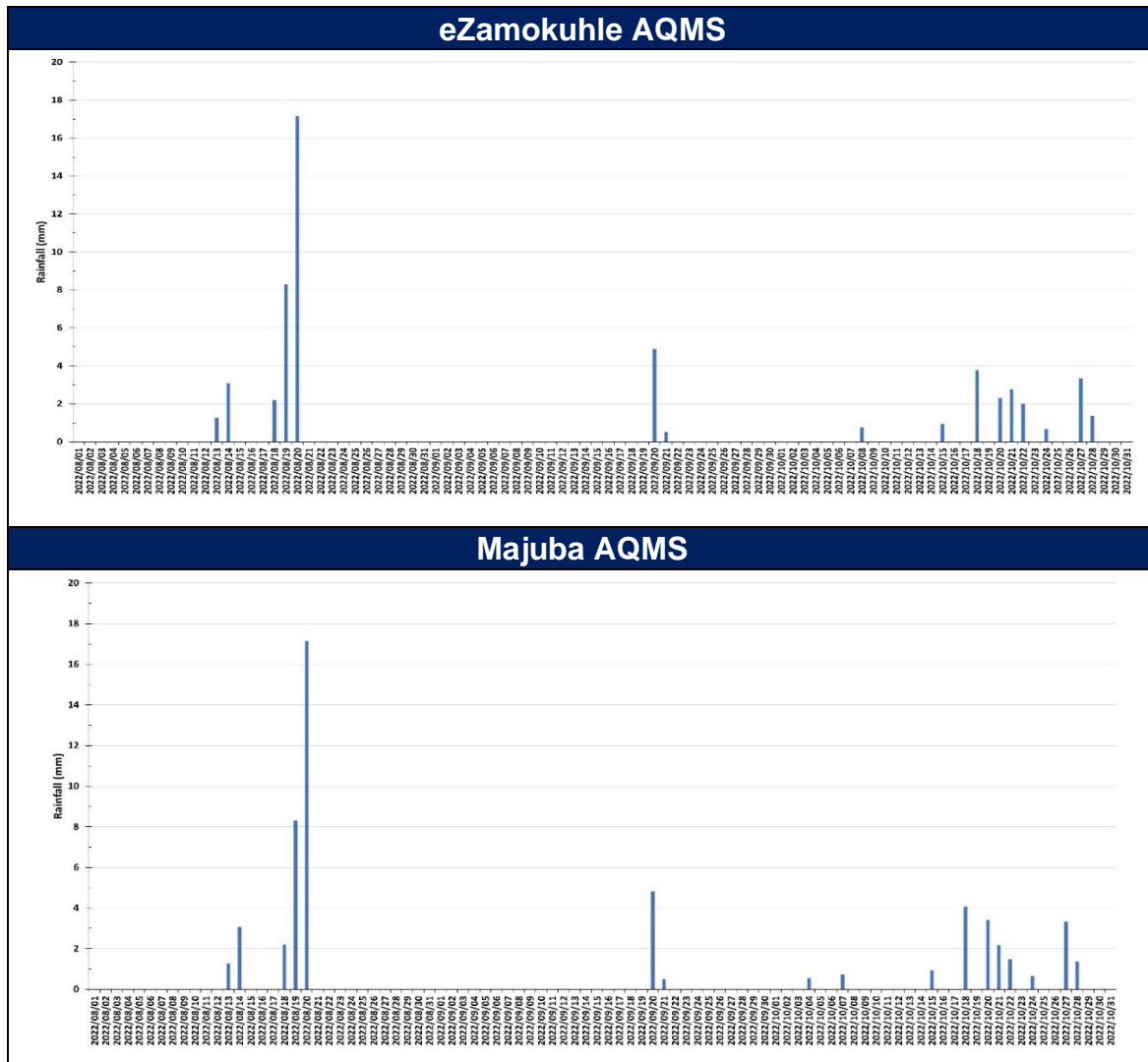


Figure 12: Daily total precipitation (rainfall) at the eZamokuhle and Majuba AQMS (mm).

3.2 POLLUTANT TREND & ANALYSIS

Openair is an air quality model for statistically analysing semi-empirical mathematical relationships between air pollutant concentration and other factors that may affect it (Tiwary, 2010). The Openair model can analyse emissions of pollutant sources, pollutant characteristics, trend estimates and model evaluations. Additionally, Openair model has the advantage of data manipulation or interpolation, statistical data analysis, creation, and visualization of high-quality graphics (Carslaw, 2015).

The Openair model has been successfully applied to determine the potential emission sources based on urban air quality measurements (Munir et al., 2016, Czernecki et al., 2016) as well as for air quality research campaigns (Crilley et al. 2017), studies concerning pollution exposure (Pattinson et al. 2016), and natural events (Salvador et al. 2014; Schweizer, Cisneros 2014). Often multiple functions provided in Openair are combined to provide comprehensive information & insight for the analysed data (Crilley et al., 2015 and Jang et al., 2016).

The relationship and trends of concentrations, including PM₁₀, PM_{2.5}, SO₂, NO₂ and meteorological parameters such as wind speed and direction, temperature for the five sampling sites were examined using the Openair model.

3.2.1 PARTICULATE MATTER (PM₁₀)

Figure 13 indicate the ambient hourly PM₁₀ concentrations recorded at the Eskom, Eskom Majuba and House 4 sampling sites. Although no NAAQS exists for hourly PM₁₀ concentrations, Figure 13 highlight that for both the eZamokuhle and Majuba sites maximum hourly concentrations of 500ug/m³ were recorded, whilst House 4 indicate maximum concentrations of 400ug/m³. Figure 14 is a graphical representation of the average hourly PM₁₀ concentrations for the sampling period. It is evident from Figure 14

that the highest average values are recorded during hours 06:00 to 08:00 for both the eZamokuhle and House 4 sites, but all three sites indicate elevated hourly values from 17:00 to 19:00. These diurnal profiles are also illustrated in Figure 15. The bi-modal particulate matter peak for both the Eskom eZamokuhle, Majuba and House 4 sites (Figure 4-8) is a typical profile for residential fuel burning. A morning peak occurs at 07:00 whilst the evening peak occurs at 18:00. The morning peaks reduces towards midday as the inversion layer rises & improves the mixing height of the planetary boundary layer. The morning peak is not that prevalent at the Majuba AQMS.

Figure 16 indicate the daily ambient PM₁₀ concentrations recorded at the Eskom eZamokuhle, Eskom Majuba and House 4 sampling sites. The daily NAAQS for PM₁₀ of 75 ug/m³ is exceeded at all three stations, especially during the colder months of August and September, which indicate higher daily ambient concentrations (Figure 16). Daily maximum PM₁₀ concentrations of 200 ug/m³ were recorded for both the Eskom eZamokuhle and Eskom Majuba sampling sites, whilst House 4 recorded maximum concentrations of approximately 120 ug/m³. Few exceedances were recorded for October. These elevated daily concentrations during the colder months are indicated in the calendar plots (Figure 17). These elevated concentrations could be attributed to colder ambient temperatures leading to an increase in residential fuel burning. Figure 18 highlights the average weekday PM₁₀ concentrations. The Eskom eZamokuhle and House 4 sampling sites indicate elevated concentrations on Thursdays, whilst the Eskom Majuba AQMS recorded elevated concentrations for Sundays and Mondays. All three stations recorded lower concentrations for Tuesdays compared to the other days in the week.

Figure 19 illustrates the monthly mean ambient PM₁₀ concentrations recorded at the Eskom eZamokuhle, Eskom Majuba and House 4 sampling sites. Both the Eskom eZamokuhle and Eskom Majuba illustrates a decrease in monthly concentrations from

August to October, whilst House 4 indicate an increase from August to September, and a significant decrease to October.

As mentioned previously, the bi-modal particulate matter peak for both the Eskom eZamokuhle, Majuba and House 4 sites (Figure 15) is a typical profile for residential fuel burning. These peaks are evident in Figure 20 illustrating the weekly diurnal ambient PM₁₀ concentrations. A morning peak occurs at 07:00 whilst the evening peak occurs at 18:00. The morning peaks are less prominent at the Eskom Majuba sampling site.

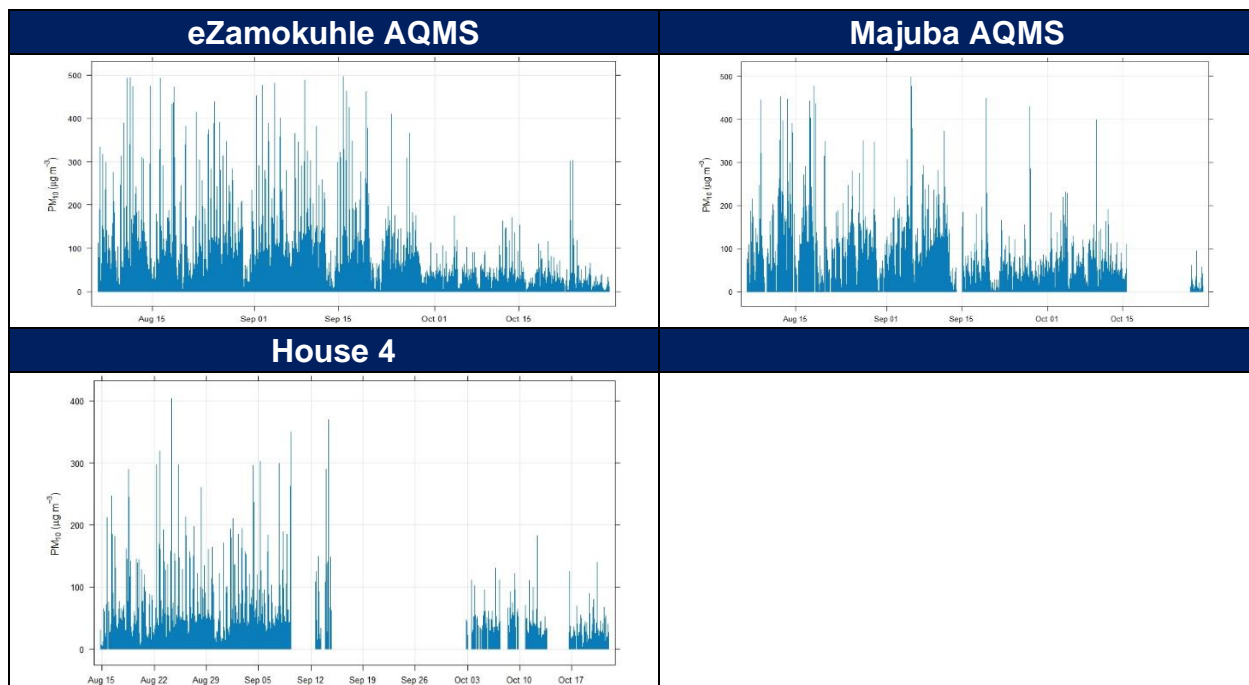


Figure 13: Hourly ambient PM₁₀ concentrations (ug/m³) measured at the sampling locations during the sampling survey.

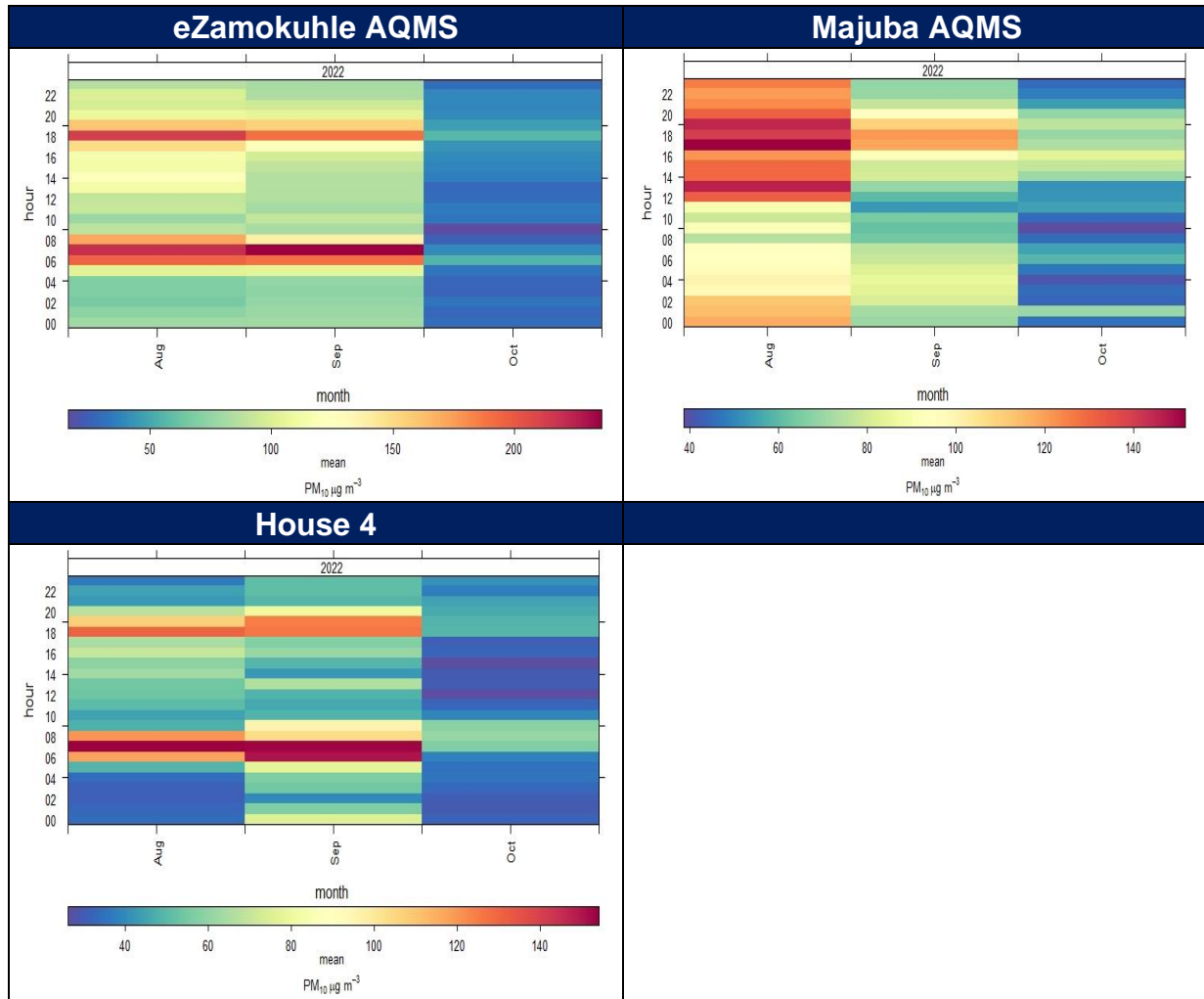


Figure 14: Mean hourly ambient PM₁₀ concentrations (ug/m³) measured at the sampling locations during the sampling survey.

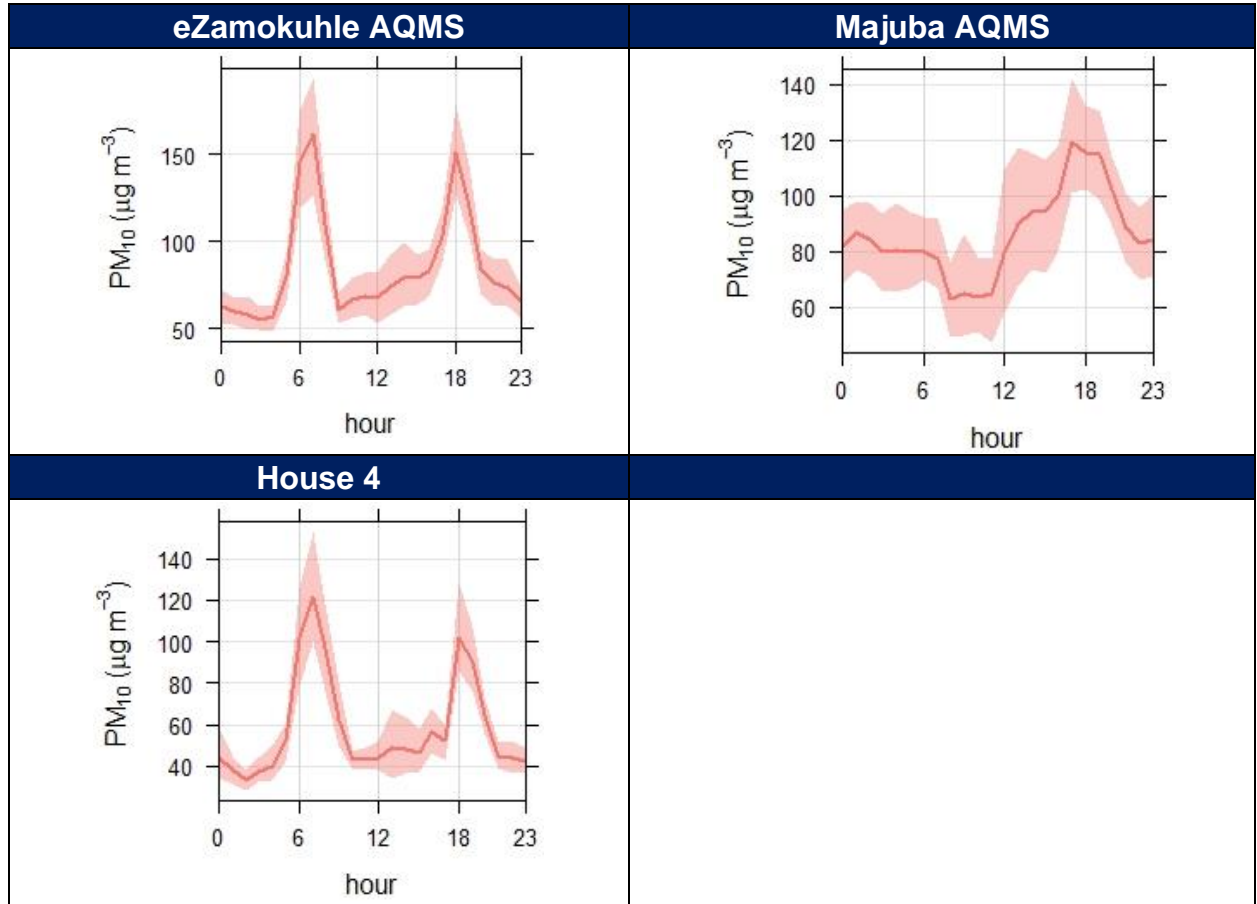


Figure 15: Mean hourly diurnal PM_{10} concentrations ($\mu g/m^3$) measured at the sampling sites during the sampling survey

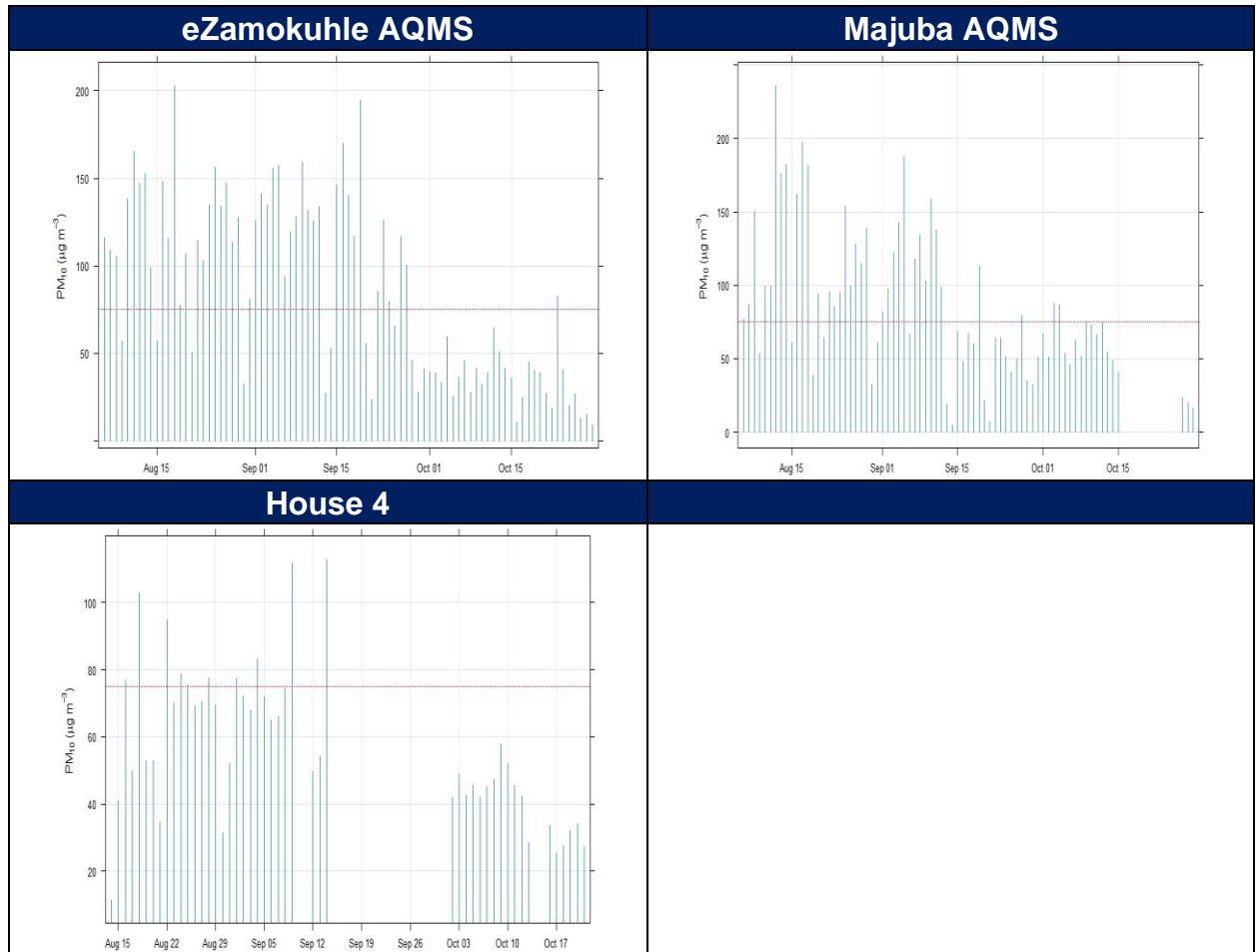


Figure 16: Daily ambient PM₁₀ concentrations ($\mu\text{g}/\text{m}^3$) measured at the sampling sites during the sampling survey

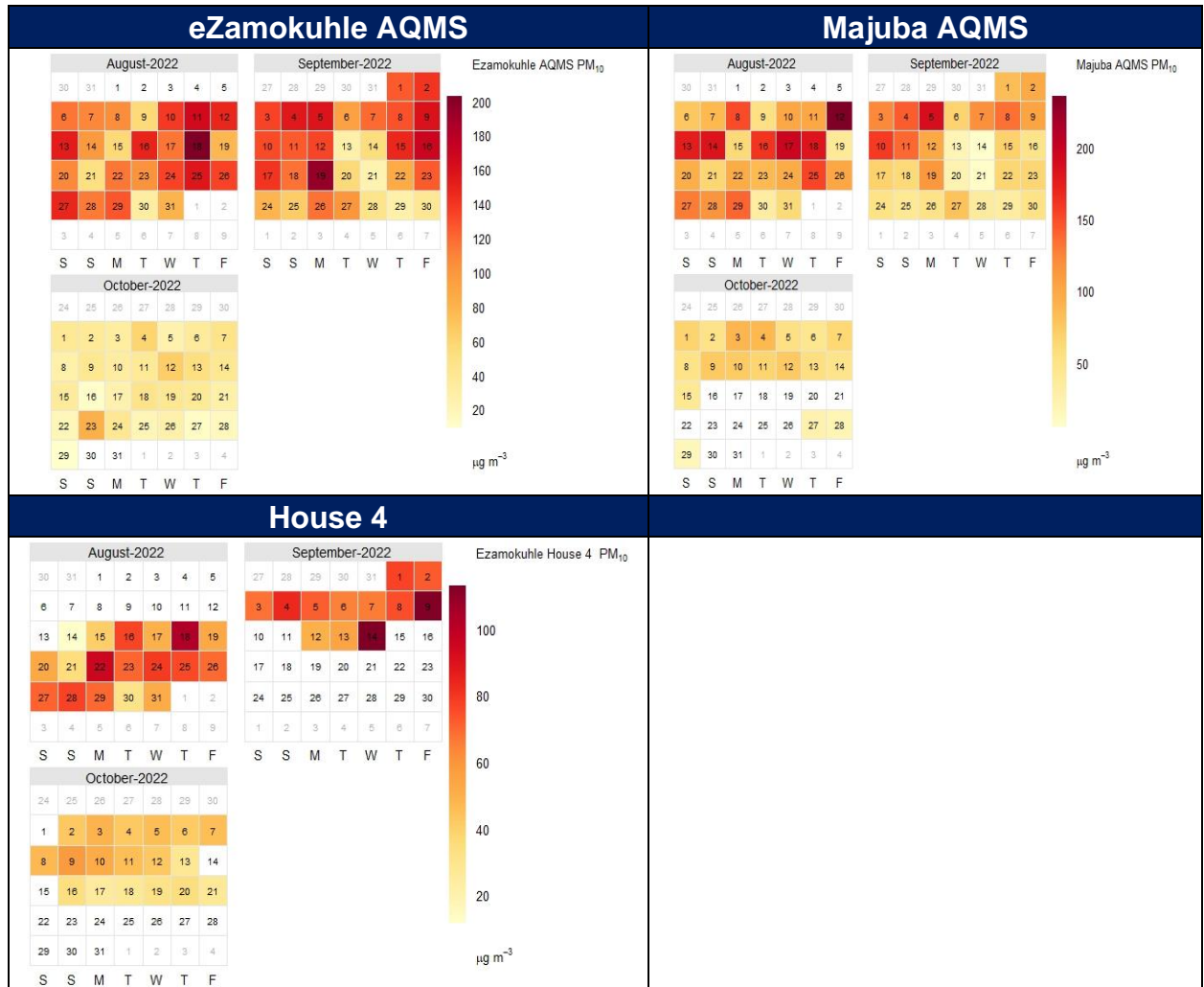


Figure 17: Daily ambient PM₁₀ concentrations (ug/m3) measured at the sampling sites during the sampling survey

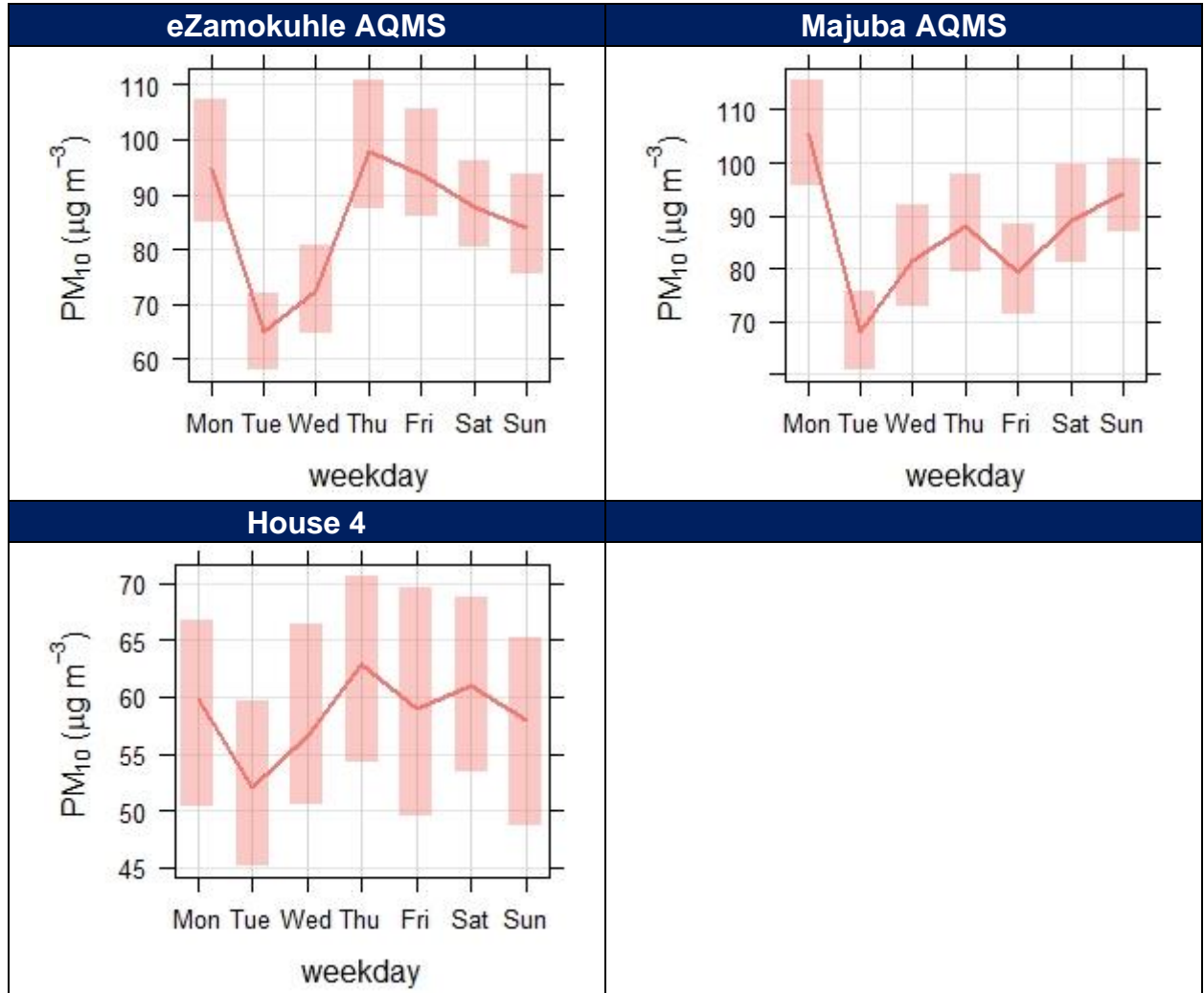


Figure 18: Average weekday ambient PM₁₀ concentrations (ug/m³) measured at sampling sites during the sampling survey

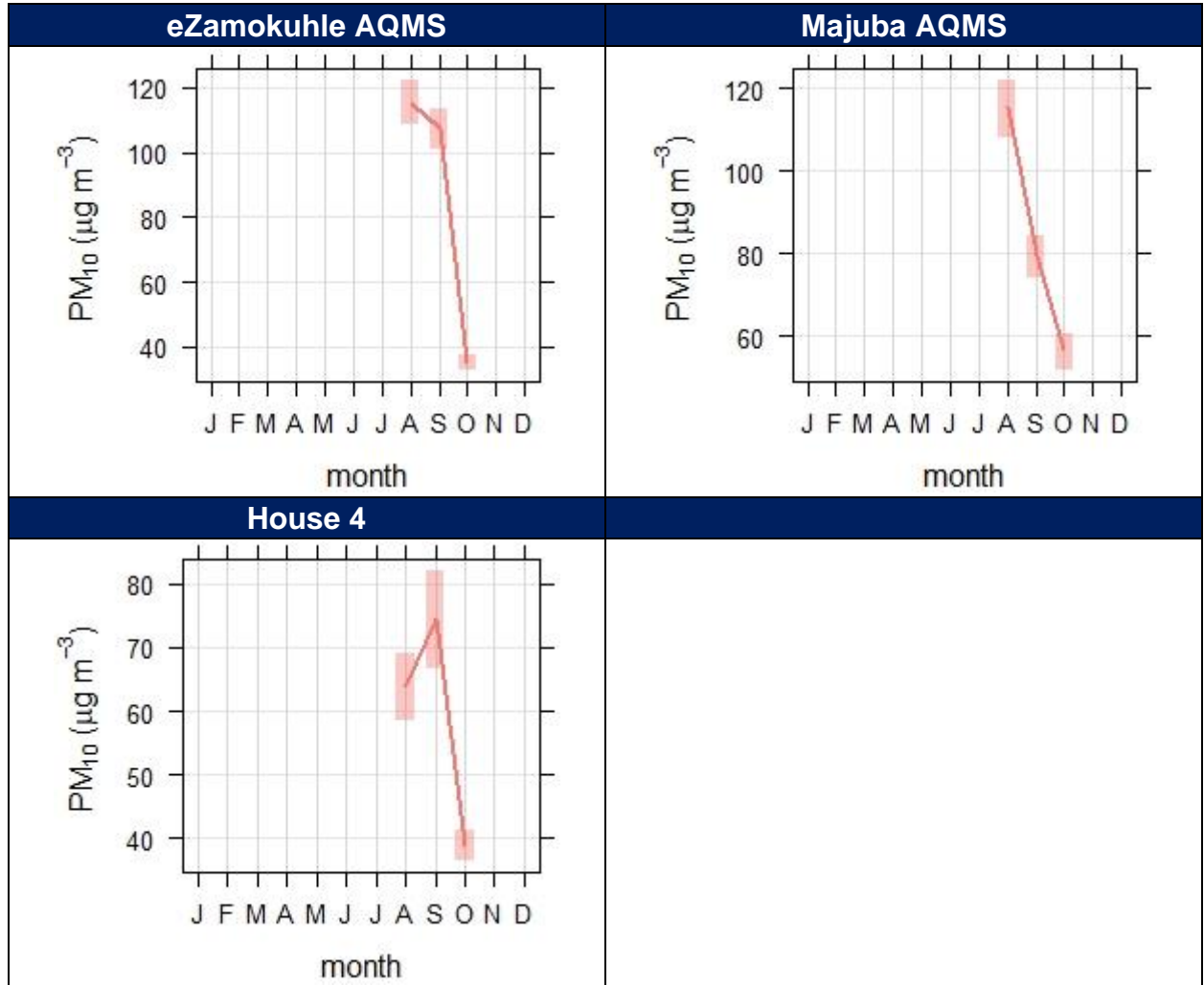


Figure 19: Monthly mean ambient **PM₁₀** concentrations (ug/m³) measured at sampling sites during the sampling survey.

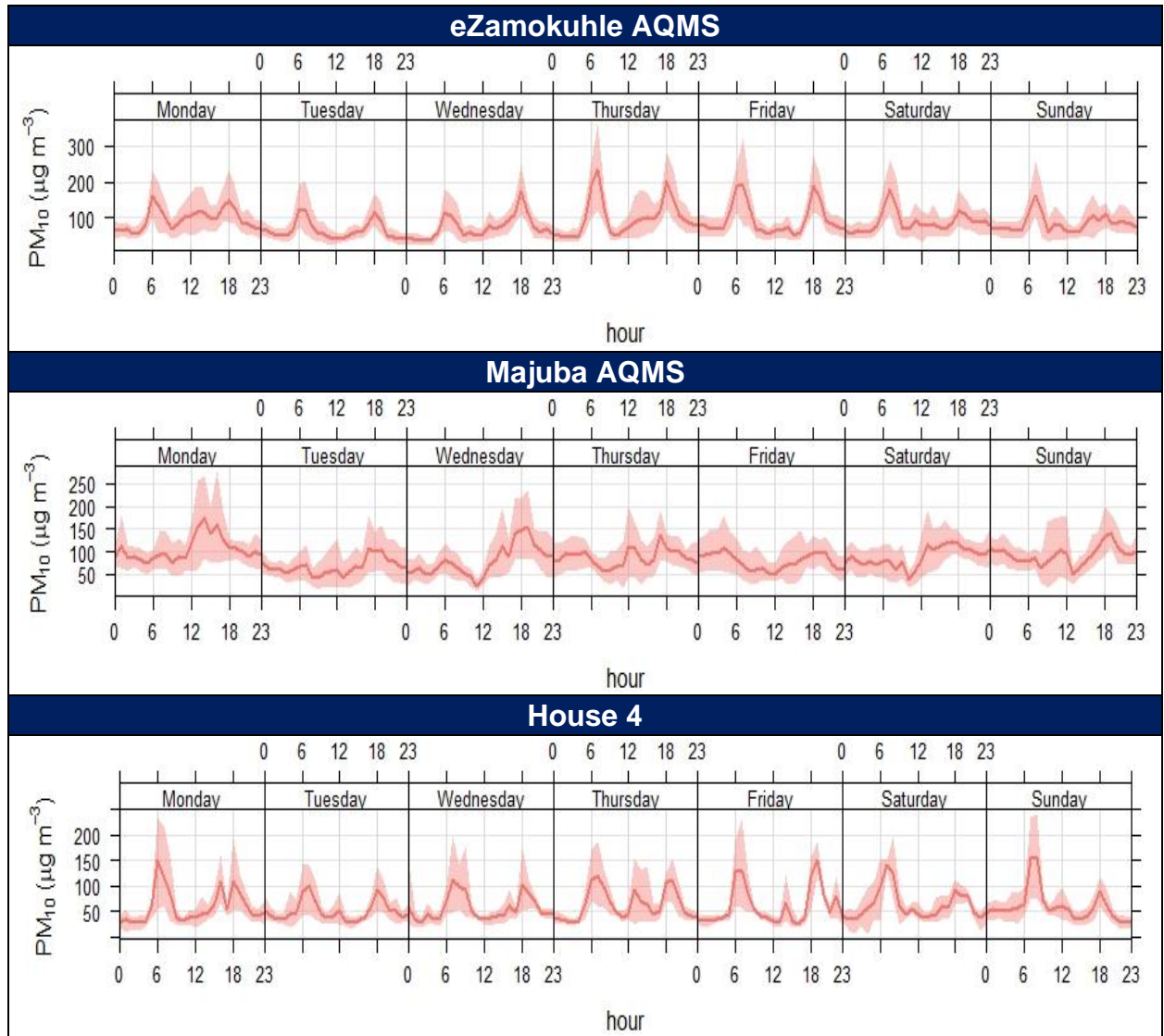


Figure 20: Weekly diurnal PM₁₀ concentrations ($\mu\text{g}/\text{m}^3$) measured at the sampling sites during the sampling survey

3.2.2 PARTICULATE MATTER (PM_{2.5})

Figure 21 indicate the ambient hourly PM_{2.5} concentrations recorded at the Eskom eZamokuhle, Eskom Majuba, House 1, and House 5 sampling sites. Although no NAAQS exist for hourly PM_{2.5} concentrations, Figure 21 highlight that for both the eZamokuhle and Majuba sites maximum hourly concentrations of 250 ug/m³ were recorded, whilst House 1 and House 5 indicate maximum concentrations of 500ug/m³. Figure 22 is a graphical representation of the mean hourly PM_{2.5} concentrations for the sampling period. It is evident from Figure 22 that the highest average values are recorded during hours 06:00 to 08:00 for both the eZamokuhle, House 1 and House 5 sites, but all four sites indicate elevated hourly values from 17:00 to 19:00. These diurnal profiles are also illustrated in Figure 23. The bi-modal particulate matter peak for both the Eskom eZamokuhle, Majuba, House 1 and House 5 sites (Figure 23) is a typical profile for residential fuel burning. A morning peak occurs at 07:00 whilst the evening peak occurs at 18:00. The morning peaks reduces towards midday as the inversion layer rises & improves the mixing height of the planetary boundary layer. As with the PM₁₀ concentrations, the morning peak is less prevalent at the Eskom Majuba station.

Figure 24 indicate the daily ambient PM_{2.5} concentrations recorded at the Eskom eZamokuhle, Eskom Majuba, House 1, and House 5 sampling sites respectively. The daily NAAQS for PM_{2.5} of 40 ug/m³ is exceeded at all four stations, although only once at the Eskom eZamokuhle site. The Eskom Majuba, House 1, and House 5 sampling sites recorded multiple exceedances of the daily NAAQS for PM_{2.5} for the sampling period. These elevated daily concentrations are indicated in the calendar plots (Figure 25). These elevated concentrations could be attributed to colder ambient temperatures leading to an increase in residential fuel burning.

Figure 26 highlights the mean weekday ambient PM_{2.5} concentrations. The Eskom eZamokuhle, House 1 and House 4 sampling sites indicate elevated concentrations on

Thursdays, whilst the Eskom Majuba AQMS recorded elevated concentrations for Sundays and Mondays.

Figure 27 illustrates the mean monthly ambient PM_{2.5} concentrations recorded at the Eskom eZamokuhle, Eskom Majuba, House 1, and House 5 sampling sites. The Eskom Majuba, House 1, and House 5 illustrates a decrease in monthly concentrations from August to October, whilst the Eskom eZamokuhle station indicate an increase from August to September, and a significant decrease to October.

As mentioned previously, the bi-modal particulate matter peak for both the Eskom eZamokuhle, Majuba and House 4 sites (Figure 23) is a typical profile for residential fuel burning. These peaks are evident in Figure 28 illustrating the weekly diurnal ambient PM_{2.5} concentrations. A morning peak occurs at 07:00 whilst the evening peak occurs at 18:00. These peaks are less prominent at the Eskom Majuba sampling site.

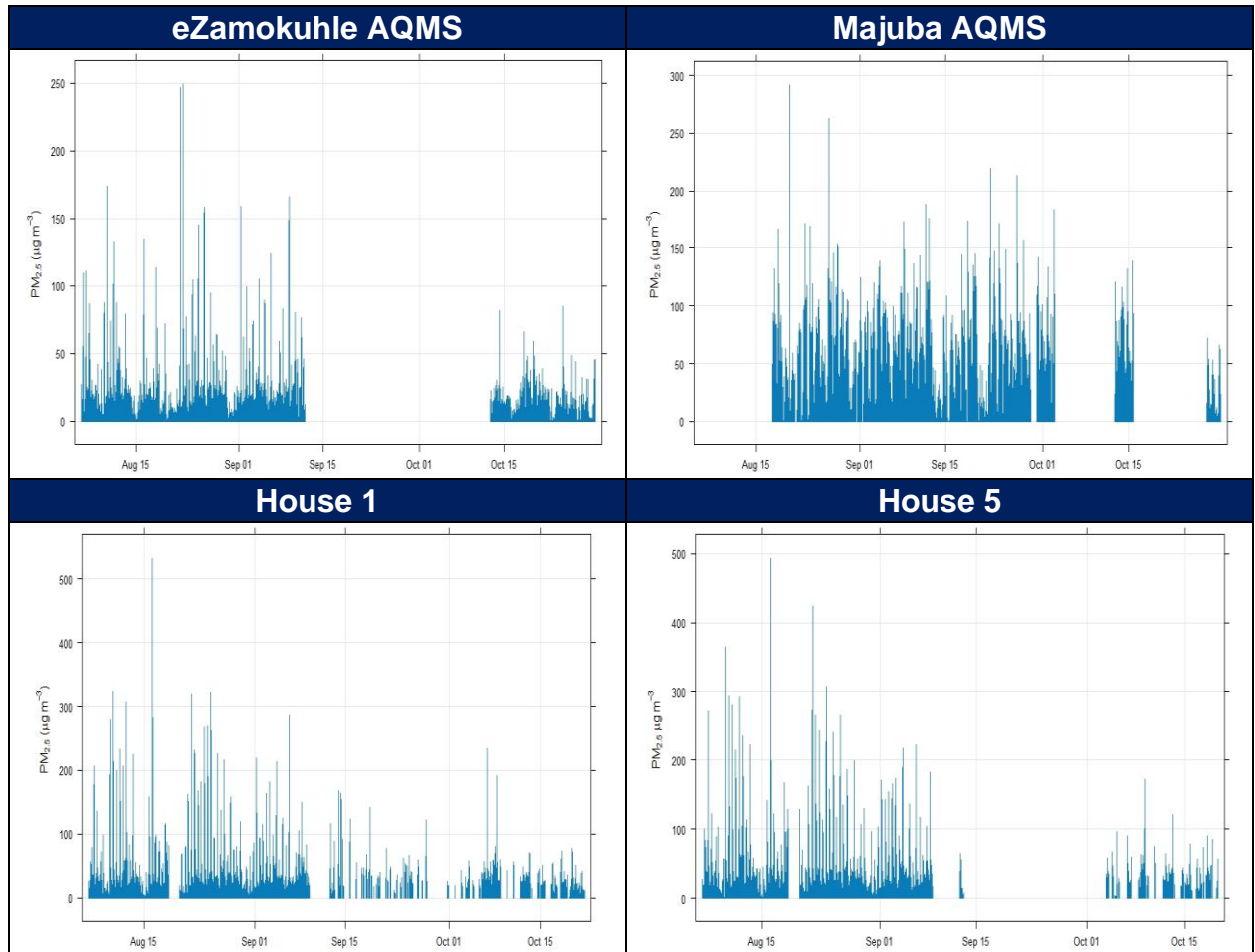


Figure 21: Hourly ambient $PM_{2.5}$ concentrations ($\mu g/m^3$) measured at the sampling sites during the sampling survey

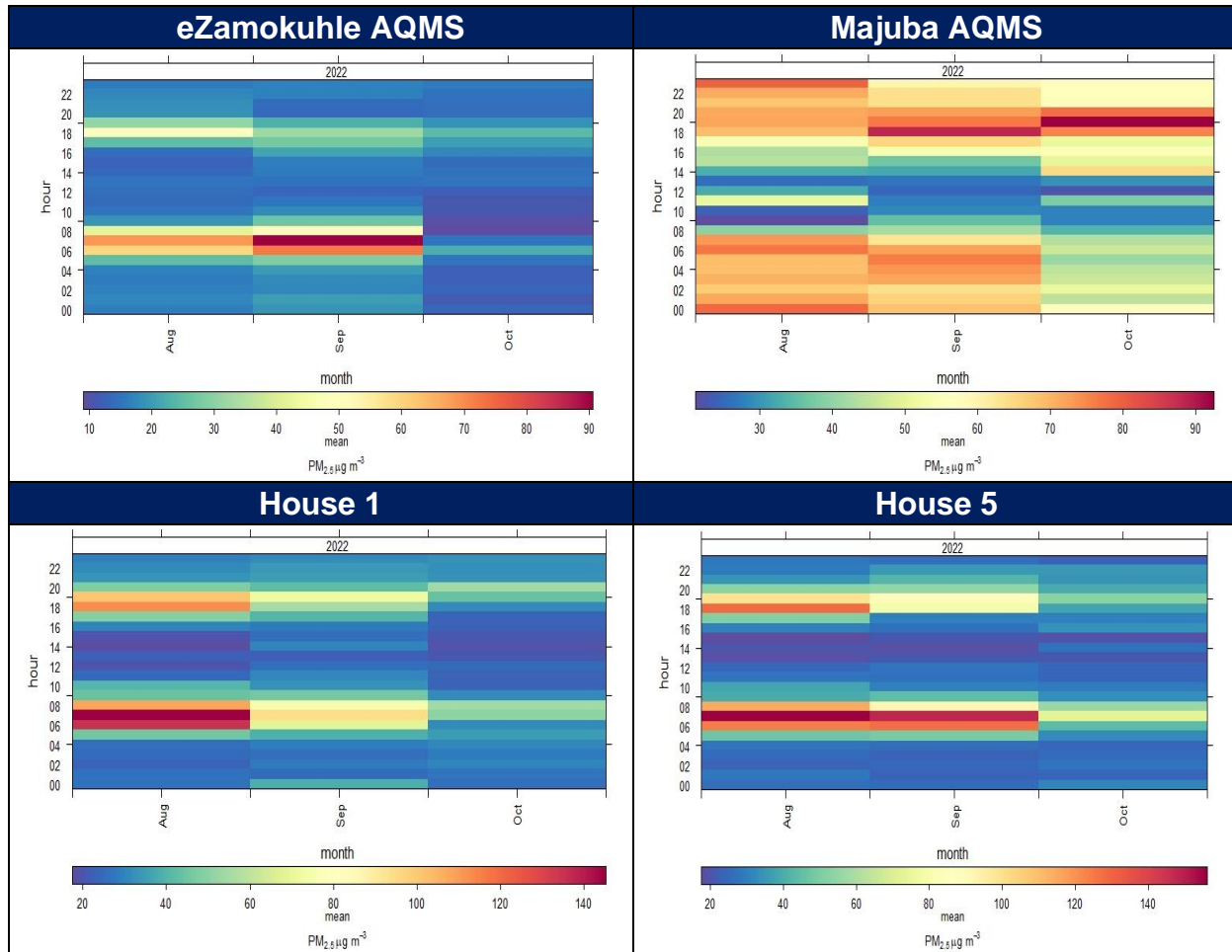


Figure 22: Mean hourly ambient PM_{2.5} concentrations ($\mu\text{g m}^{-3}$) measured at the sampling sites during the sampling survey.

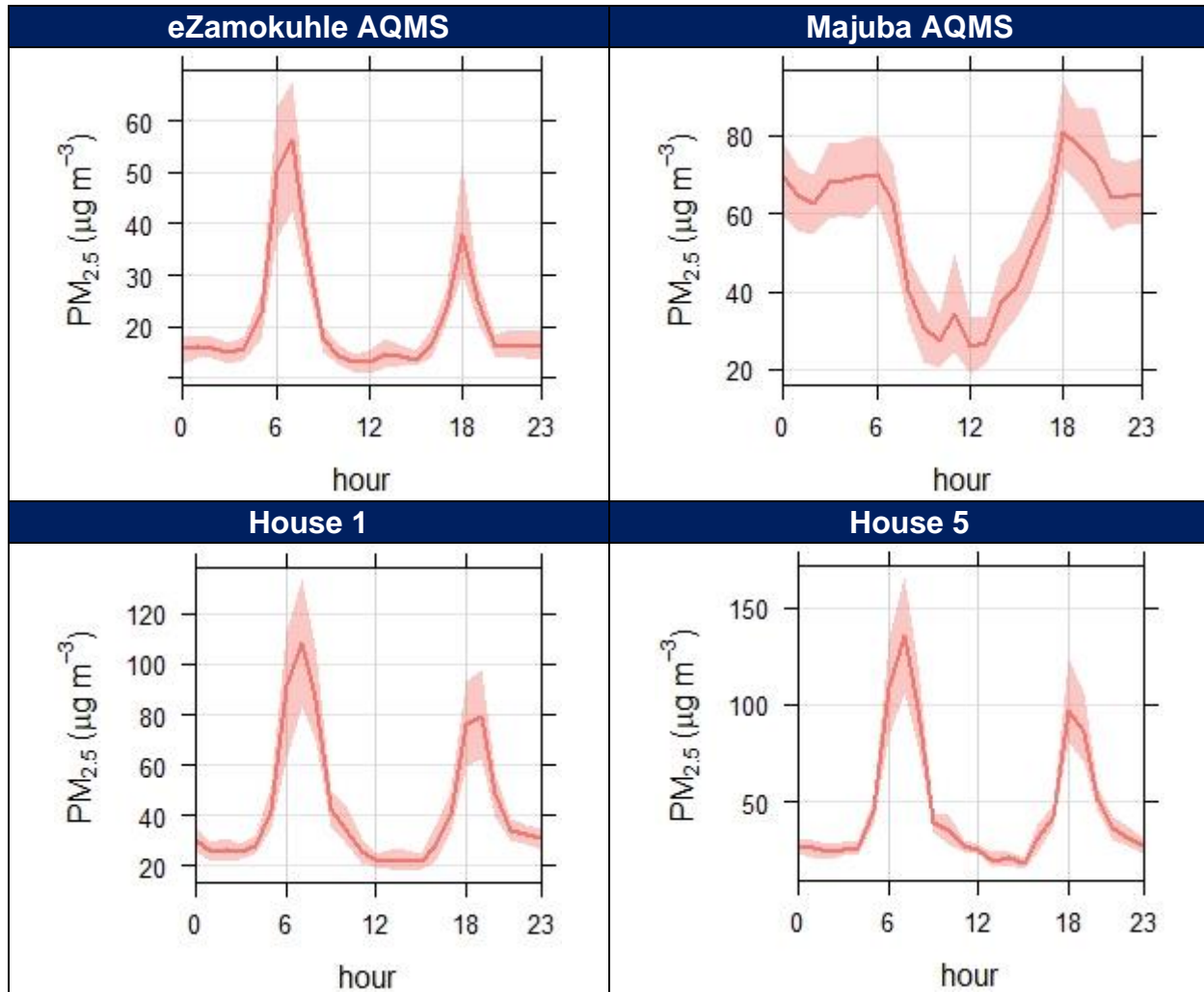


Figure 23: Hourly diurnal PM_{2.5} concentrations ($\mu\text{g/m}^3$) measured at the sampling sites during the sampling survey.

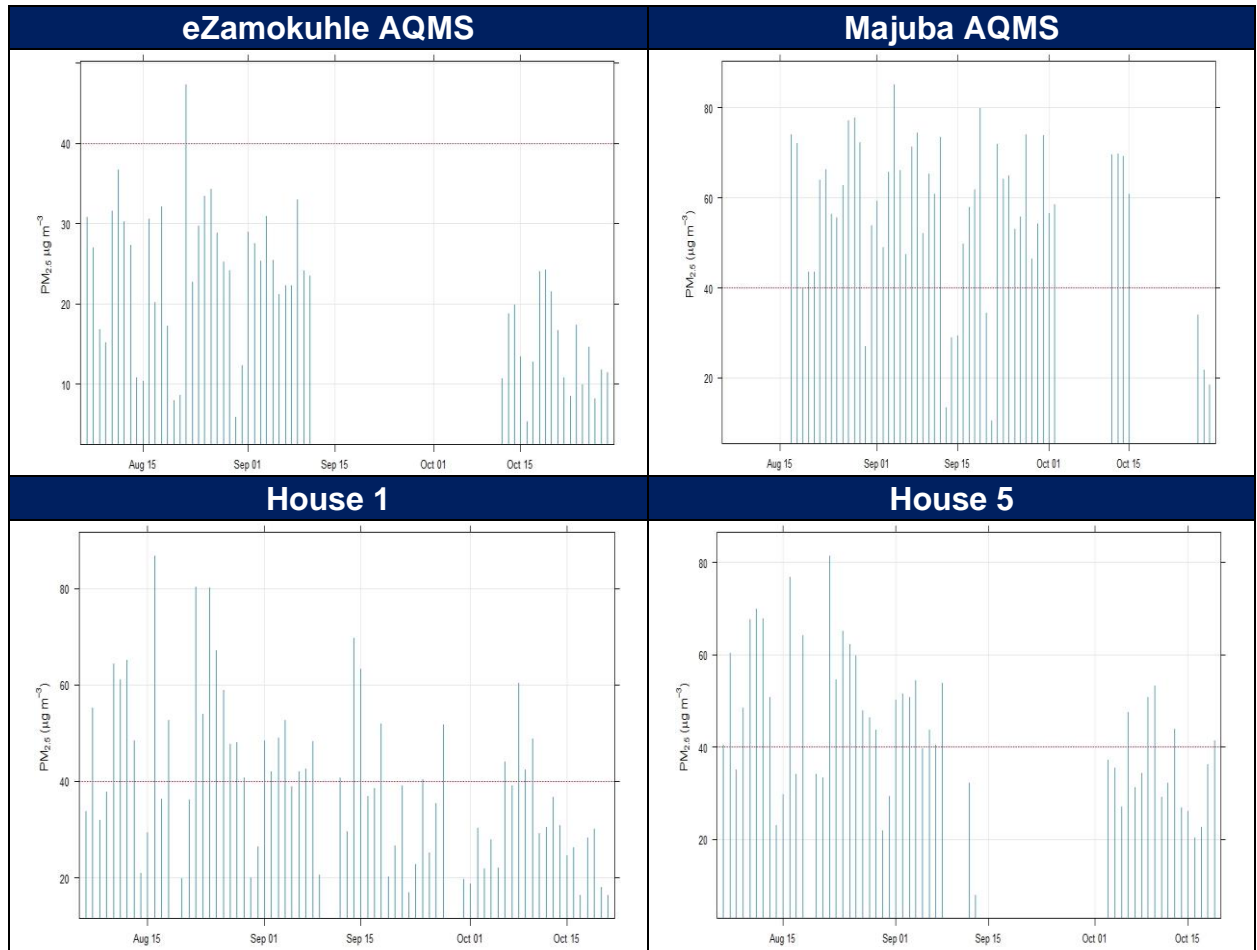


Figure 24: Daily ambient PM_{2.5} concentrations ($\mu\text{g m}^{-3}$) measured at the sampling sites during the sampling survey

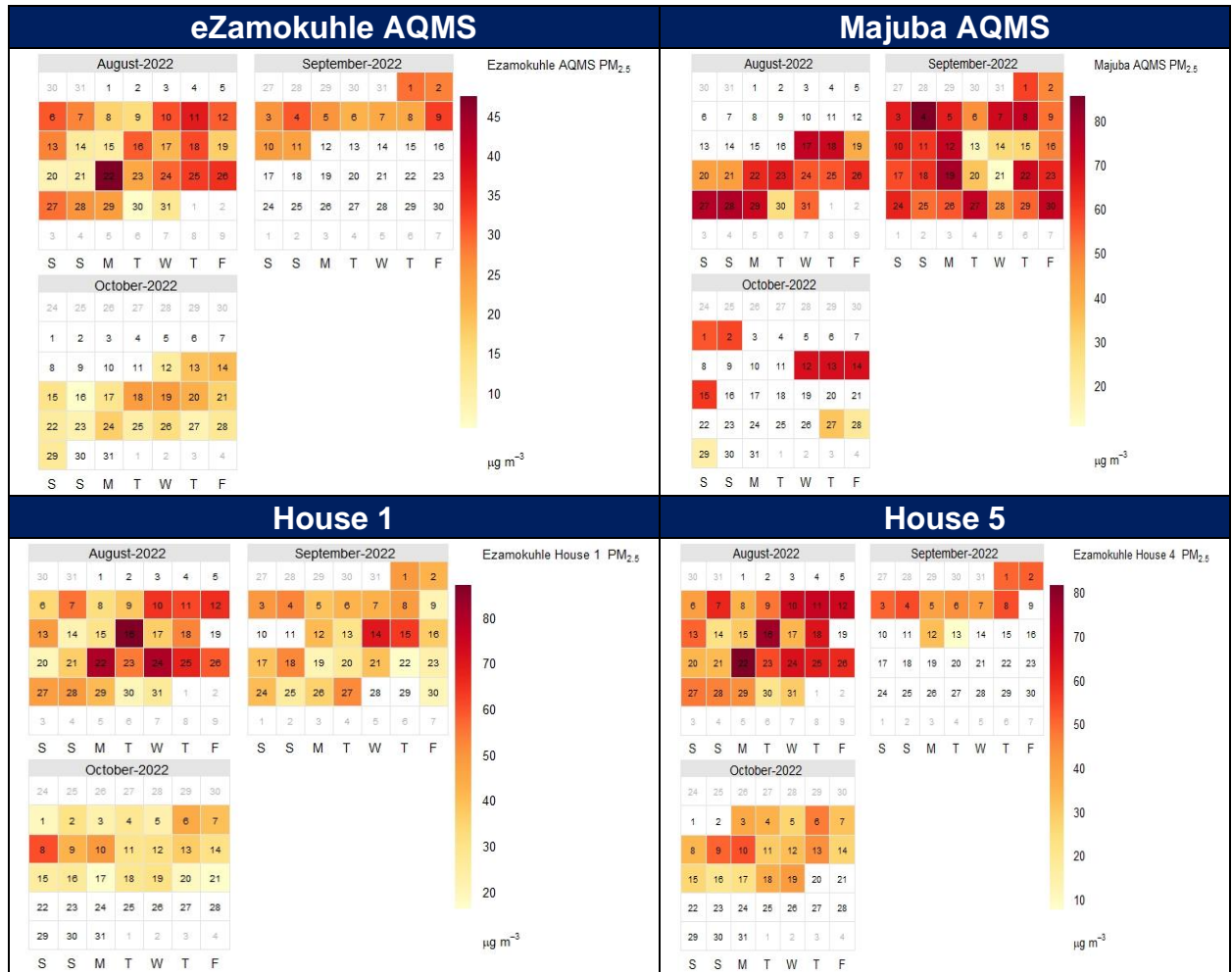


Figure 25: Daily ambient PM_{2.5} concentrations ($\mu\text{g}/\text{m}^3$) measured at the sampling sites during the sampling survey

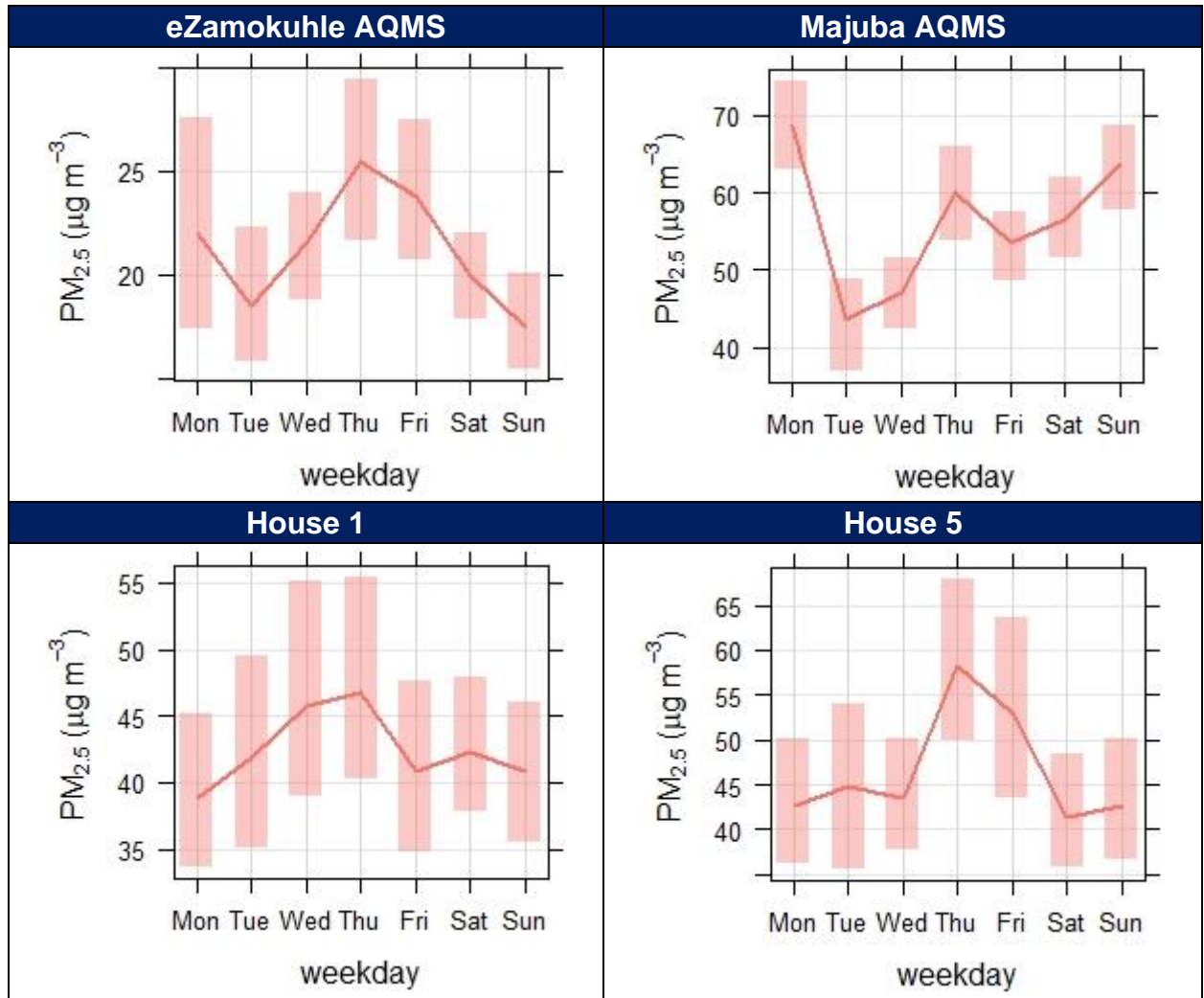


Figure 26: Weekday ambient PM_{2.5} concentrations ($\mu\text{g m}^{-3}$) measured at the sampling sites during the sampling survey

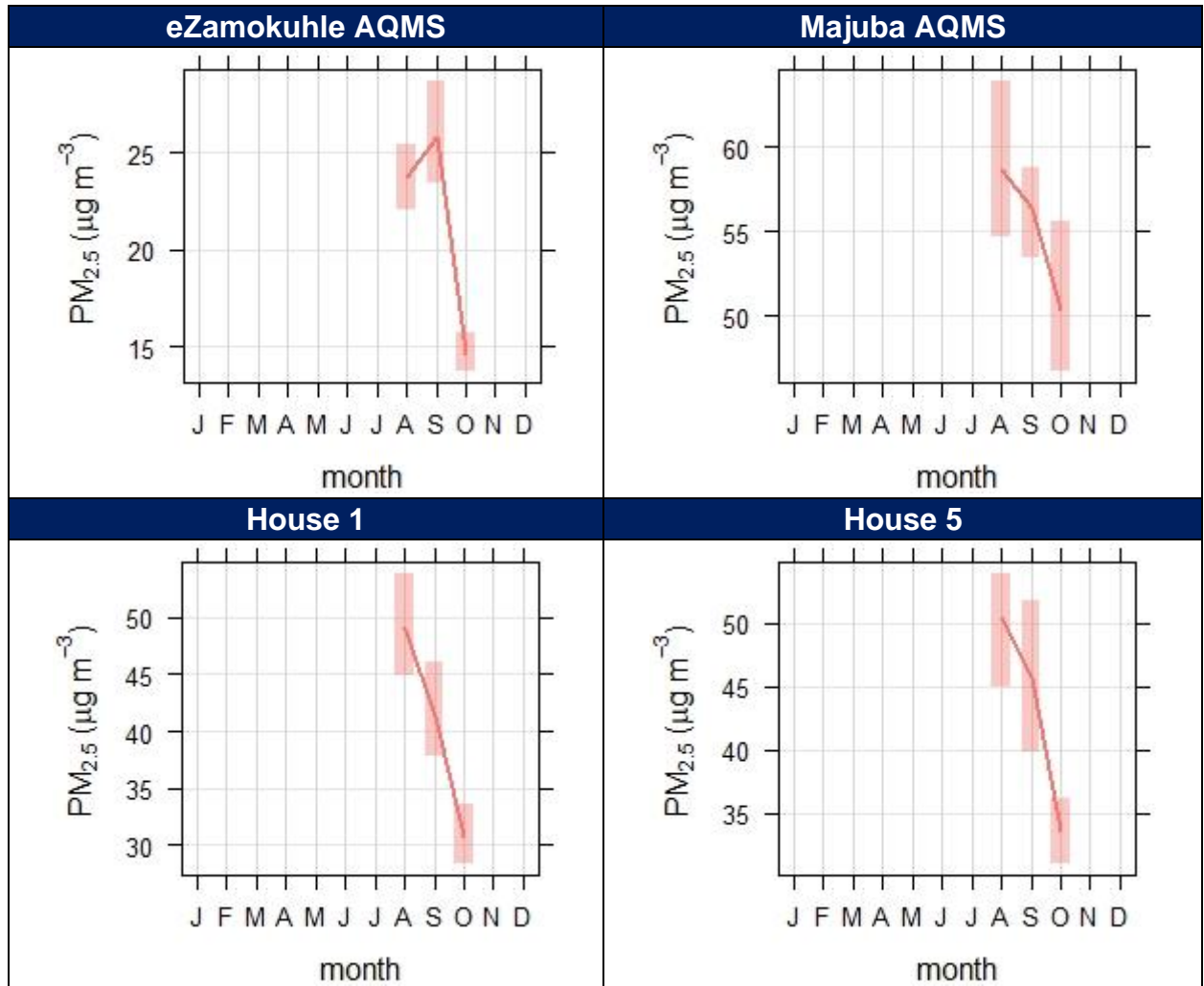


Figure 27: Mean monthly ambient $PM_{2.5}$ concentrations ($\mu g/m^3$) measured at sampling sites during the sampling survey.

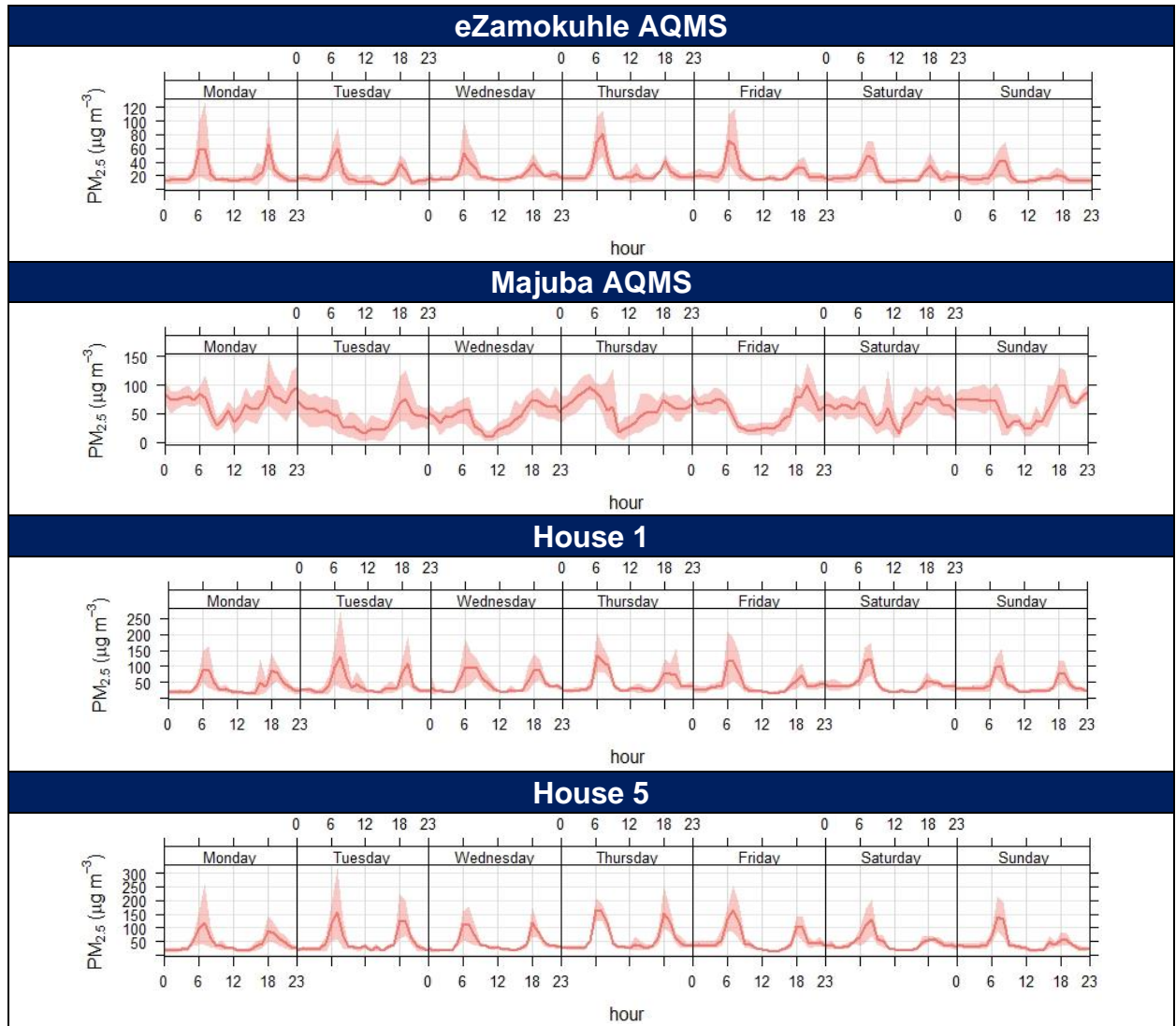


Figure 28: Weekly diurnal PM_{2.5} concentrations ($\mu\text{g/m}^3$) measured at sampling sites during the sampling survey.

3.2.3 SULPHUR DIOXIDE (SO₂)

Figure 29 indicate the hourly ambient SO₂ concentrations recorded at the Eskom eZamokuhle and Eskom Majuba AQMS. The NAAQS for hourly SO₂ concentrations is 134ppb. No exceedances of the hourly NAAQS were recorded for an hourly time average for both stations. Figure 29 highlight maximum hourly SO₂ concentrations of 80ppb at the Eskom eZamokuhle station, whilst maximum concentrations of above 150ppb were recorded for the Eskom Majuba AQMS.

Figure 30 is a graphical representation of the mean hourly SO₂ concentrations for the sampling period. It is evident from Figure 3 that the highest mean concentrations were recorded during hours 10:00 to 14:00 and 18:00 for both stations, although the 18:00 peak is less prevalent at the Eskom Majuba station. These diurnal profiles are also illustrated in Figure 31. Figure 31 indicates a typically industrial signature with increased SO₂ concentrations as just before midday due to the break-up of an elevated inversion layer, in addition to the development of daytime convective conditions causing the plume to be brought down to ground level relatively close to the point of release from tall stacks. The 18:00 peak recorded for the Eskom eZamokuhle station is indicative of the impact of residential fuel burning emissions.

Figure 32 indicate the daily ambient SO₂ concentrations recorded at the Eskom eZamokuhle and Eskom Majuba AQMS. No exceedances of the daily NAAQS for SO₂ were recorded for both stations during the sampling period. Daily maximum SO₂ concentrations of above 20ppb were recorded for both stations. Figure 32 also indicate lower daily SO₂ concentrations during October for the Eskom eZamokuhle station compared to the Eskom Majuba station. These lower daily concentration in October could be related to lower domestic fuel burning practices that have a direct impact on the Eskom eZamokuhle station. These daily concentrations are indicated in calendar plots (Figure 33). Both stations indicate lower concentrations for October, compared to August and

September, and could be attributed to colder ambient temperatures leading to an increase in residential fuel burning.

Figure 34 highlights the mean weekday and mean monthly ambient SO₂ concentrations. The Eskom eZamokuhle station as well as the Eskom Majuba station indicate higher recorded ambient concentrations on a Thursday. Both stations also illustrate a decrease in monthly concentrations from August to September, but a slight elevation in October were recorded for the Eskom Majuba station.

Figure 35 is indicative of the mean weekly SO₂ concentrations. It is evident for the Eskom eZamokuhle station (Figure 28) a second less pronounced peak compared to midday, that occurs consistently throughout the entire week at 18:00. A comparison of the trend level plot for eZamokuhle (Figure 30) clearly indicates that the 18:00 peak occurs in winter (August) thus indicating the impact of residential fuel burning emissions. The evening (18:00) peak is less prominent at the Eskom Majuba sampling site.

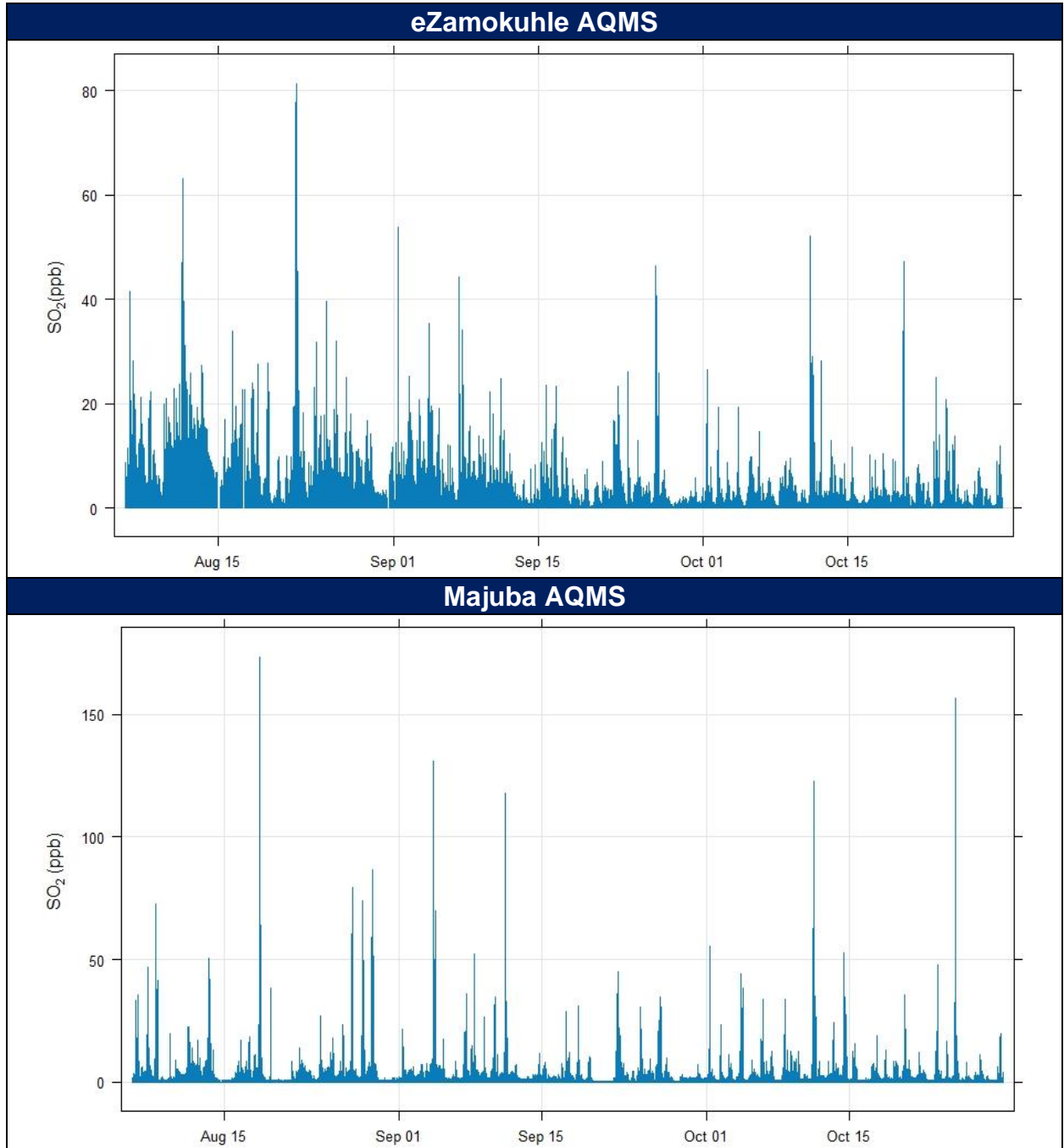


Figure 29: Hourly ambient SO₂ concentrations (ppb) measured at the Eskom eZamokuhle and Eskom Majuba AQMS during the sampling survey (Hourly SO₂ NAAQS = 134ppb)

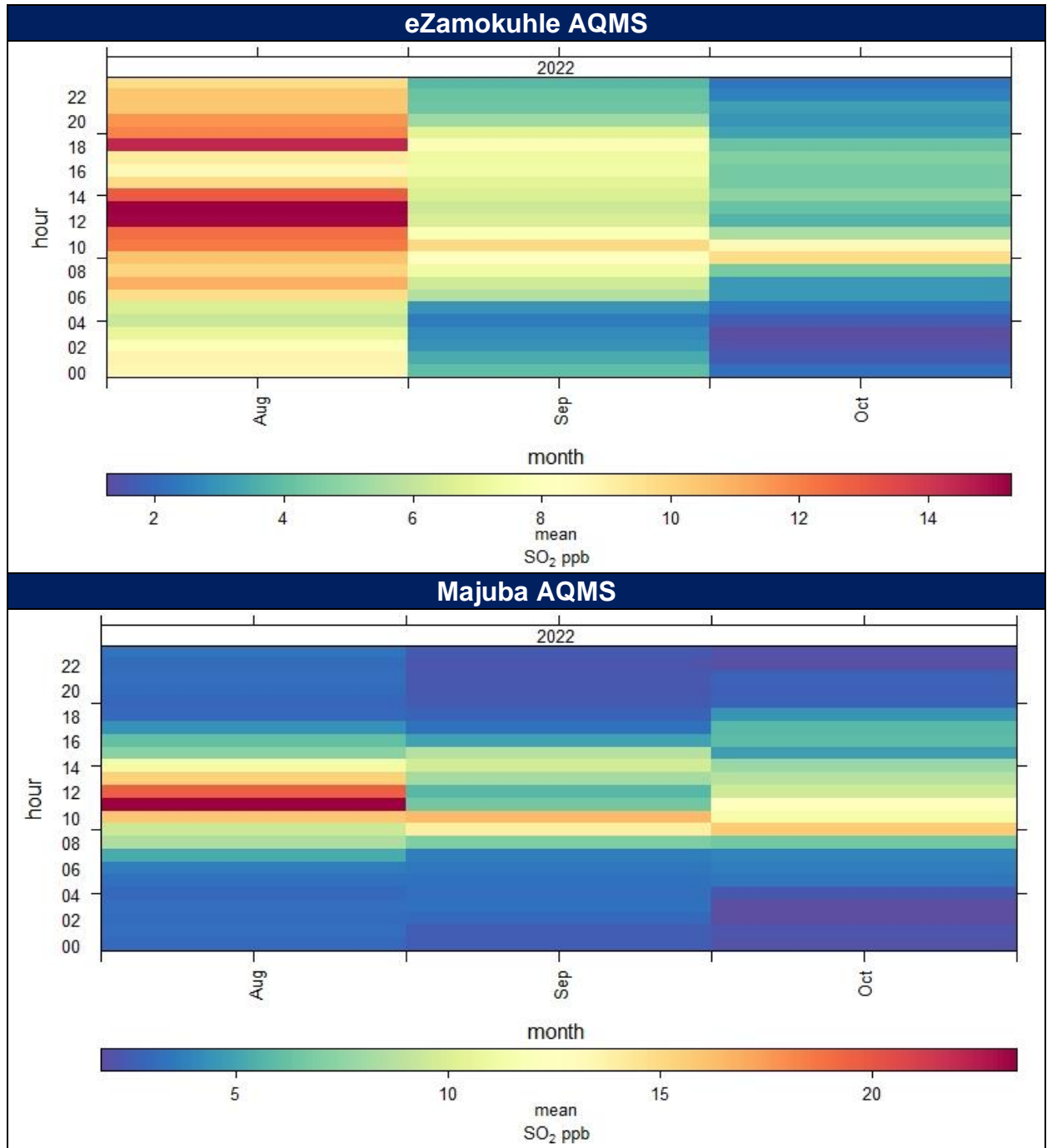


Figure 30: Hourly mean ambient SO₂ concentrations (ppb) measured at the Eskom eZamokuhle and Eskom Majuba AQMS during the sampling survey (Hourly SO₂ NAAQS = 134ppb)

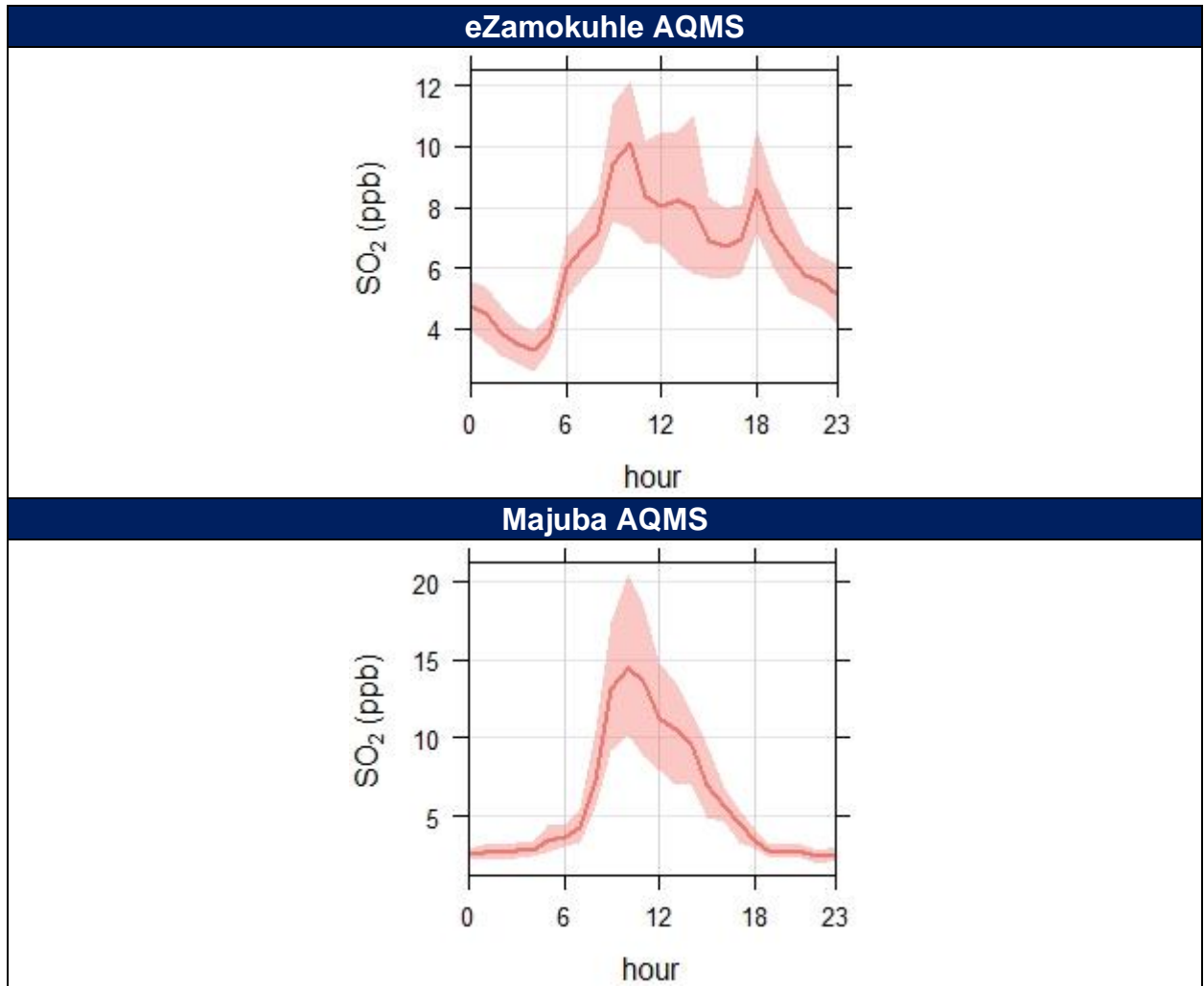


Figure 31: Mean hourly diurnal ambient SO₂ concentrations (ppb) measured at sampling sites during the sampling survey

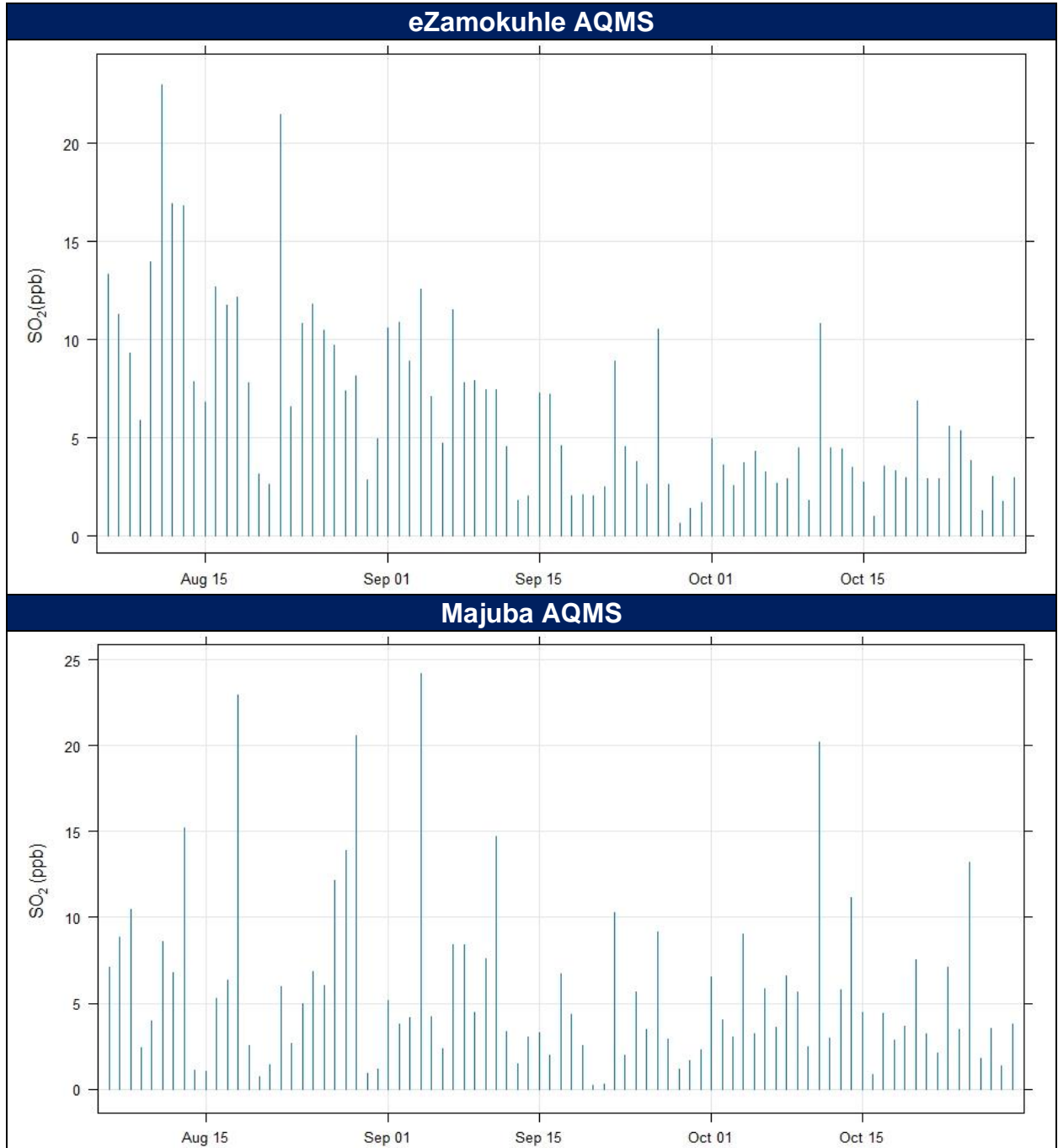


Figure 32: Daily ambient SO₂ concentrations (ppb) measured at the Eskom eZamokuhle and Eskom Majuba AQMS during the sampling survey (Hourly SO₂ NAAQS = 48ppb)

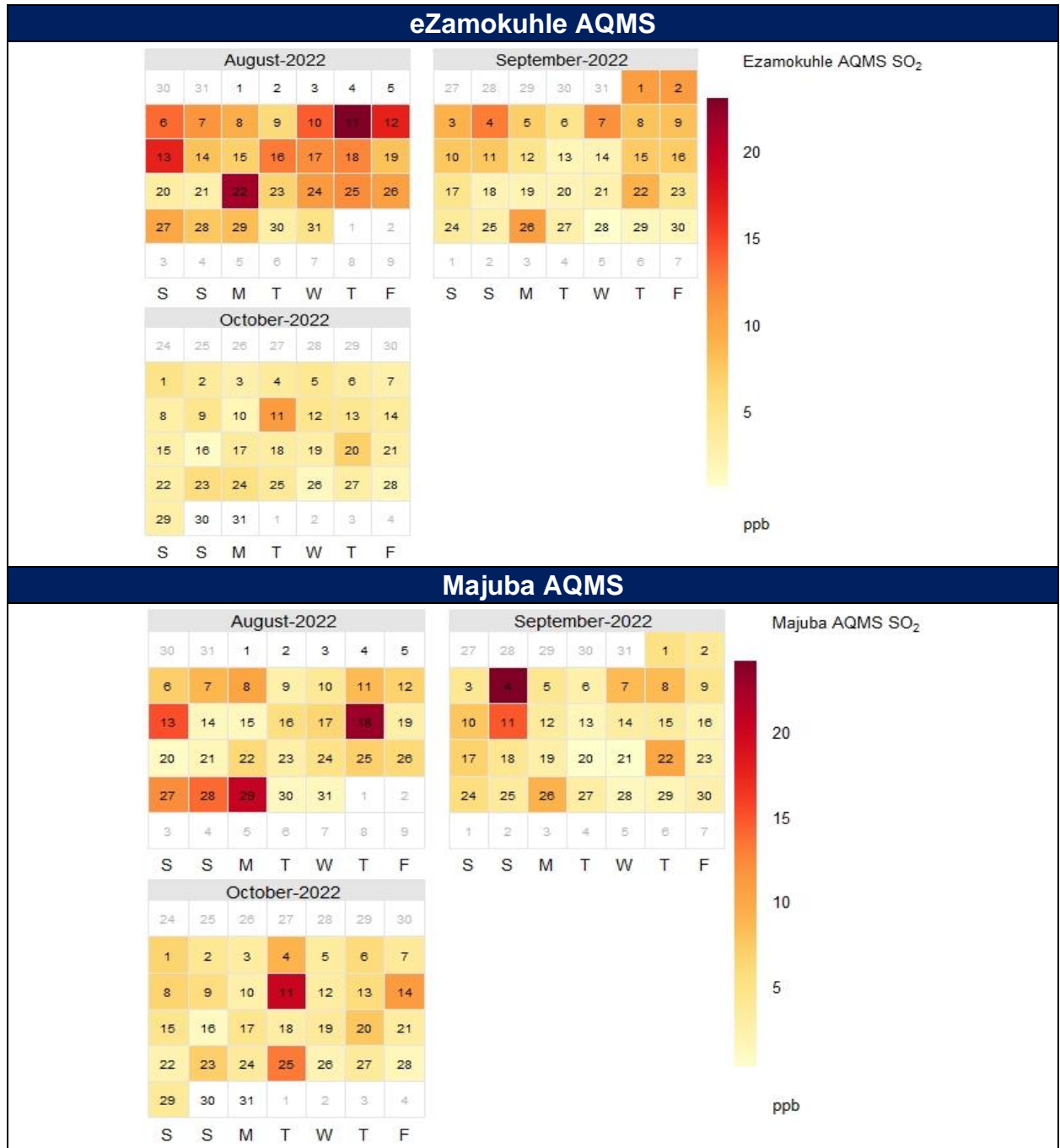


Figure 33: Daily ambient SO₂ concentrations (ppb) measured at the Eskom eZamokuhle and Eskom Majuba AQMS during the sampling survey (Hourly SO₂ NAAQS = 48ppb).

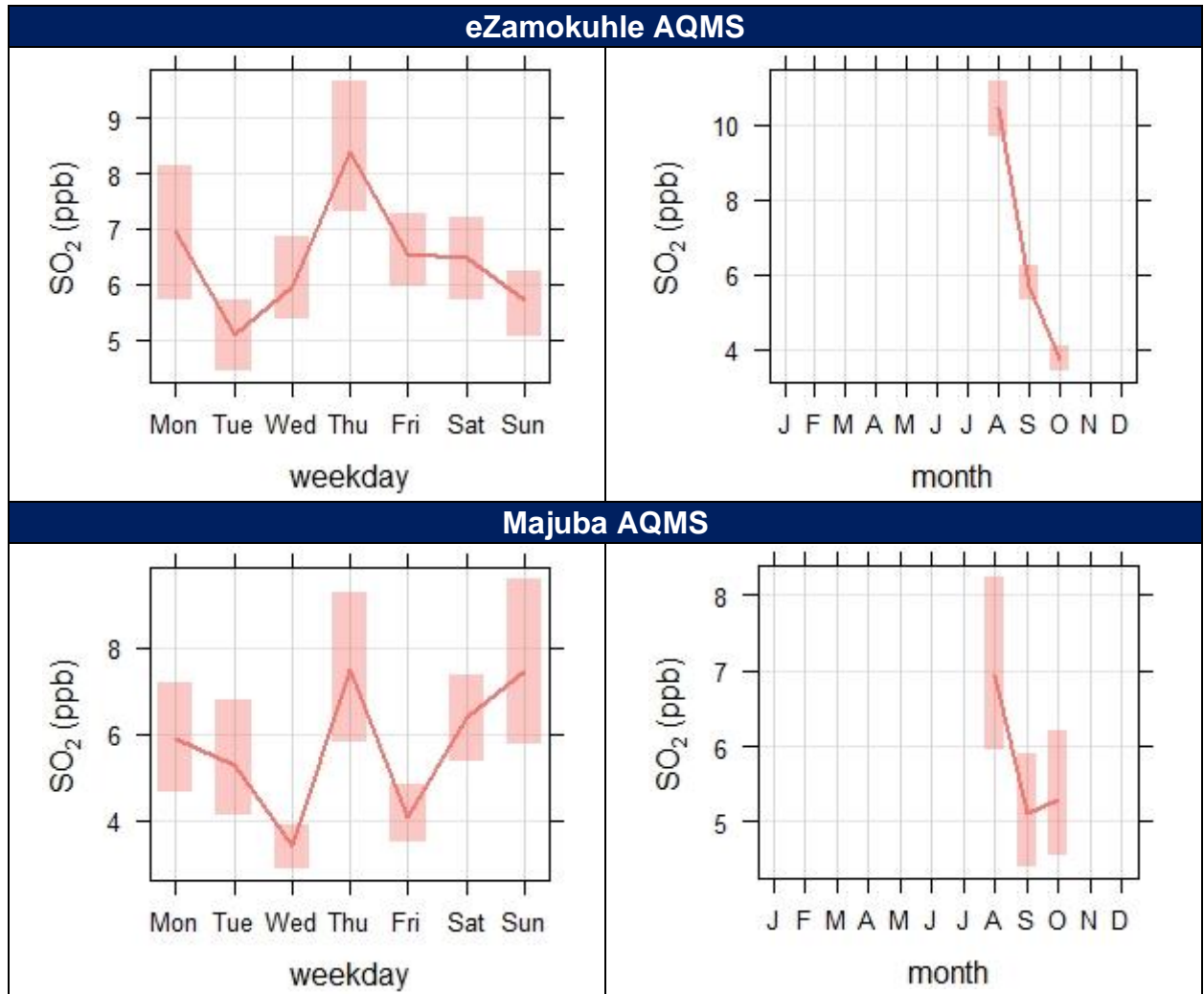


Figure 34: Mean weekday and mean monthly ambient SO₂ concentrations (ppb) measured at sampling sites during the sampling survey

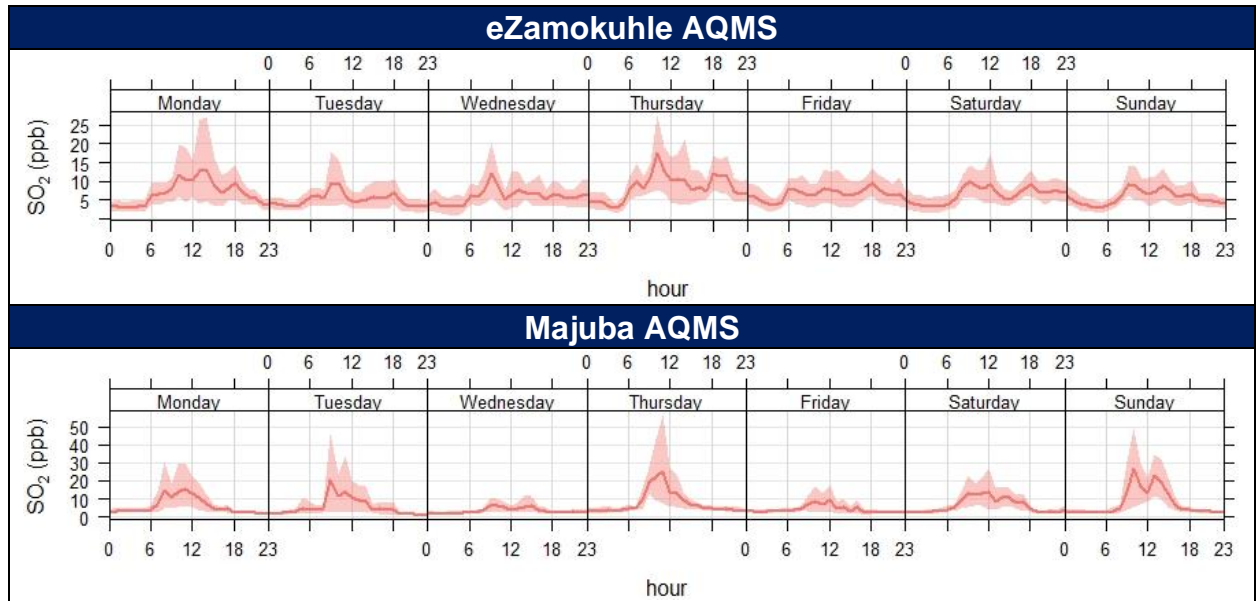


Figure 35: Weekly diurnal SO₂ concentrations (ppb) measured at sampling sites during the sampling survey

3.2.4 NITROGEN DIOXIDE (NO₂)

Figure 36 indicate the hourly ambient NO₂ concentrations recorded at the Eskom eZamokuhle and Eskom Majuba AQMS. The NAAQS for hourly NO₂ concentrations is 106ppb. No exceedances of the hourly NAAQS were recorded for an hourly time average for both stations. Figure 36 highlight maximum hourly NO₂ concentrations of approximately 25ppb at the Eskom eZamokuhle station, whilst maximum concentrations of 40ppb were recorded for the Eskom Majuba AQMS.

Figure 37 is a graphical representation of the mean hourly NO₂ concentrations for the sampling period. It is evident from Figure 30 that the highest mean concentrations were recorded during hours 06:00 to 08:00 and 16:00 to 18:00 for the Eskom eZamokuhle station, whilst elevated concentrations were recorded at 10:00 to 12:00 for the Eskom Majuba station. These diurnal profiles are also illustrated in Figure 38. The Eskom eZamokuhle signature in Figure 38 explicitly reveal that the variability of this pollutant concentration is conditioned by vehicle emissions. The diurnal cycle corresponds to the cyclical nature of traffic volume with marked peaks in concentration on weekdays around the early-morning and late-afternoon rush-hours. For the Eskom Majuba station (Figure 38), there is an increased NO₂ concentrations at just before midday due to the break-up of an elevated inversion layer, in addition to the development of daytime convective conditions causing the plume to be brought down to ground level relatively close to the point of release from tall stacks.

Figure 39 indicate the daily ambient NO₂ concentrations recorded at the Eskom eZamokuhle and Eskom Majuba AQMS. No daily NAAQS for NO₂ exists. Daily maximum NO₂ concentrations of approximately 10ppb were recorded for both stations. These daily mean NO₂ concentrations are graphically presented in Figure 40.

Figure 40 highlights the mean weekday and mean monthly ambient NO₂ concentrations. Both stations indicate higher recorded ambient concentrations on a Thursday, as well as a decrease in monthly concentrations from August to October.

Figure 41 is indicative of the mean weekly NO₂ concentrations. It is evident for the Eskom eZamokuhle station that the weekly diurnal cycle corresponds to the cyclical nature of traffic volume with marked peaks in concentration on weekdays around the early-morning and late-afternoon rush-hours. For the Eskom Majuba station (Figure 41), there is an increased NO₂ concentrations at just before midday due to the break-up of an elevated inversion layer, in addition to the development of daytime convective conditions causing the plume to be brought down to ground level relatively close to the point of release from tall stacks.

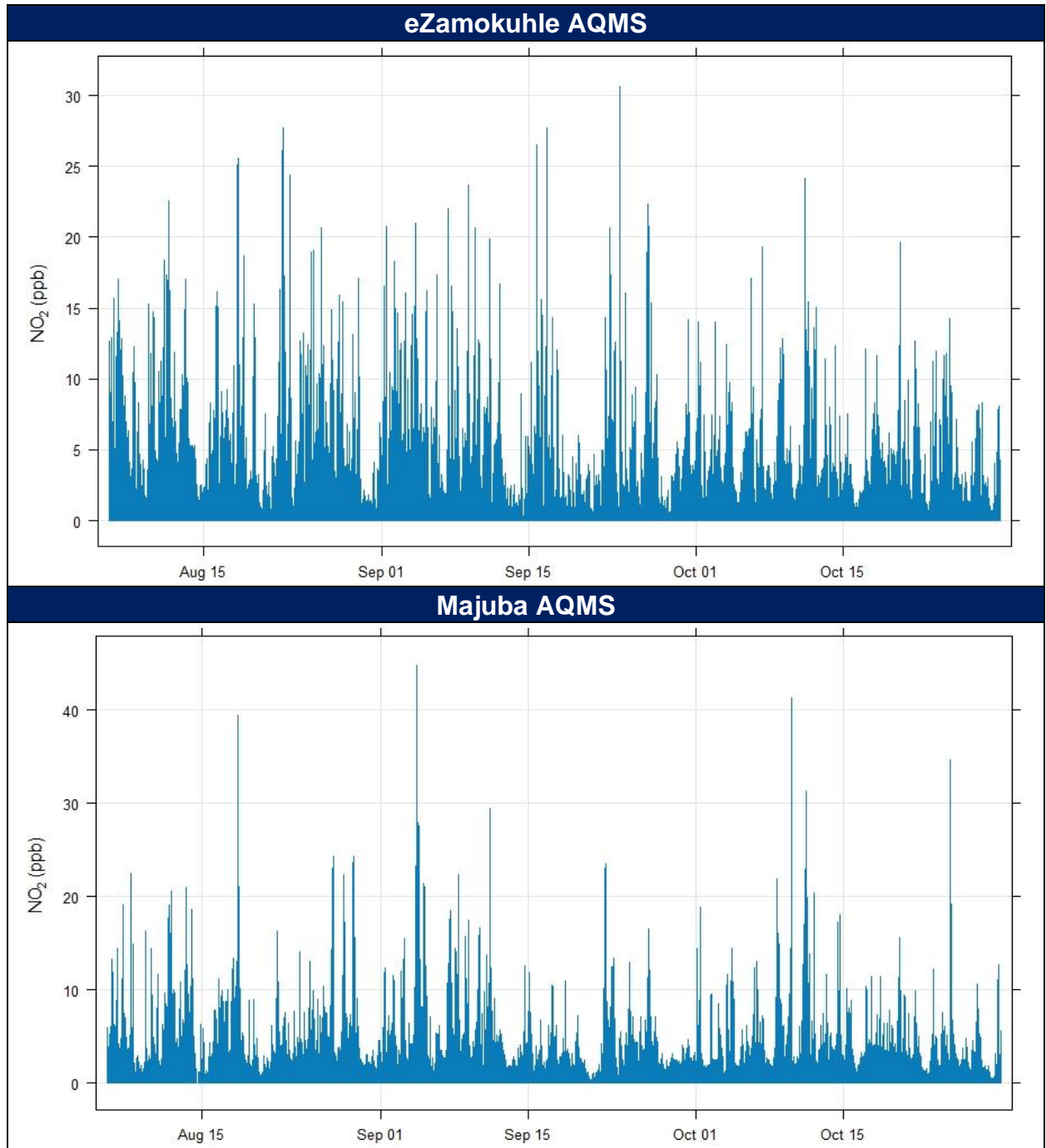


Figure 36: Hourly ambient NO₂ concentrations (ppb) measured at Eskom eZamokuhle AQMS during the sampling survey (Hourly NO₂ NAAQS = 106ppb).

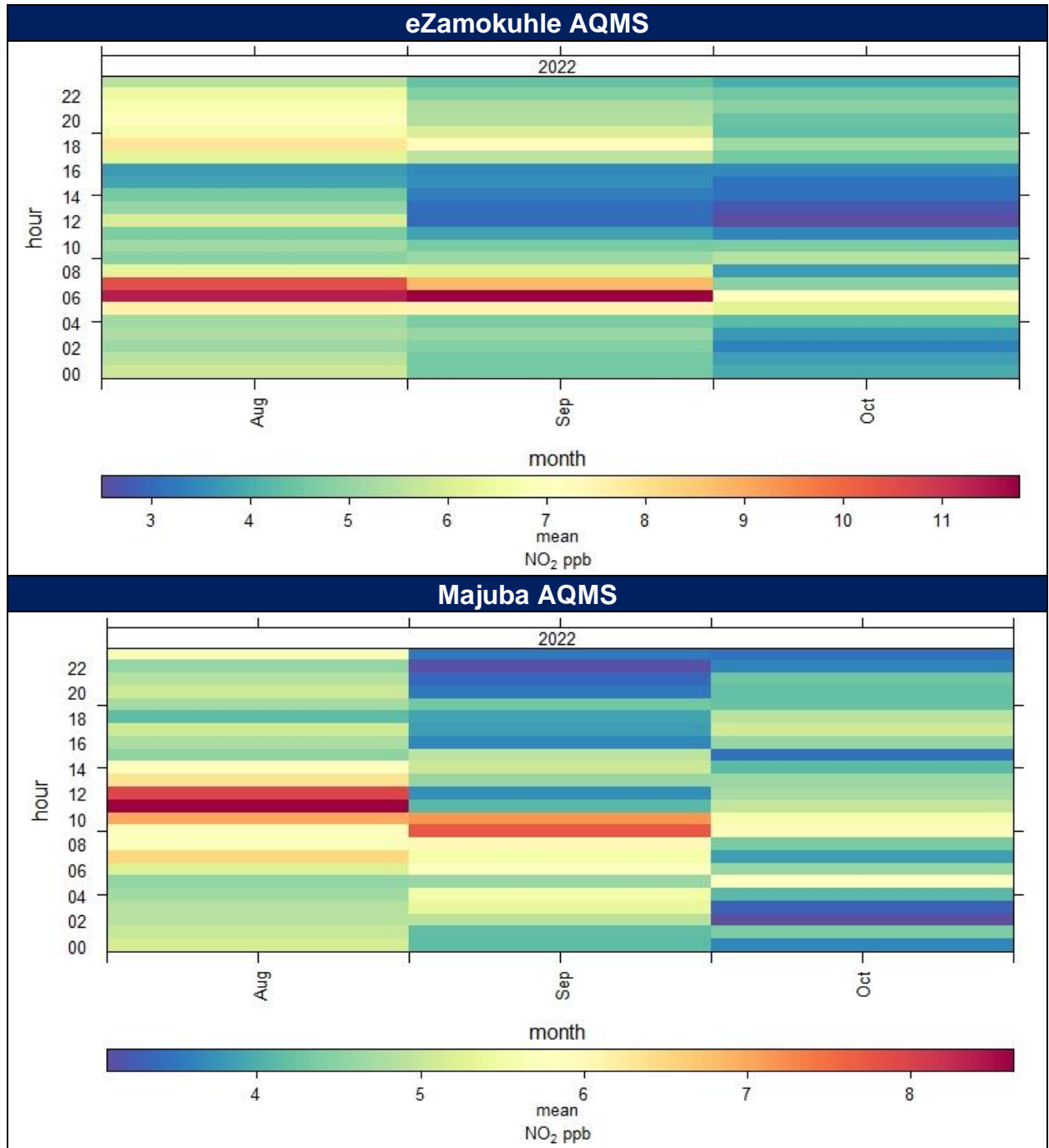


Figure 37: Hourly mean ambient NO₂ concentrations (ppb) measured at Eskom eZamokuhle AQMS during the sampling survey (Hourly NO₂ NAAQS = 106ppb).

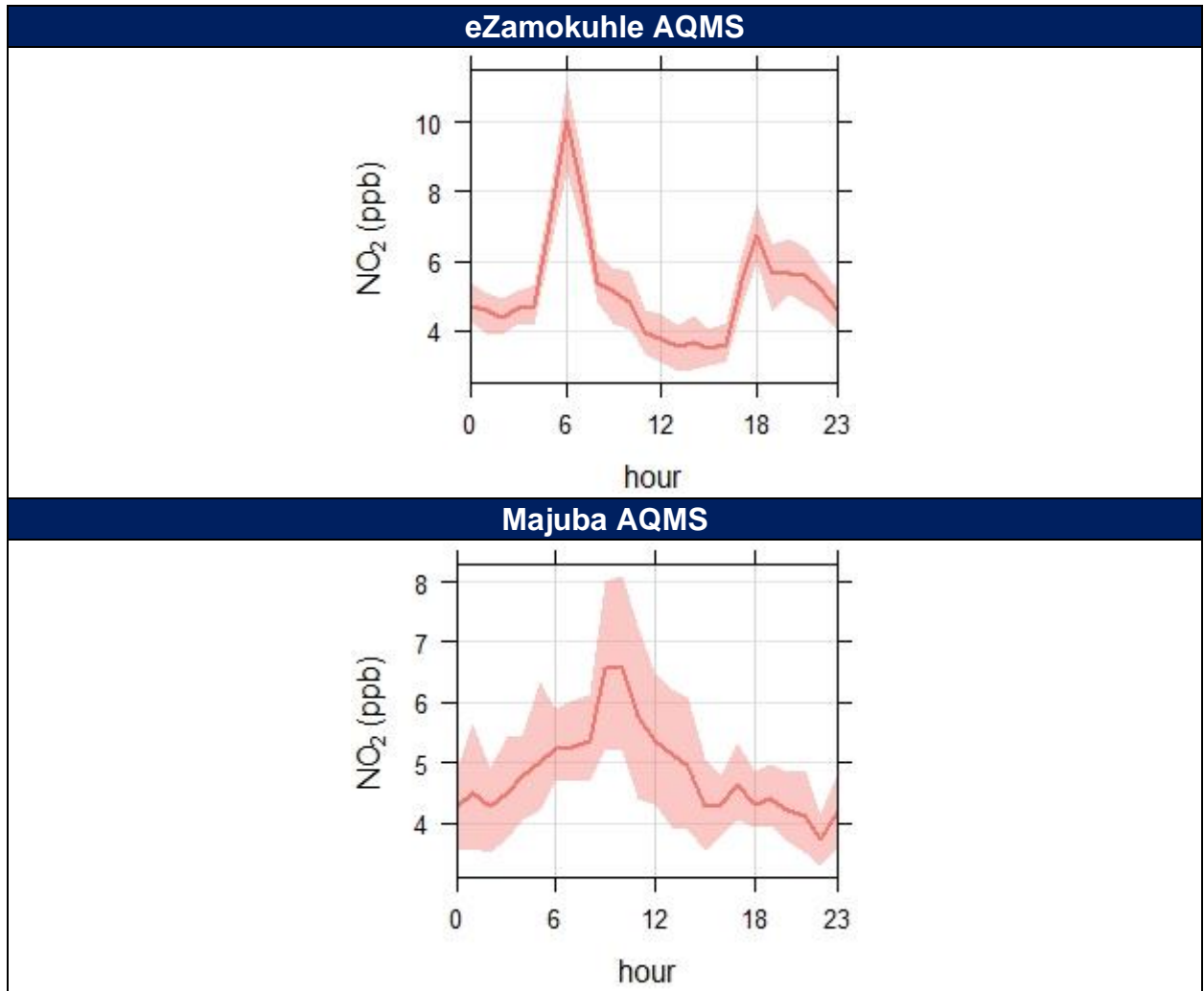


Figure 38: Mean hourly diurnal NO₂ concentrations (□g/m³) measured at sampling sites during the sampling survey

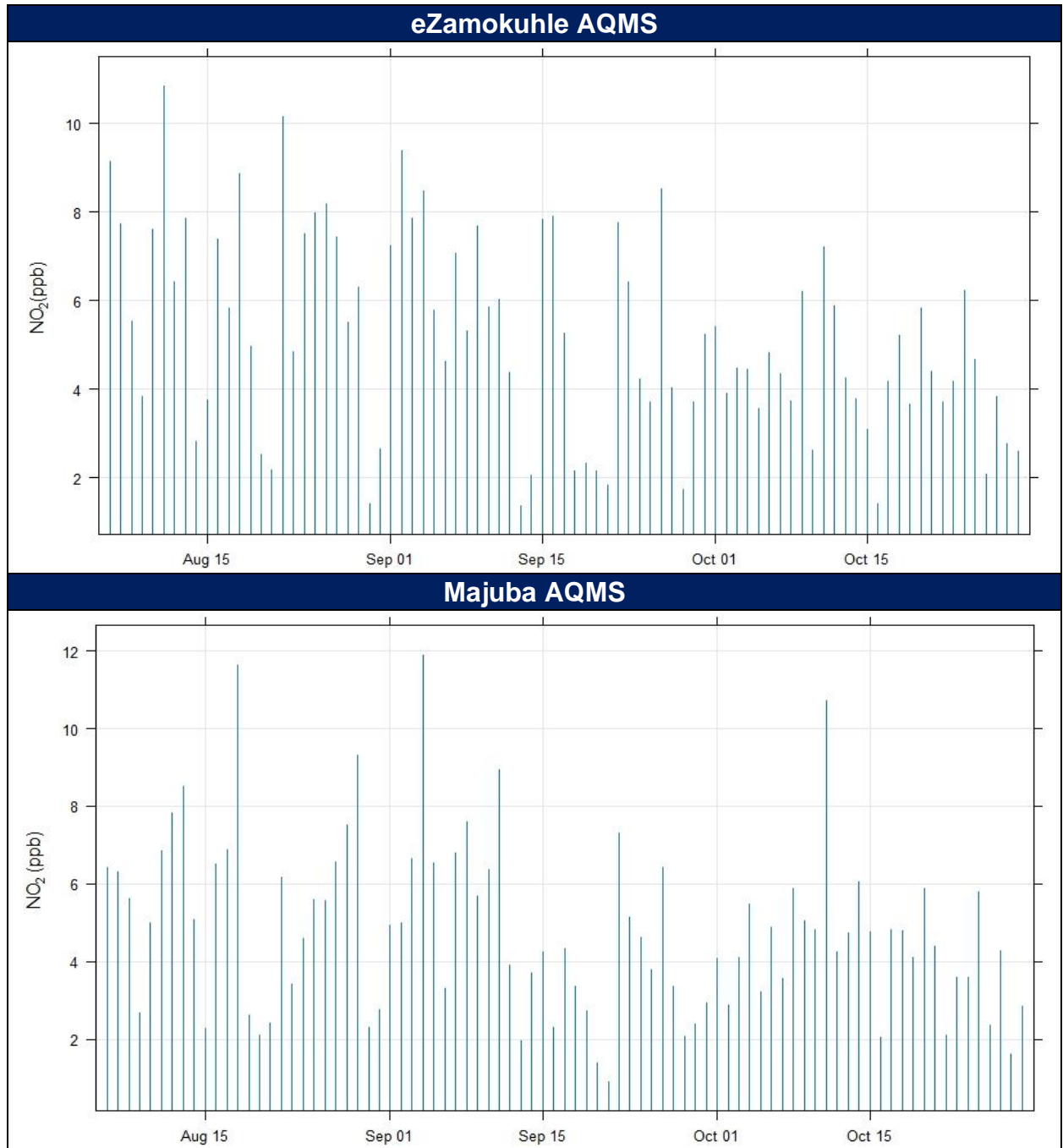


Figure 39: Daily ambient NO₂ concentrations (ppb) measured at Eskom eZamokuhle AQMS during the sampling survey

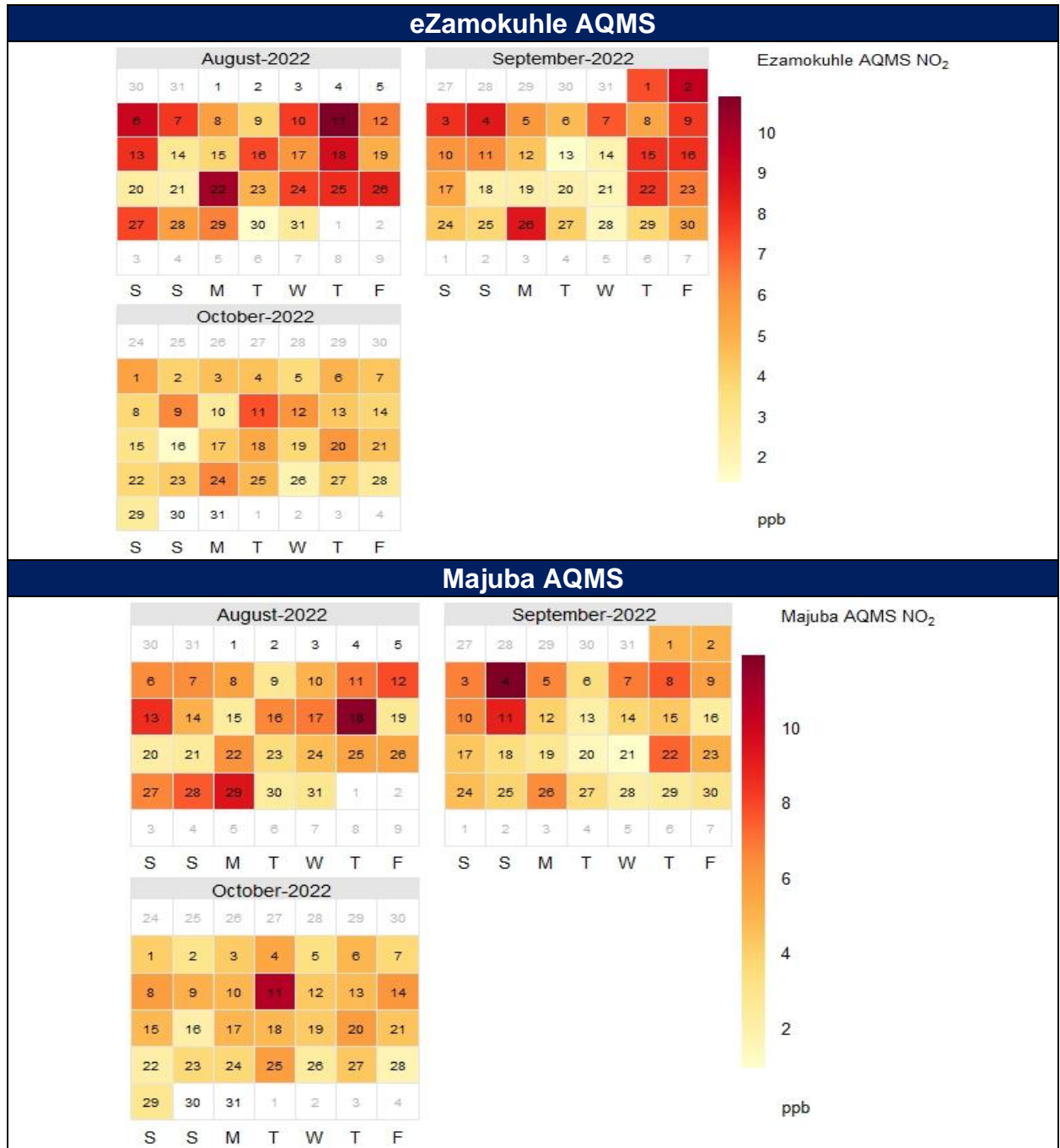


Figure 40: Daily ambient NO₂ concentrations (ppb) measured at Eskom eZamokuhle AQMS during the sampling survey

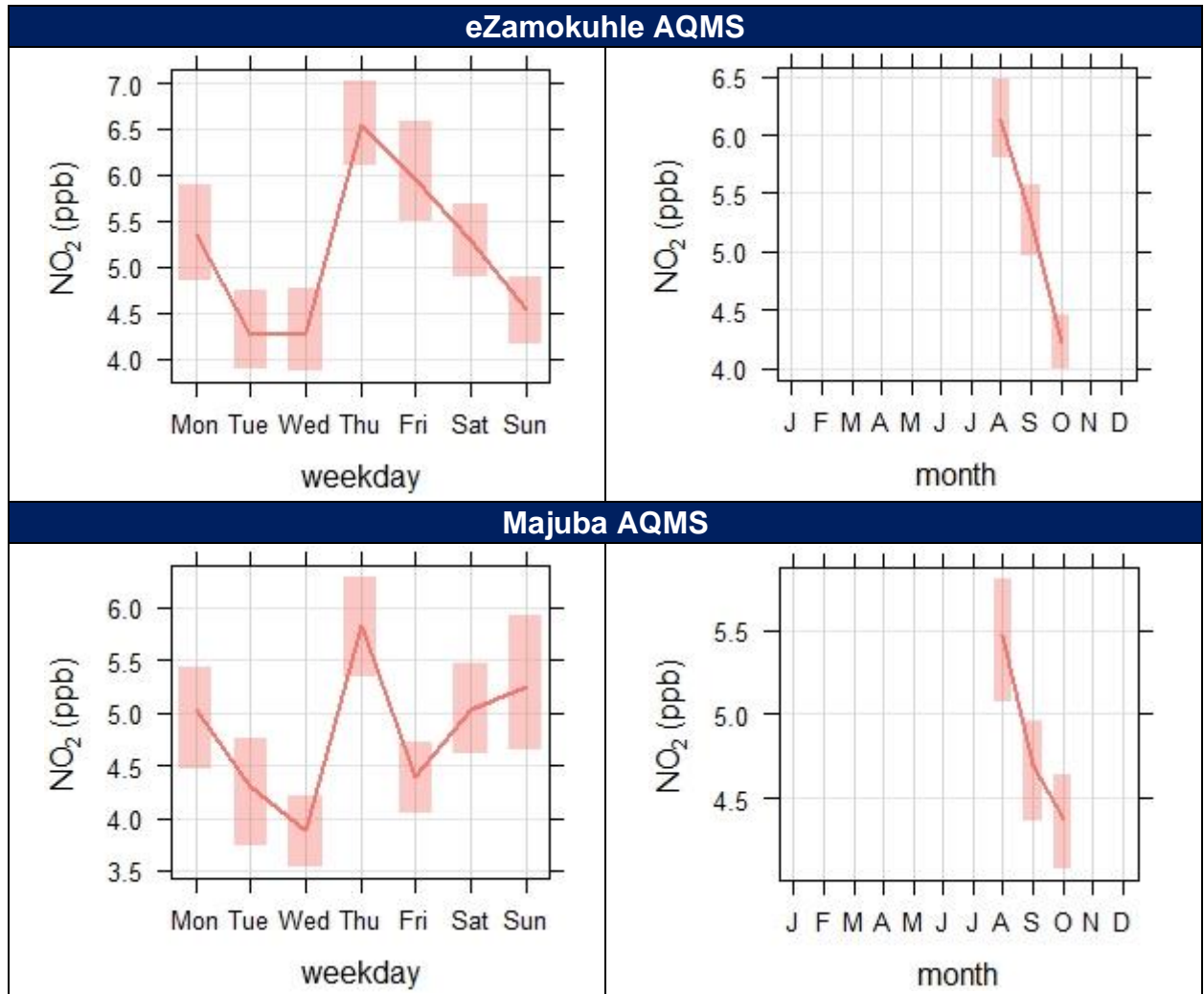


Figure 41: Mean weekday and mean monthly ambient NO₂ concentrations (ppb) measured at sampling sites during the sampling survey

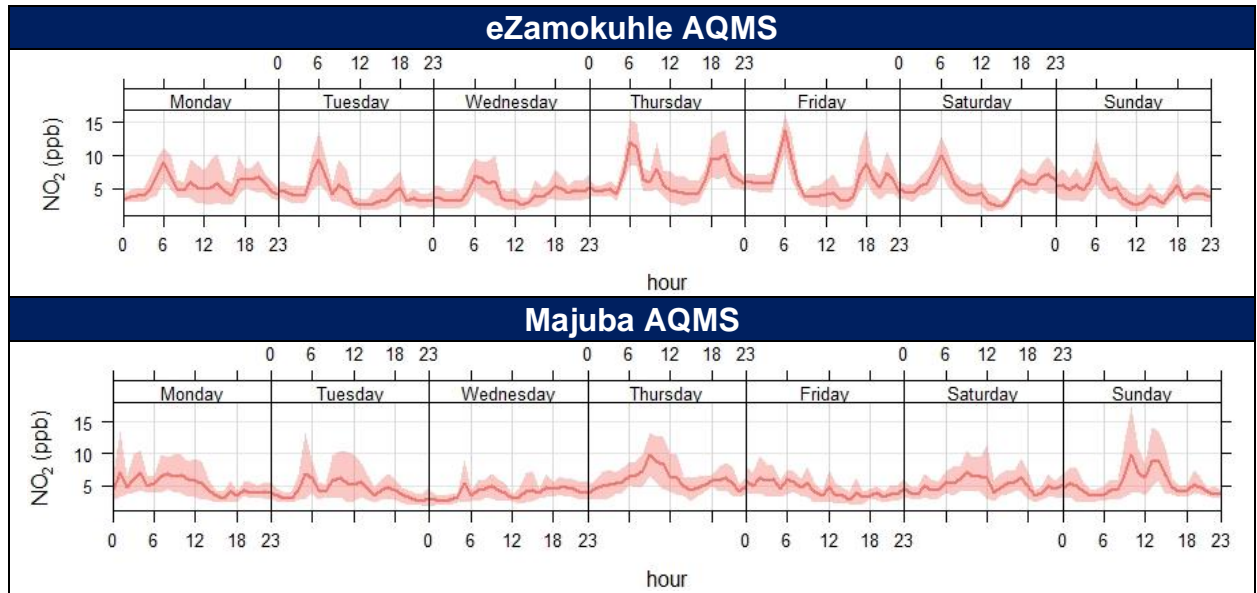


Figure 42: Weekly diurnal NO₂ concentrations ($\mu\text{g}/\text{m}^3$) measured at sampling sites during the sampling survey

4.3 EMISSION SOURCE CONTRIBUTION

The emission performance of an individual air-pollution source can be inferred from an ambient record by isolating its signal of impacts. However, ambient data are not conventionally used for such purposes because individual signals tend to be modified, obscured, or complicated by confounding factors (Szulecka et al., 2017). However, more detailed and source-specific information can be extracted if analyses are performed using a subset of the data that has been “conditionally-selected” to exclude superimposed impacts from non-relevant sources (Malby et al., 2013). Numerous studies (Carslaw, 2007; Griffin et al., 2009; Malby et al., 2008; Shu et al., 2017) have demonstrated that these signals can successfully be used for source attribution. A common method for source characterisation is the use of pollution roses and bivariate polar plots (Carslaw et al., 2006; Westmoreland et al., 2007; Carslaw and Beevers, 2013; Uria Tellaetxe and Carslaw, 2014).

Bivariate polar plots have proved to be extremely valuable for identifying and understanding sources of air pollution (Carslaw et al., 2006; Westmoreland et al., 2007). Bivariate polar plots provide an effective graphical means of discriminating different source types and characteristics as these plots show how the concentration of a pollutant varies by two different variables at a specific receptor.

4.3.1 POLLUTION ROSES

The pollution rose is useful for considering pollutant concentrations by wind direction, or more specifically the percentage time the concentration is in a particular range. This type of approach can be very informative for air pollutant species (Henry et al. 2009).

4.3.1.1 Particulate Matter (PM₁₀)

Figure 43 illustrates the pollution roses for PM₁₀ measured at the Eskom eZamokuhle & Majuba stations. These plots are very useful for understanding which wind directions control the overall mean concentrations. The pollution rose clearly indicates that high episodes of pollutant levels are primarily related to winds from the: west-, north-westerly direction; east-, north easterly direction, as well a south westerly direction. A comparison of the annual wind rose for the Eskom eZamokuhle station and the Eskom Majuba station (Figure 8) to the pollution roses (Figure 43) shows higher pollutant concentrations occur at higher wind speeds. Conversely lower wind speeds (Figure 8) are associated with lower concentrations (Figure 43). It should be noted that higher wind speeds are typically associated with elevated emissions from tall stack sources whilst low-level emissions behave differently, and higher concentrations would normally be observed during weak-wind conditions.

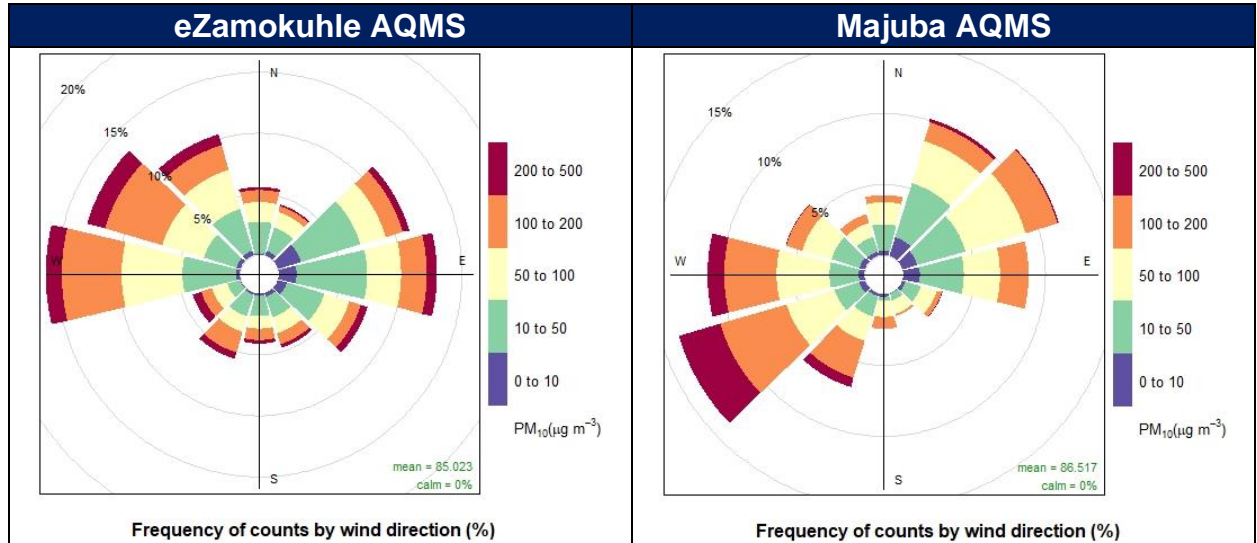


Figure 43: Pollution roses indicating which wind directions contribute most to overall mean concentrations for PM₁₀

4.3.1.2 Particulate Matter (PM_{2.5})

Figure 44 illustrates the pollution roses for PM_{2.5} measured at the Eskom eZamokuhle & Majuba stations. The pollution rose clearly indicates that high episodes of pollutant levels are primarily related to winds from the: west-, north-westerly direction; east-, north easterly direction, as well a south westerly direction.

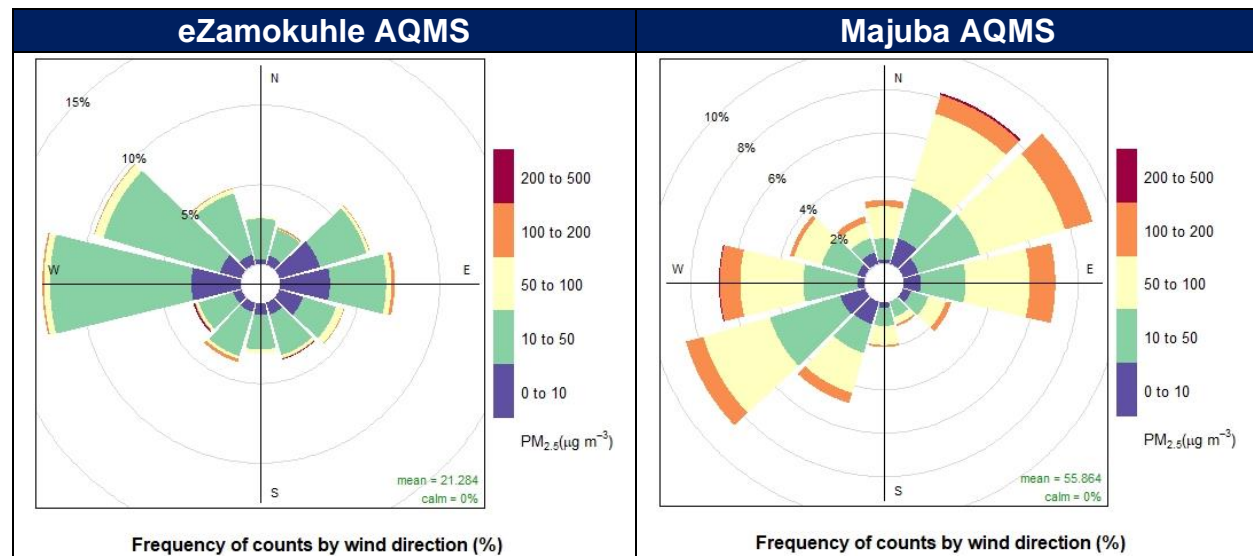


Figure 44: Pollution roses indicating which wind directions contribute most to overall mean concentrations for PM_{2.5}

4.3.1.3 Sulphur Dioxide (SO₂)

Figure 45 illustrates the pollution roses for SO₂ measured at the Eskom eZamokuhle & Majuba stations. The pollution rose clearly indicates that high episodes of pollutant levels are primarily related to winds from the: west-, north-westerly direction; east-, north easterly direction, as well a south westerly direction. Figure 45 illustrates that hourly mean concentrations of 10 to 50ppb SO₂, recorded at the Eskom eZamokuhle station are predominantly associated with sources emanating from a westerly/west north-westerly direction.

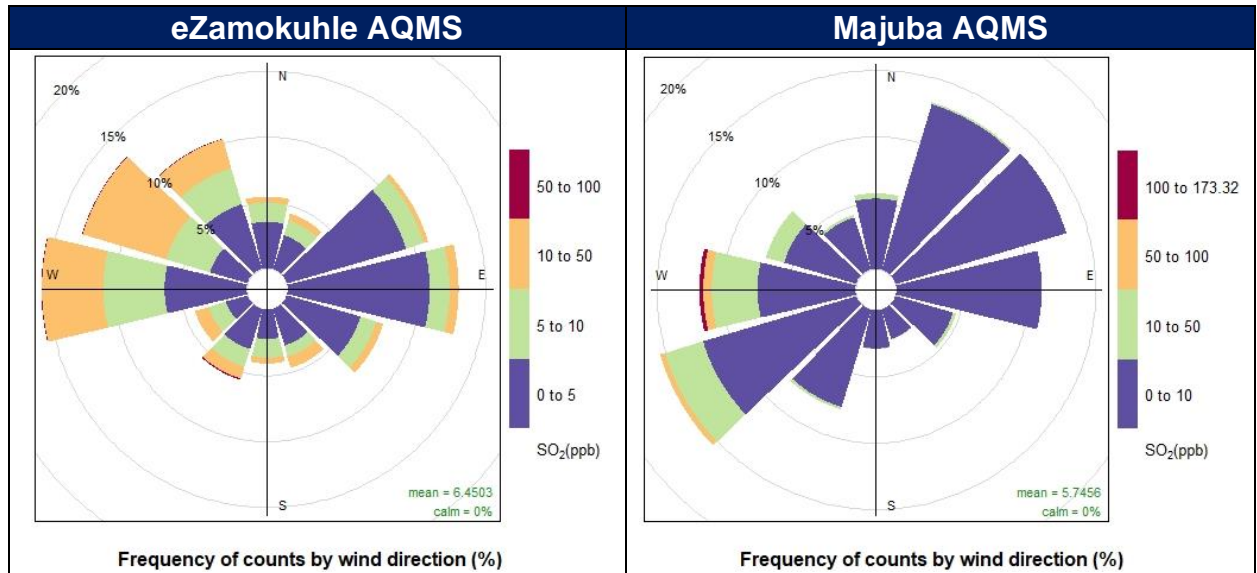


Figure 45: Pollution roses indicating which wind directions contribute most to overall mean concentrations for SO₂

4.3.1.4 Nitrogen Oxide (NO₂)

Figure 46 illustrates the pollution roses for NO₂ measured at the Eskom eZamokuhle & Majuba stations. The pollution rose clearly indicates that high episodes of pollutant levels are primarily related to winds from the: west-, north-westerly direction; east-, north easterly direction, as well a south westerly direction. Figure 46 illustrates those hourly mean concentrations of 10 to 50 ppb NO₂, recorded at the Eskom eZamokuhle station are predominantly associated with sources emanating from a westerly/south-westerly direction.

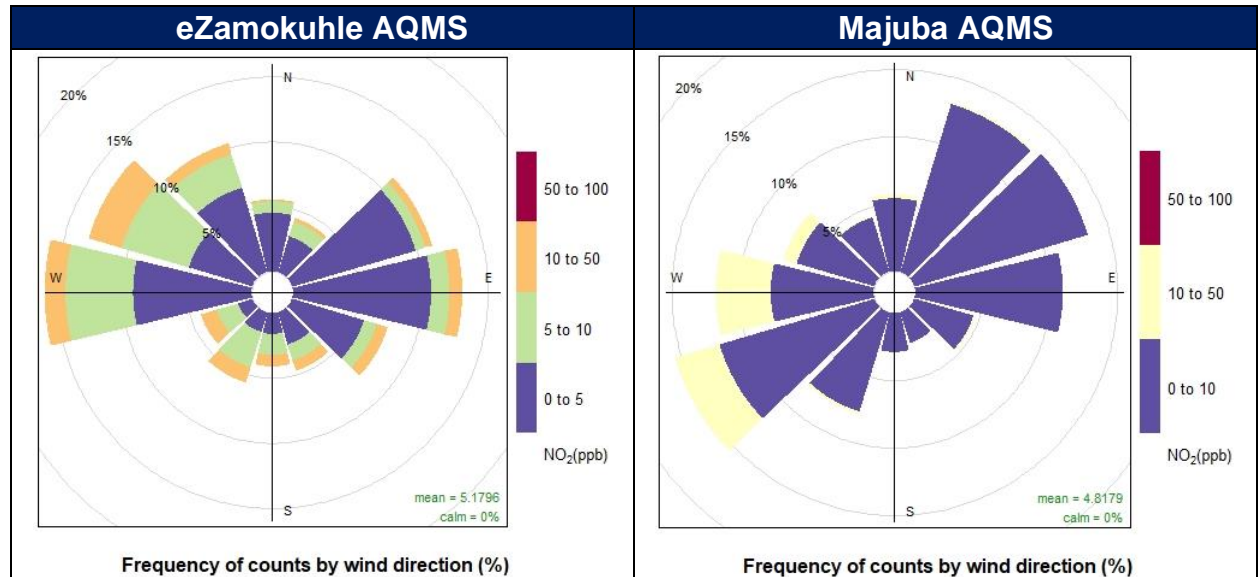


Figure 46: Pollution roses indicating which wind directions contribute most to overall mean concentrations for NO₂

4.3.2 BIVARIATE POLAR PLOTS FOR MEAN CONCENTRATION & WIND SPEED

Bivariate plots indicate how the concentration of a pollutant varies by wind direction and wind speed at a receptor. The wind speed dependence of a source can provide important information concerning the source type and characteristics (Carslaw et al., 2006; Jones et al., 2010). High ground level concentrations from tall stack emissions are more prevalent during stronger wind speeds during stable conditions whilst conversely low-level emissions, and higher concentrations would normally be observed during weak-wind conditions.

4.3.2.1 Particulate Matter (PM₁₀)

Elevated particulate (PM₁₀) concentrations at Eskom eZamokuhle show source contributions from the north-west and the south-east at higher (between 8 and 12 m/s) wind speeds (Figure 47). At low wind speeds the symmetrical plot shows a localised contribution, most likely the result of residential fuel burning (Figure 47). The Eskom Majuba station indicate source contributions from a westerly, south-westerly as well as a north-easterly direction. The higher concentrations (400 to 450 $\mu\text{g}/\text{m}^3$) is associated with sources from a south-westerly direction (10 to 14m/s).

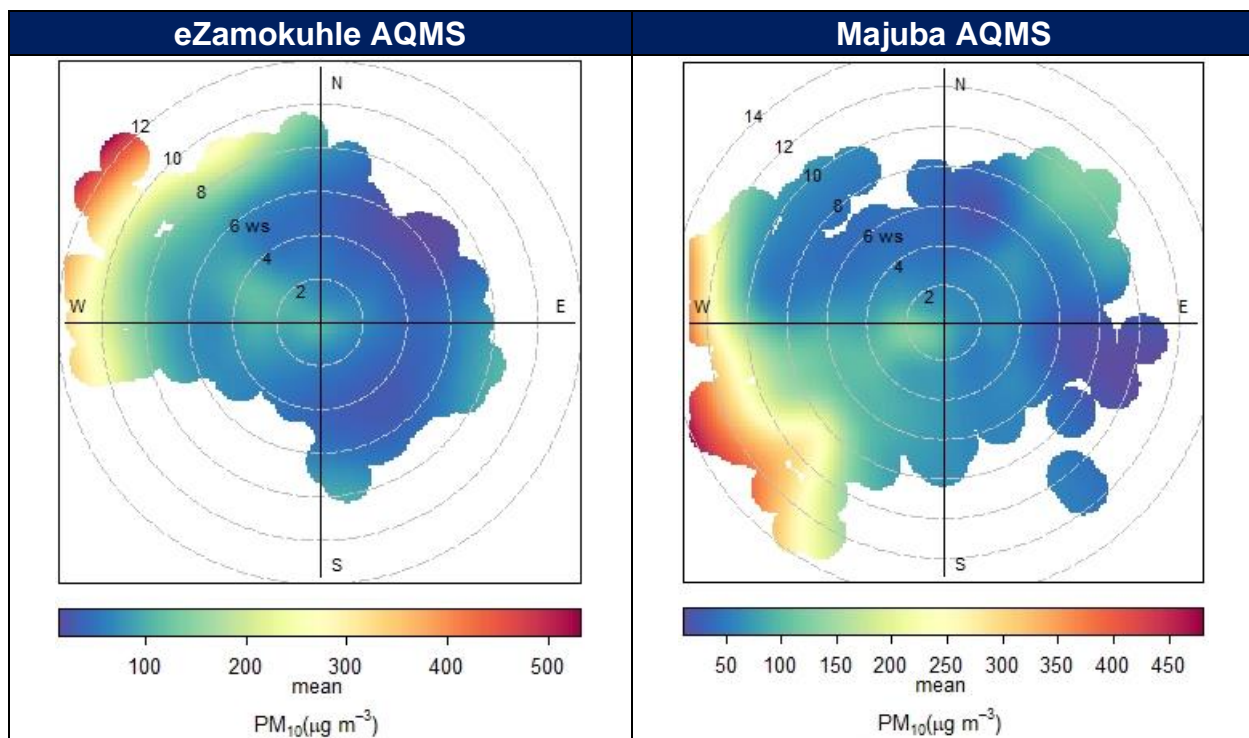


Figure 47: Polar plot of hourly mean PM₁₀ concentration at the Eskom AQMS for the sampling period

4.3.2.2 Particulate Matter (PM_{2.5})

Elevated particulate (PM_{2.5}) concentrations at Eskom eZamokuhle show source contributions from the north-west and the south-east at higher (between 8 and 12 m/s) wind speeds (Figure 48). At low wind speeds the symmetrical plot shows a localised contribution, most likely the result of residential fuel burning (Figure 48). The Eskom Majuba station indicate the highest source contribution from a westerly direction. These high concentrations (>120 ug/m³) is associated with sources from a westerly direction and wind speeds of 12 to 14 m/s.

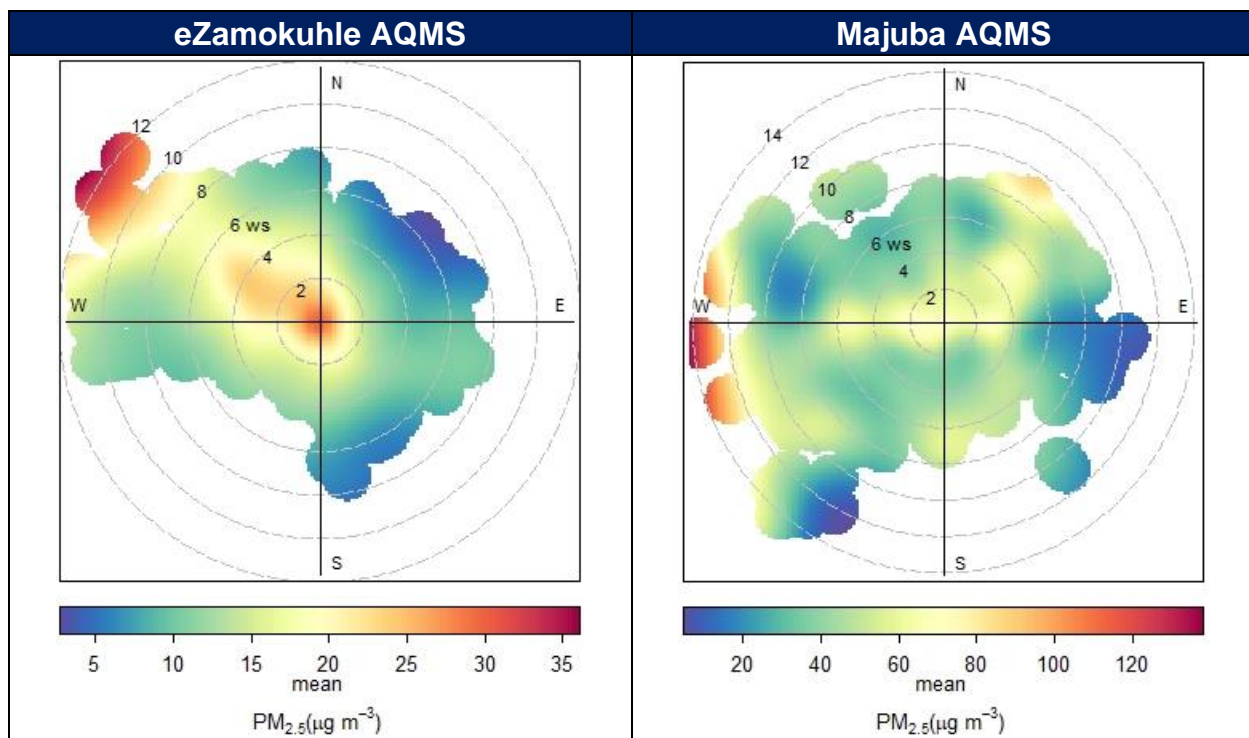


Figure 48: Polar plot of hourly mean PM_{2.5} concentration at the Eskom AQMS for the sampling period

4.3.2.3 Sulphur Dioxide (SO₂)

The SO₂ concentrations observed at the Eskom eZamokuhle station (Figure 49) show two distinct wind directions, namely from the south-west and the north-west. High concentrations present at high wind speeds are indicative of emissions from stacks rather than non-buoyant ground-level sources. Hence the higher SO₂ concentrations associated with the south-westerly winds are most likely due to emissions from the Eskom Majuba power station. Similarly, the SO₂ concentrations from the north-west indicates a distinct tall stack emission source and this corresponds to the exact direction of a significant petrochemical facility located in Secunda which may be the likely emission source.

SO₂ concentrations (Figure 49) observed at the Eskom Majuba AQMS clearly show that the highest SO₂ concentrations occur when the wind is blowing from the west/north-west. These high concentrations occur under very high wind speeds conditions (between 10 to 15 m/s) from the south-west which is most likely due to emissions from the Eskom Majuba power station. At low wind speeds the symmetrical plot shows a localised contribution, most likely the result of residential fuel burning (Figure 49).

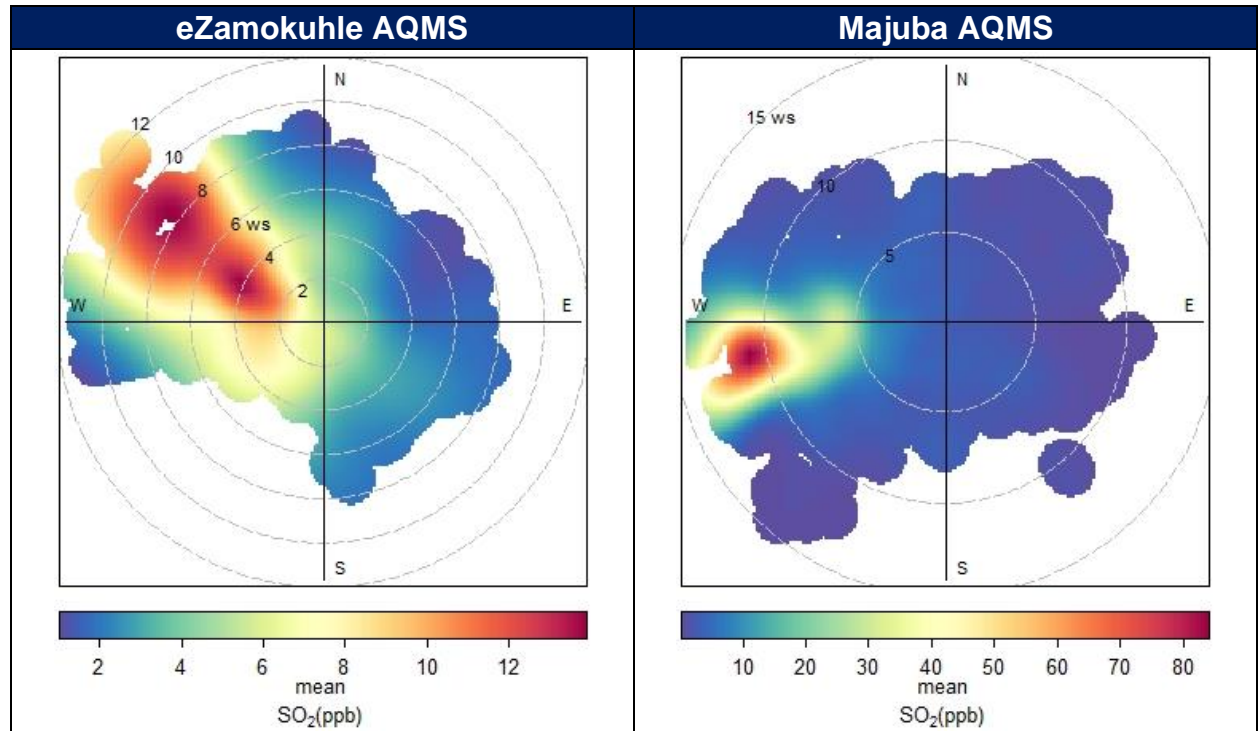


Figure 49: Polar plot of hourly mean SO_2 concentration at the Eskom AQMS for the sampling period

4.3.2.3 Nitrogen Dioxide (NO_2)

Figure 50 indicate the bivariate NO_2 polar plots for the Eskom eZamokuhle and Majuba AQMS. The highest concentrations occur under very low wind speed conditions (0 to 2m/s) from the south-west. These high concentrations occur under stable atmospheric conditions when non-buoyant ground-level sources are important such as road transport emissions. Figure 48 confirms that these NO_2 concentrations are the likely impact of vehicle emissions. The bivariate polar plot also indicates an area of high concentration to the north-west that occur at high wind speeds (8 to 12m/s), possibly corresponding to the activities of a petrochemical facility located in Secunda.

NO₂ concentrations (Figure 50) observed at the Eskom Majuba station clearly show that the highest NO₂ concentrations occur when the wind is blowing from the south-west. The high concentrations occur under very high wind speeds conditions (between 10 to 15 m/s) from the north-west which is most likely due to emissions from the Eskom Majuba power station. At low wind speeds the symmetrical plot shows a localised contribution, most likely the result of residential fuel burning in the region.

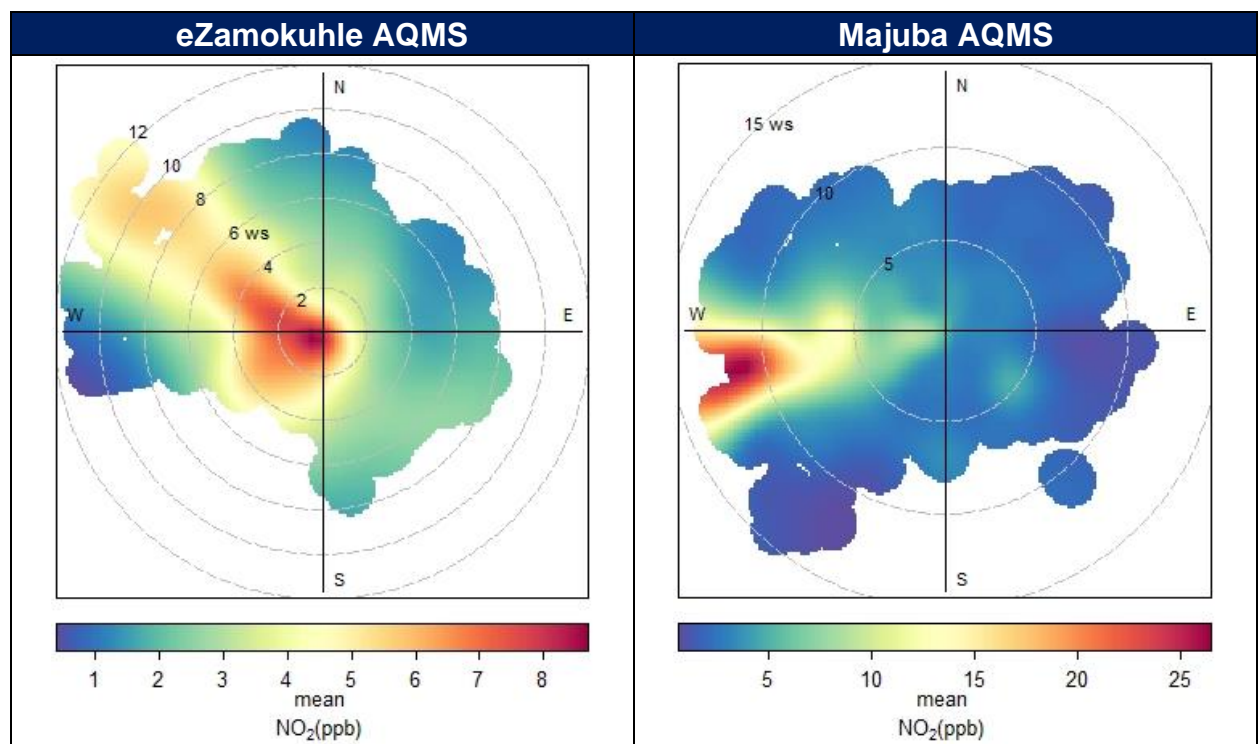


Figure 50: Polar plot of hourly mean NO₂ concentration at the Eskom AQMS for the sampling period

4.3.3 BIVARIATE POLAR PLOT FOR MEAN CONCENTRATION & TEMPERATURE

These plots show how the concentration of a pollutant varies by wind direction and temperature at a receptor. Temperature can help reveal high-level sources brought down to ground level in unstable atmospheric conditions or show the effect a source emission dependent on temperature e.g., residential burning for space heating.

4.3.3.1 Particulate Matter (PM₁₀)

Figure 51 indicates the bivariate polar plots for PM₁₀ concentrations as a function of wind direction and surface temperature for both the Eskom eZamokuhle and Eskom Majuba AQMS. The highest concentrations occur during low temperatures, which results mostly from residential fuel burning.

4.3.3.2 Particulate Matter (PM_{2.5})

Figure 52 indicates the bivariate polar plots for PM_{2.5} concentrations as a function of wind direction and surface temperature for both the Eskom eZamokuhle and Eskom Majuba AQMS. Lower localised concentrations occur during low temperatures, which results mostly from residential fuel burning.

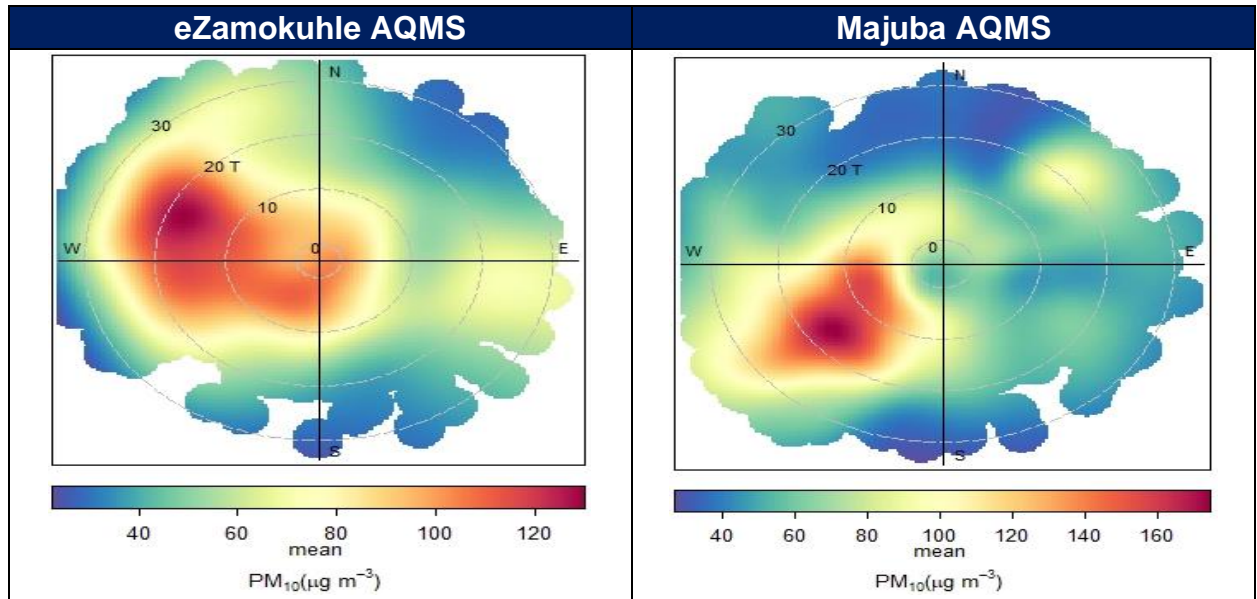


Figure 51: Polar plot of hourly mean PM_{10} concentration at the Eskom AQMS for the sampling period

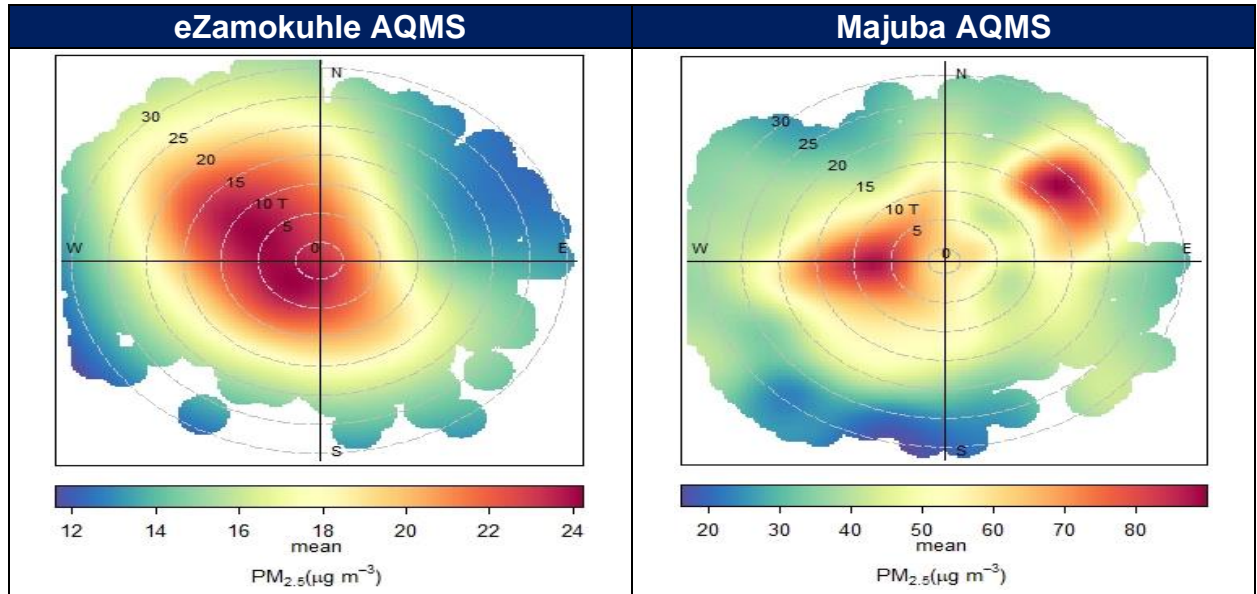


Figure 52: Polar plot of hourly mean $PM_{2.5}$ concentration at the Eskom AQMS for the sampling period

4.3.3.3 Sulphur Dioxide (SO₂)

Figure 53 indicate the bivariate polar plot for hourly SO₂ concentrations as a function of wind direction and surface temperature. It is apparent that there is a clear dependence of SO₂ concentrations with increasing ambient temperature for both the Eskom eZamokuhle and Eskom Majuba AQMS. These concentrations increase with increasing temperature can be attributed to dispersing plumes from tall stacks that are brought down to ground level under unstable atmospheric conditions when thermal turbulence is increased. The bivariate polar plot (Figure 53) also indicates an area of high concentration to the north-west that occur at higher temperatures (20 to 30°C), possibly corresponding to the activities of a petrochemical facility located in Secunda.

The area of high concentration for the Eskom Majuba station toward the west could possibly correspond to the Eskom Majuba power station, located towards the west of the Eskom Majuba AQMS.

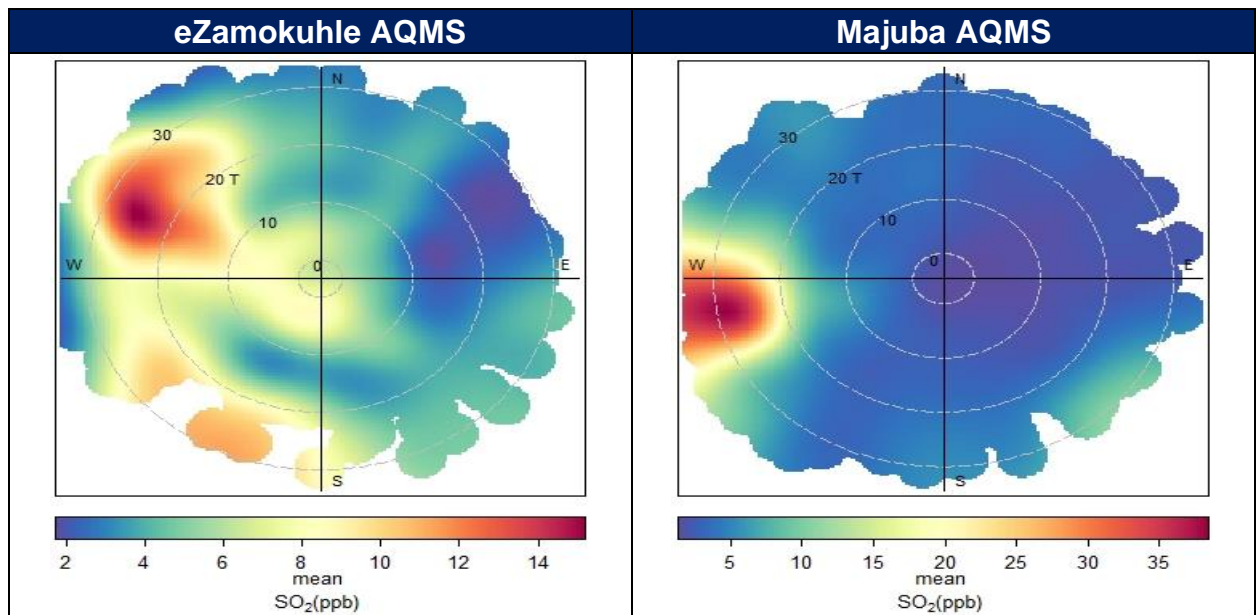


Figure 53: Polar plot of hourly mean SO₂ concentration at the Eskom AQMS for the sampling period

4.3.3.4 Nitrogen Dioxide (NO₂)

Figure 54 indicate the bivariate polar plot for hourly NO₂ concentrations as a function of wind direction and surface temperature. It is apparent that there is a clear dependence of NO₂ concentrations with increasing ambient temperature for both the Eskom eZamokuhle and Eskom Majuba AQMS. These concentrations increase with increasing temperature can be attributed to dispersing plumes from tall stacks that are brought down to ground level under unstable atmospheric conditions when thermal turbulence is increased. The bivariate polar plot (Figure 54) also indicates an area of high concentration to the north-west that occur at higher temperatures (20°C), possibly corresponding to the activities of a petrochemical facility located in Secunda. The area of high concentration in the south-westerly direction at temperatures from 0 to 30°C could correspond to vehicle emissions.

The area of high concentration for the Eskom Majuba station (Figure 54) toward the west could possibly correspond to the Eskom Majuba power station, located towards the west of the Eskom Majuba AQMS.

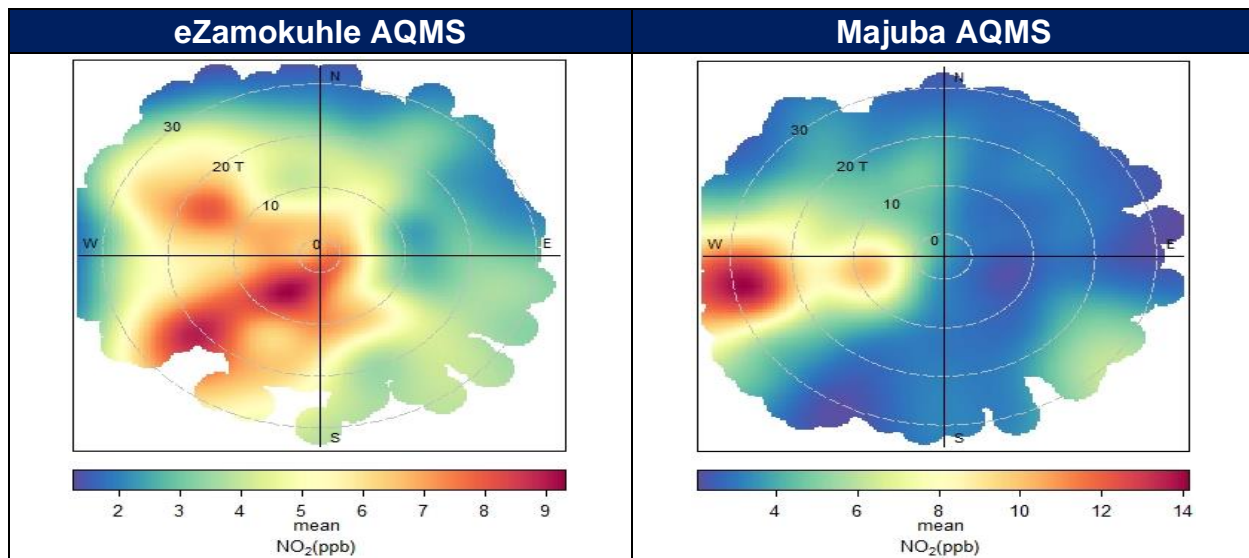


Figure 54: Polar plot of hourly mean NO₂ concentration at the Eskom AQMS for the sampling period

5. CONCLUSIONS

5.1 PARTICULATE MATTER (PM₁₀)

The bi-modal hourly diurnal cycle at House 4 is indicative of residential fuel burning. Maximum hourly ambient PM₁₀ concentrations of 400 ug/m³ were recorded at House 4 during the survey. Maximum daily ambient concentrations of 120 ug/m³ were recorded, with exceedances of the daily NAAQS for PM₁₀. These exceedances were prominent during the colder months during the sampling period. No exceedances of the daily NAAQS for PM₁₀ were recorded for the second half of September, as well as the October at House 4. A daily mean ambient PM₁₀ concentration of 57.1ug/m³ was recorded for House 4 during the sampling period. The results are conclusive that residential fuel burning is the major contributing emission source to these measured PM₁₀ concentrations.

5.2 PARTICULATE MATTER (PM_{2.5})

The bi-modal hourly diurnal cycle at House 1 and House 5 are indicative of residential fuel burning. Maximum hourly ambient PM₁₀ concentrations of 500 ug/m³ were recorded at House 1 and House 5 during the survey. Maximum daily ambient concentrations of 80ug/m³ were recorded at both Houses, with exceedances of the daily NAAQS for PM_{2.5}. These exceedances were prominent during the colder months during the sampling period, but exceedances were also reported during October for both Houses respectively. A daily mean ambient PM_{2.5} concentration of 40.0 ug/m³ and 43.7 ug/m³ were recorded for House 1 and House 5 respectively during the sampling period.

For both PM_{10} and $PM_{2.5}$ the results are conclusive that residential fuel burning is the major contributing emission source to the elevated concentrations measured in eZamokuhle. These elevated concentrations were more pronounced in the winter months with the increased space heating requirements of the eZamokuhle households in winter. Hence there is an opportunity herein to reduce human exposure to harmful levels of air pollution by reducing emissions from residential burning. Thus supporting the roll-out of Eskom's PMV air quality offset intervention project in Ezamokuhle.

6. ACKNOWLEDGEMENTS

Air Resource Management would like to thank the following individuals for their assistance in this study:

- Ms Bontle Moiloa for timeously providing the team with the ambient air quality monitoring data for the Eskom Majuba and eZamokuhle stations;
- Mr Motshewa Matimolane and Mr Bryan McCourt for their technical comments and support.

7. REFERENCES

1. S. Munir, T. M. Habeebullah, A. M. F. Mohammed, E. A. Morsy, M. Rehan, and K. Ali, "Analysing PM_{2.5} and its association with PM₁₀ and meteorology in the arid climate of Makkah, Saudi Arabia," *Aerosol and Air Quality Research*, vol. 17, no. 2, pp. 453–464, 2017.
2. J. Hu, Y. Wang, Q. Ying, and H. Zhang, 2014. "Spatial and temporal variability of PM_{2.5} and PM₁₀ over the north China plain and the Yangtze River Delta, China," *Atmospheric Environment*, vol. 95, pp. 598–609, 2014.
3. Doucet, P., Sloep, P.B. 1992. "Mathematical Modeling in the Life Sciences", King's College, London, 1992
4. Tiwary, A., Colls, J. "Air Pollution: Measurement, Modeling, and Mitigation", 3rd Edition, Routledge, New York, 2010
5. Carslaw D.C., Ropkins K. 2012. "Openair – an r package for air quality data analysis". *Environmental Modelling and Software*, pp27–28: pp52–61
6. Appel, K.W., Gilliam, R.C., Davis, N., Zubrow, A., and Howard, S.C., 2011. "Overview of the atmospheric model evaluation tool (amet) v1.1 for evaluating meteorological and air quality models". *Environmental Modelling and Software*, Vol 26 (4), pg434-443. <http://www.sciencedirect.com/science/article/pii/S1364815210002653>
7. Carslaw, D. "The Openair Manual Open-Source Tools for Analysing Air Pollution Data", King's College, London, 2015.
8. Czernecki B., Pólrolniczak M., Kkolendowicz L., Marosz M., Kendzierski S., Pilgij N. 2016. "Influence of the Atmospheric Conditions on PM₁₀ Concentrations in Poznan, Poland". *Journal of Atmospheric Chemistry*, vol 74(1), pp. 1-25. View at: https://www.researchgate.net/publication/308477377_Influence_of_the_atmospheric_conditions_on_PM10_concentrations_in_Poznan_Poland

9. Crilley L.R., Lucarelli F., Bloss W.J., Harrison R.M., Beddows D.C., Calzolari G., Navab S., Vallid G., Bernardoni V., Vecchi R. 2017. "Source apportionment of fine and coarse particles at a roadside and urban background site in London during the 2012 summer ClearfLo campaign". *Environmental Pollution* 220: pp766–778
10. Pattinson W., Kingham S., Longley I., Salmond J. 2016. "Potential Pollution Exposure Reductions from Small-Distance Bicycle Lane Separations". *Journal of Transport & Health*, Vol 4, pp40-52. View at: <https://www.sciencedirect.com/science/article/abs/pii/S2214140516303504>
11. Salvador P., Alonso-Pérez S., Pey J., Artíñano B., Debustos J.J., Alastuey A., Querol X. 2014. "African dust outbreaks over the western Mediterranean Basin: 11-year characterization of atmospheric circulation patterns and dust source areas". *Atmospheric Chemistry and Physics* Vol 14(13): pp6759–6775. View at: https://www.researchgate.net/publication/263036412_African_dust_outbreaks_over_the_western_Mediterranean_Basin_11-Year_characterization_of_atmospheric_circulation_patterns_and_dust_source_areas
12. Schweizer D., and Cisneros R. 2014. "Wildland Fire Management and Air Quality in the Southern Sierra Nevada: Using the Lion Fire as a case study with a multi-year perspective on PM_{2.5} impacts and fire policy". *Journal of Environmental Management* Vol 144: pp 265–278. View at: <https://www.sciencedirect.com/science/article/pii/S0301479714003089?via%3Dihub>
13. Crilley L.R., Bloss W.J., Yin J., Beddows D.C., Harrison R.M., Allan J.D., Young D.E., Flynn M., Williams P., Zotter P., Prevot A.S.H., Heal M.R., Barlow J.F., Halios C.H., Lee J.D., Szidat S., Mohr C., Prevot A.S. 2015. "Sources and contributions of wood smoke during winter in London: Assessing local and regional influences".

- Atmospheric Chemistry and Physics Vol 15(6): pp 3149–3171. View at: <https://acp.copernicus.org/articles/15/3149/2015/>
14. Jang E., Do W., Park,G., Kim M., Yoo E. 2016. “Spatial and temporal variation of urban air pollutants and their concentrations in relation to meteorological conditions at four sites in Busan, South Korea”. Atmospheric Pollution Research Vol 8(1): pp 89–100. View at: <https://www.sciencedirect.com/science/article/abs/pii/S1309104216301192?via%3Dihub>
15. Szulecka,A., Oleniacz R , and Rzeszutek,M. 2017. “Functionality of Openair Package in Air Pollution Assessment and Modeling — A Case Study of Krakow”. Environmental Protection and Natural Resources,Vol 28(2):pp 22-27. View at: https://content.sciendo.com/view/journals/oszn/28/2/article-p22.xml?language=en&tab_body=abstract
16. Malby, A.R., Whyatt, J.D., and Timmis, R.J. 2013. “Conditional Extraction of Air-Pollutant Source Signals from air-quality monitoring”. Atmospheric Environment, Vol 74(2013):pp 112-122
17. Carslaw, D.C.,and Carslaw, N., 2007. “Detecting and characterising small changes in ur-ban nitrogen dioxide concentrations”. Atmospheric Environment Vol 41(22): pp 4723-4733.View at: <http://dx.doi.org/10.1016/j.atmosenv.2007.03.034>
18. Malby, A.R., Timmis, R.J., Whyatt, J.D., 2008. “Combining modelling and monitoring to Estimate Fugitive Releases from a Heavily-Industrialised Site”. Proceedings from the 12th Conference on Harmonisation within Atmospheric Dispersion Modelling for Regulatory Purposes (HARMO 12), Cavtat, Croatia,October 6-9, 2008, pp. 939-943. View at: <http://www.harmo.org/Conferences/Cavtat/12harmo.asp>
19. Shu,M., Dang,D., Nguyen,T., Hsu,B., and Pham,K. 2017. “The application of bivariate polar plots and k-means clustering to analysis air pollution in Taoyuan,

- Taiwan”. International Journal of Advance Engineering and Research Development, Vol 4(4),pp 553-557
20. Carslaw, D.C., Beevers, S.D., Ropkins, K., Bell, M.C., 2006. “Detecting and quantifying aircraft and other on-airport contributions to ambient nitrogen oxides in the vicinity of a large international airport”. Atmospheric Environment 40 (28),pp 5424-5434. View at: <https://www.sciencedirect.com/science/article/abs/pii/S1352231006004250?via%3Dihub>
21. Westmoreland, E.J., Carslaw, N., Carslaw, D.C., Gillah, A., and Bates, E., 2007. “Analysis of air quality within a street canyon using statistical and dispersion modelling techniques”. Atmospheric Environment, Vol 41(39), pp 9195-9205. View at: <https://doi.org/10.1016/j.atmosenv.2007.07.057>
22. Carslaw D.C., and Beevers S.D. 2013. “Characterising and understanding emission sources using bivariate polar plots and k-means clustering”. Environmental Modelling and Software, Vol 40: pp 325–329. View at: <https://doi.org/10.1016/j.envsoft.2012.09.005>
23. Jones, A.M., Harrison, R.M., Baker, J., 2010. “The wind speed dependence of the concentrations of airborne particulate matter and nox”. Atmospheric Environment Vol 44(13), pp 1682-1690. View at: <http://www.sciencedirect.com/science/article/B6VH3-4Y7P72C-2/2/f6c65e5f49ac3e9862d4c1803d4735c0>.
24. Tellaetxe, I.U., and Carslaw, D.C. “Conditional bivariate probability function for source identification”, Environmental Modelling & Software, Vol 59, pp 1-9. View at: <https://www.sciencedirect.com/science/article/pii/S1364815214001339?via%3Dihub>
25. Thangprasert, N., and Suwanarat, S. 2017. “The Relationships between Wind Speed and Temperature Time Series in Bangkok, Thailand. Journal of Physics:

- Conference Series, 901 (2017) 01204. View at: <https://iopscience.iop.org/article/10.1088/1742-6596/901/1/012043>
26. Grundstrom, M., Tang, L., Hallquist, M., Nguyen, H., Chen, D., and Pleijel, H. "Influence of atmospheric circulation patterns on urban air quality during the winter" *Atmospheric Pollution Research*, Vol 6(2), pp 278-285. View at: <https://doi.org/10.5094/APR.2015.032>.
27. Garstang, M., Tyson, P.D., Swap, R., Edwards, M., Källberg, P. and Lindesay, J.A. (1996). Horizontal and vertical transport of air over Southern Africa. *Journal of Geophysical Research*, 101 (D19), 23721-23736.
28. Swap, R., Garstang, M., Macko, S.A., Tyson, P.D., Maenhaut, W., Artaxo, P., Kallberg, P. and Talbot, R. (1996). The long-range transport of southern African aerosols to the tropical south Atlantic. *Journal of Geophysical Research*, 101 (D19), 23777-23791.
29. Held, G., Gore, B.J., Surridge, A.D., Tosen, G.R. and Walmsley, R.D. (eds) (1996), *Air Pollution and its Impacts on the South African Highveld*, Environmental Scientific Association, Cleveland, 144 pp.
30. DEFF (2010), *Air Quality Baseline Assessment for the Highveld Priority Area*
31. Merrill, J.T., Bleck, R. and Boudra, D.B. (1986). Techniques of Lagrangian trajectory analysis in isentropic coordinates. *Monthly Weather Review*, 114, 571-581.
32. Lacaux J.P (2003), *IGACtivities Newsletter*, issue no.27, January 2003, (http://www.igac.noaa.gov/newsletter/igac27/Jan_2200_IGAC_27.pdf)
33. Martins J.J, Dhammapala R.S, Lachmann G, Galy-Lacaux C and Pienaar J.J., (2007): 'Long-term measurements of sulphur dioxide, nitrogen dioxide, ammonia, nitric acid and ozone in southern Africa using passive samplers', *South African Journal of Science*, 103, 1-7

34. Mphopya J.N. 2004, 'Precipitation Chemistry in Semi-Arid Areas of Southern Africa: A Case Study of a Rural and an Industrial Site', *Journal of Atmospheric Chemistry* 47: 1–24.
35. Van Zyl, P.G., Conradie, E.H., Pienaar, J.J., Beukes, J.P., Galy-Lacaux, C., Swartz, J., Liousse, C., and Mkhathshwa, G.V., An assessment of precipitation chemistry at the South African DEBITS sites, 13th Quadrennial Symposium of the International Commission on Atmospheric Chemistry and Global Pollution, (iCACGP) 13th Science Conference of the International Global Atmospheric Chemistry Project, (IGAC), Natal Convention Center (NCC), Natal, Brazil 22-26th September 2016
36. Van Zyl, P.G., Beukes, J.P.; Conradie, E.H.; Pienaar, J.J.; Mkhathshwa, G.; Fourie, G.D. and Galy-Lacaux, C., Deposition measurements in southern Africa, Workshop on Atmospheric Deposition Processes, The Abdus Salam International Centre for Theoretical Physics, Trieste, Italy, 21-25 May 2012.
37. P. Maritz, J.P. Beukes, P.G. van Zyl, E.H. Conradie, A.D. Venter, J.J. Pienaar, C. Liousse, C. Galy-Lacaux, Spatial and temporal assessment of atmospheric organic and black carbon concentrations at South African DEBITS sites, 16th International Union of Air Pollution Prevention Association (IUAPPA) Congress, 29 September – 4 October 2013, International Convention Centre, Cape Town, South Africa.

DISCLAIMER

Air Resource Management (Pty) Ltd has prepared this report based on an agreed scope of work and acts in all professional matters as an advisor to the Client and exercises all reasonable skill and care in the provision of its professional services in a manner consistent with the level of care and expertise exercised by air quality management professionals.

Reports are commissioned by and prepared for the exclusive use of the Client. They are subject to and issued in accordance with the agreement between the Client and Air Resource Management (Pty) Ltd. Air Resource Management (Pty) Ltd is not responsible and will not be liable to any other person or organisation for or in relation to any matter dealt within this Report, or for any loss or damage suffered by any other person or organisation arising from matters dealt with or conclusions expressed in this report (including without limitation matters arising from any negligent act or omission of Air Resource Management (Pty) Ltd or for any loss or damage suffered by any other party relying upon the matters dealt with or conclusions expressed in this Report). Other parties should not rely upon the report or the accuracy or completeness of any conclusions and should make their own inquiries and obtain independent advice in relation to such matters.

Except where expressly stated, Air Resource Management (Pty) Ltd has not verified the validity, accuracy or comprehensiveness of any information supplied to Air Resource Management (Pty) Ltd for its reports.

Reports prepared by Air Resource Management (Pty) Ltd cannot be copied or reproduced in whole or part for any purpose without the prior written agreement of Air Resource Management (Pty) Ltd.

Where site inspections, testing or fieldwork have taken place, the report is based on the information made available by the client or their nominees during the visit, visual observations and any subsequent discussions with regulatory authorities. The validity and comprehensiveness of supplied information has not been independently verified and, for

the purposes of this report, it is assumed that the information provided to Air Resource Management (Pty) Ltd is both complete and accurate. It is further assumed that normal activities were being undertaken at the site on the day of the site visit(s), unless explicitly stated otherwise.

COPYRIGHT

The information contained in this document is the property of Air Resource Management (Pty) Ltd. Use or copying of this document in whole or in part without the written permission of Air Resource Management (Pty) Ltd constitutes an infringement of copyright.